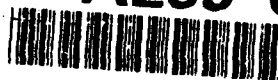


AFIT/GA/ENY/92D-02

AD-A259 000



EFFECT OF TRANSVERSE VIBRATION  
ON THE CAPILLARY LIMIT OF A  
WRAPPED SCREEN WICK COPPER/  
WATER HEAT PIPE

THESIS

Mark C. Charlton, Captain, USAF

AFIT/GA/ENY/92D-02

DTIC  
ELECTE  
JAN 08 1993  
S E D

93-00029



Approved for public release; distribution unlimited

93 1 04 040

AFIT/GA/ENY/92D-02

EFFECT OF TRANSVERSE VIBRATION ON THE CAPILLARY LIMIT  
OF A WRAPPED SCREEN WICK COPPER/WATER HEAT PIPE

THESIS

Presented to the Faculty of the School of Engineering  
of the Air Force Institute of Technology

Air University

In Partial Fulfillment of the  
Requirements for the Degree of  
Master of Science in Astronautical Engineering

DTIC QUALITY INSPECTED

Mark C. Charlton, B.S.  
Captain, USAF

December, 1992

Accession For	
NTIS	CRA&I <input checked="checked" type="checkbox"/>
DTIC	TAB <input checked="checked" type="checkbox"/>
Unannounced <input type="checkbox"/>	
Justification .....	
By .....	
Distribution /	
Availability Codes	
Dist	Avail and/or Special
A-1	

Approved for public release; distribution unlimited

### *Acknowledgements*

In arriving at this finished product, there has been a great deal of help from others. My faculty advisor, Major W. Jerry Bowman, has been instrumental in addressing the many difficulties that arose along the way, and in the preparation of this manuscript. Furthermore, Dr. William Elrod and Major David Coulliette invested a great deal of time in reviewing the manuscript. A word of thanks to Dr. Jerry Beam of the Power and Technology Branch for the initial research topic, technical support, and financial sponsorship. In the design and construction of the apparatus, I have a number of people to thank. John Brohas at the AFIT Model Shop worked hard to provide short turn-around times on hardware needed to fix the things that inevitably go awry in an experimental thesis. Also Don Reinmuller and John Tennant at the Power and Technology Branch exhibited exceptional patience in the construction and fill of the heat pipe during the many attempts to get it right. The Aero/Astro Lab Technicians, Jay Anderson and Andy Pitts spent many hours helping to work out the gremlins in the instrumentation and data acquisition systems. Finally, I wish to thank my wife April for her understanding and support on the many late nights sacrificed by both of us to put this together.

Mark C. Charlton

## Table of Contents

	Page
Acknowledgements . . . . .	ii
List of Figures . . . . .	v
List of Tables . . . . .	vi
List of Symbols . . . . .	vii
Abstract . . . . .	x
I. Introduction . . . . .	1.1
Background . . . . .	1.1
Objective . . . . .	1.9
Approach . . . . .	1.9
II. Theory . . . . .	2.1
Heat Pipe Operating Principles . . . . .	2.1
Temperature Drop Along Heat Pipe Operating in Heat Pipe Mode . . . . .	2.8
Temperature Gradient Along Evaporator Section Assuming Pure Conduction . . . . .	2.14
Temperature Gradient Along Adiabatic Section Assuming Pure Conduction . . . . .	2.19
III. Experiment Design . . . . .	3.1
Heat Pipe Design . . . . .	3.1
Heat Pipe Construction . . . . .	3.13
Heating Apparatus . . . . .	3.25
Coolant Control System . . . . .	3.26
Vibration Input Apparatus . . . . .	3.27
Data Acquisition System . . . . .	3.30
Experimental Test Procedure . . . . .	3.36
IV. Experiment Analysis . . . . .	4.1
Temperature Measurements . . . . .	4.1
Vibration Data . . . . .	4.5
Coolant Flow Measurement . . . . .	4.8
Heat Pipe Inclination Measurement . . . . .	4.9
Determination of Accumulated Experimental Error . . . . .	4.10
V. Experimental Results . . . . .	5.1
Determination of Heat Pipe Performance With no Vibration . . . . .	5.1

Determination of Heat Pipe Performance During Transverse Vibration . . . . .	5.3
Comparison of Vibration Data to Static Data . . . . .	5.5
VI. Conclusions and Recommendations . . . . .	6.1
Conclusions . . . . .	6.1
Recommendations . . . . .	6.2
Appendix A: Thermophysical Properties of Saturated Water . . . . .	A.1
Appendix B: Table of Test Run Results . . . . .	B.1
Appendix C: Reduced Test Run Data . . . . .	C.1
Bibliography . . . . .	BIB.1
Vita . . . . .	VIT.1

## List of Figures

Figure	Page
1.1 The Basic Heat Pipe (4:3) . . . . .	1.3
2.1 Heat Flow Path Through a Heat Pipe (1:70) . .	2.11
2.2 Heat Flow Path During Pure Conduction . . . .	2.16
3.1 Heat Pipe Container Dimensions . . . . .	3.3
3.2 Analytical $Q_{c,max}$ vs. $T_{op}$ . . . . .	3.14
3.3 Experimental Heat Pipe . . . . .	3.15
3.4 Endcap Construction . . . . .	3.17
3.5 Fill Station Apparatus . . . . .	3.23
3.6 Vibration Fixture . . . . .	3.29
3.7 Accelerometer Locations . . . . .	3.31
3.8 Thermocouple Locations . . . . .	3.33
3.9 Coolant Thermocouple . . . . .	3.34
3.10 Experimental Setup . . . . .	3.37
5.1 $Q_{c,max}$ vs. $T_{op}$ : Static and Predicted . . . .	5.3
5.2 $Q_{c,max}$ vs. $T_{op}$ : Static and Vibration Results .	5.6
5.3 $Q_{c,max}$ vs. $T_{op}$ : Vibration at 1.0 g . . . . .	5.7
5.4 $Q_{c,max}$ vs. $T_{op}$ : Vibration at 2.5 g . . . . .	5.8
5.5 $Q_{c,max}$ vs. $T_{op}$ : Vibration at 5.0 g . . . . .	5.9
5.6 $Q_{c,max}$ vs. $T_{op}$ : Vibration at 30 Hz . . . . .	5.10
5.7 $Q_{c,max}$ vs. $T_{op}$ : Vibration at 250 Hz . . . . .	5.11
5.8 $Q_{c,max}$ vs. $T_{op}$ : Vibration at 1000 Hz . . . . .	5.12

*List of Tables*

Table		Page
A.1	Thermophysical Properties of Saturated Water (5:A22) . . . . .	A.1
B.1	Test Run Results . . . . .	B.1

## List of Symbols

Symbol	Definition
$A_c$	pipe wall cross-sectional area ( $m^2$ )
$A_s$	area of wick pore at wick-vapor interface ( $m^2$ )
$A_s$	pipe surface area in contact with heater ( $m^2$ )
$A_v$	vapor core cross-sectional area ( $m^2$ )
$A_w$	wick cross-sectional area ( $m^2$ )
ASME	American Society of Mechanical Engineers
$C_s$	wetted perimeter of wick pore at wick-vapor interface (m)
$C_{p,l}$	specific heat of liquid (J/kg-K)
cps	cycles per second
$d$	screen wire diameter (m)
$d_i$	inner pipe diameter (m)
$d_o$	outer pipe diameter (m)
$d_v$	vapor core diameter (m)
$E_{rss}$	root-sum square error
$\dot{E}_g$	rate of energy generation (W)
$\dot{E}_{in}$	rate of energy transfer in (W)
$\dot{E}_{out}$	rate of energy transfer out (W)
$\dot{E}_{st}$	rate of energy storage (W)
$F_l$	liquid frictional coefficient $[(N/m^2)/(W-m)]$
$F_v$	vapor frictional coefficient $[(N/m^2)/(W-m)]$
$f_{max}$	maximum hoop stress ( $N/m^2$ )
ft	feet
$f_v$	drag coefficient for vapor flow
$g$	force of gravity ( $m/s^2$ )
$I$	current (amps)
$K$	wick permeability ( $m^2$ )
$k$	thermal conductivity (W/m-K)
$k_e$	effective thermal conductivity of liquid-saturated wick (W/m-K)
$k_{e,c}$	effective thermal conductivity of liquid-saturated wick at condenser (W/m-K)
$k_{e,e}$	effective thermal conductivity of liquid-saturated wick at evaporator (W/m-K)
$k_l$	thermal conductivity of liquid (W/m-K)
$k_p$	thermal conductivity of pipe material (W/m-K)
$k_w$	thermal conductivity of wick material (W/m-K)
$L$	cylinder length (m)
$L_a$	length of adiabatic section (m)
$L_c$	length of condenser section (m)
$L_e$	length of evaporator section (m)
$L_t$	total heat pipe working length (m)
$m$	fluid inventory mass (kg)
$m$	mass of collected coolant (kg)
$\dot{m}$	mass flow rate of coolant (g/s)
$N$	screen mesh number ( $m^{-1}$ )
$P$	power (W)
$P$	pressure differential across wall ( $N/m^2$ )



$P_c$	capillary pressure ( $N/m^2$ )
$P_g$	hydrostatic pressure ( $N/m^2$ )
$Q$	heat transport rate (W)
$Q_{b,max}$	boiling limited heat transport rate (W)
$Q_{c,max}$	capillary limited heat transport rate (W)
$Q_{e,max}$	entrainment limited heat transport rate (W)
$Q_{in}$	heat transfer into pipe (W)
$Q_{max}$	maximum heat transport rate (W)
$Q_{out}$	heat transfer out of pipe (W)
$Q_{s,max}$	sonic limited heat transport rate (W)
$(QL)_{c,max}$	capillary limitation on the heat transport factor (W-m)
$q$	heat transfer rate into evaporator (W)
$q_1''$	heater power density ( $W/m^2$ )
$q_2''$	conduction heat flux down pipe wall ( $W/m^2$ )
$R$	thermal resistance ( $m^2-K/W$ )
$R_v$	vapor gas constant ( $J/kg-K$ )
$Re_v$	vapor flow Reynolds number
$r_c$	effective capillary radius (m)
$r_{h,s}$	surface pore hydraulic radius (m)
$r_{h,v}$	vapor core hydraulic radius (m)
$r_i$	inner radius of pipe (m)
$r_n$	minimum radius of nucleation (m)
$r_o$	outer radius of pipe (m)
$r_v$	vapor core radius (m)
$r_1$	cylinder inner radius (m)
$r_2$	cylinder outer radius (m)
SCR	signal conditioning rectifier
$T$	temperature (K)
$T_{in}$	temperature of coolant entering manifold (K)
$T_{op}$	heat pipe operating temperature (K)
$T_{out}$	temperature of coolant leaving manifold (K)
$T_{p,c}$	pipe wall temperature at condenser (K)
$T_{p,e}$	pipe wall temperature at evaporator (K)
$T_{pw,c}$	pipe-wick interface temperature at condenser (K)
$T_{pw,e}$	pipe-wick interface temperature at evaporator (K)
$T_v$	vapor stagnation temperature (K)
$T_{v,c}$	vapor temperature at condenser (K)
$T_{v,e}$	vapor temperature at evaporator (K)
$T_{wv,c}$	wick-vapor interface temperature at condenser (K)
$T_{wv,e}$	wick-vapor interface temperature at evaporator (K)
TC	thermocouple
TIG	tungsten inert gas
T1	first thermocouple channel
T2	second thermocouple channel
T3	third thermocouple channel
T4	fourth thermocouple channel
T5	fifth thermocouple channel
T6	sixth thermocouple channel
T7	seventh thermocouple channel
T8	eighth thermocouple channel
T9	ninth thermocouple channel
T10	tenth thermocouple channel

$t$	time interval of coolant collection (s)
$t$	wall thickness (m)
$t_s$	screen thickness (m)
$t_w$	wick thickness (m)
UTS	ultimate tensile strength (N/m <sup>2</sup> )
$u_1$	first independent variable
$u_2$	second independent variable
$u_n$	nth independent variable
$V$	voltage (volts)
$v_l$	specific volume of liquid (m <sup>3</sup> /kg)
$v_v$	specific volume of vapor (m <sup>3</sup> /kg)
$w$	wire spacing (m)
$x$	distance from evaporator end of heat pipe (m)
$x$	x-axis, pipe transverse axis, normal to actuator
$y$	y-axis, pipe longitudinal axis
$z$	z-axis, pipe transverse axis, actuator axis
$\Delta C_{p,l}$	error in specific heat of liquid (J/kg-K)
$\Delta m$	error in coolant mass collected (kg)
$\Delta \dot{m}$	error in mass flow rate (kg/s)
$\Delta P$	normal hydrostatic pressure (N/m <sup>2</sup> )
$\Delta Q$	error in calculated heat transport rate (W)
$\Delta T$	change in temperature of coolant (K)
$\Delta T_{in}$	error in temperature of coolant entering manifold (K)
$\Delta T_{out}$	error in temperature of coolant leaving manifold (K)
$\Delta t$	error in time interval of coolant collection (s)
$\Delta u_1$	error in first independent variable
$\Delta u_2$	error in second independent variable
$\Delta u_n$	error in nth independent variable
$\Delta(\Delta T)$	error in change in temperature of coolant (K)
$\epsilon$	wick porosity
$\gamma_v$	vapor specific heat ratio
$\lambda$	latent heat of vaporization (J/kg)
$\mu_l$	liquid viscosity (N-s/m <sup>2</sup> )
$\mu_v$	vapor viscosity (N-s/m <sup>2</sup> )
$\rho_l$	liquid mass density (kg/m <sup>3</sup> )
$\rho_v$	vapor mass density (kg/m <sup>3</sup> )
$\sigma$	surface tension coefficient (N/m)
$\psi$	heat pipe inclination angle (°)

*Abstract*

The effect of transverse vibration on the capillary limit of a copper/water heat pipe with a tightly wrapped screen wick was investigated. The capillary limit was measured over a range of operating temperatures under static conditions. A bench-top shaker was used to provide vibration normal to the longitudinal axis of the pipe, and the capillary limit was measured at vibration frequencies of 30, 250, and 1000 Hz. At each of these frequencies, tests were run at vibration levels of 1.0, 2.5, and 5.0 G. The pipe was maintained at a zero degree inclination angle and power throughput was increased until dryout was achieved. The power throughput at dryout was considered to be the capillary limit under the conditions imposed for that test. The measured capillary limit from each vibration test was compared to those from the static tests. The results spanned pipe operating temperatures from 50° C to 75° C. For the frequencies and amplitudes tested, there was found to be little or no effect on the capillary limit due to vibration normal to the longitudinal axis. It is recommended that further study in this area be concentrated on vibration parallel to the longitudinal axis.

# EFFECT OF TRANSVERSE VIBRATION ON THE CAPILLARY LIMIT OF A WRAPPED SCREEN WICK COPPER/WATER HEAT PIPE

## *I. Introduction*

### *Background*

Heat pipes are fascinating things. With virtually no moving parts, they have proven to be a reliable and nearly maintenance free method of conducting energy from one location to another in the form of heat. Many applications exist where the heat pipe is, arguably, a desirable alternative to the current device or method used for energy transfer. Indeed, there may yet be situations discovered where a heat pipe provides the only viable energy transfer method. It is the multitude of uses for heat pipes which drives this and similar research.

The growing number of current and potential applications brings with it an expanding set of environmental conditions under which the heat pipe must function. This research is a step toward evaluating what effect, if any, these environmental conditions have on the capabilities of heat pipes. In particular, this experiment examined how a heat pipe might operate in an environment where it is subjected to vibration.

*What is a Heat Pipe?* As alluded to above, a heat pipe is a heat transfer device. It is a closed system that utilizes a working fluid to transfer heat from one location to another. The particular design may vary considerably, but they all operate using the same basic principles. A basic heat pipe is illustrated in Figure 1.1. It typically consists of a sealed chamber containing the working fluid and a wick structure. Some portion of the pipe acts as an evaporator and another serves as a condenser, with these sections connected by the wick structure. The wick is filled with the liquid form of the working fluid while the remainder of the volume is, ideally, filled with the vapor form.

While the device is operating in what is known as the heat pipe mode, heat will be applied to the evaporator section by some external source, causing the fluid in that section to be vaporized. The condenser section is simultaneously transferring heat from the pipe to a heat sink. This loss of heat causes the working fluid in that section to condense from the vapor phase to the liquid phase, releasing the heat of vaporization. The resulting drop in pressure between these sections causes the vapor to travel down the pipe from the evaporator to the condenser. Once in its liquid form, the working fluid enters the wick structure and is transported via a capillary pumping action from the condenser back to the evaporator section of the pipe. The wick must be composed of a porous structure to

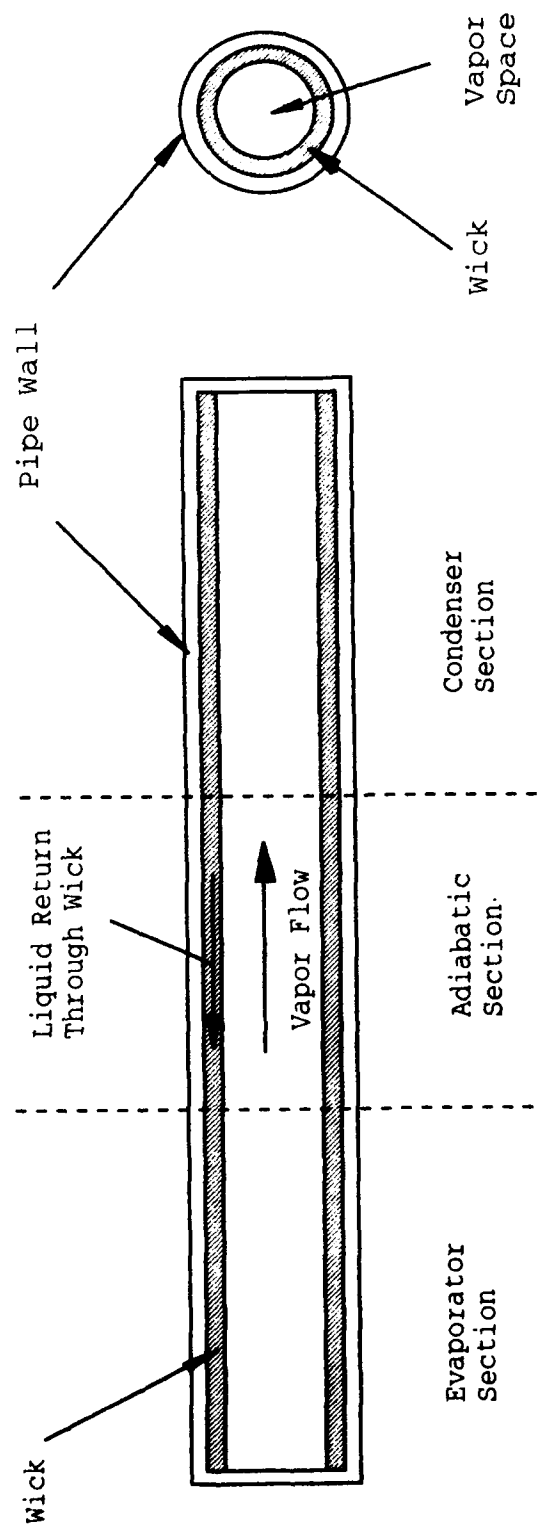


Figure 1.1 The Basic Heat Pipe (4:3)

enable the generation of adequate capillary forces for this to occur. The working fluid, therefore, makes a complete cycle. It begins in the evaporator section, is vaporized, travels in vapor form to the condenser section, condenses, enters the wick, and is pumped via capillary action back to the evaporator section, where the process begins again. This process is continuous as long as the pipe is operating in the heat pipe mode.

In the most basic heat pipes there are no moving parts and herein lies the simplicity that makes them so reliable. There is also no requirement for replenishment of the working fluid since the system is sealed and the fluid merely changes phase, but does not escape. In addition to its inherent reliability and simplicity, a significant advantage of the heat pipe is that "The amount of heat that can be transported is usually several orders of magnitude larger than that which can be transported as sensible heat in a conventional convective system" (1:1). Likewise, as Chi points out in his work, its lighter weight and smaller temperature drop make it superior to solid conductors in many applications (1:2).

*Air Force Interest.* The Air Force has expressed interest in heat pipes for some years now. Most of the research appears to have been done in the late 1960s and throughout the 1970s. In the intervening years research has been conducted at a somewhat less energetic pace. Currently, with the advent of new and challenging thermal

control concerns, the heat pipe is once again being evaluated as a means of addressing difficult heat transfer problems. The Air Force is involved in a number of programs where the heat pipe may be a desirable, and perhaps the only, solution to thermal control concerns.

One area of interest is satellite thermal control. Here is a prime example of an application where light weight, low maintenance, and high heat transfer rate are of great importance. "The first use of heat pipes for satellite thermal control was on GEOS-B, launched from Vandenburg Air Force Base in 1968" (4:11). Like this application, heat pipes are most often used on spacecraft to normalize temperatures between areas which are physically separated from one another. They may also be used to transport heat from some area to a radiator, where it can be shed to space. Other spacecraft related applications include cooling radioisotope thermoelectric generators, cooling individual electronic components, and thermal control and cooling of sensor surfaces (1:14).

Another significant area of Air Force interest is in the realm of high temperature surfaces. With the never-ending push to expand the operating envelope of all Air Force systems, the material constraints of many components are being reached. In order to increase performance, without developing new materials, a way must be found to keep these components at a temperature such that the material properties are not exceeded. The cooling of high



speed turbine blades is one possible example. Another is the search for a way to cool the leading edge of the wings on the National Aerospace Plane and other high speed aircraft. These may be applications suited to the use of heat pipes.

The areas described above are merely a sampling of the substantial number of possibilities for Air Force use of heat pipes in current and future systems. These systems operate in a wide range of environments including those found on the ground, in the atmosphere, and in space. It is clear that a better understanding of heat pipe operation, and the effect of its operating environment on performance, is of importance to the Air Force.

*The Importance of Vibration.* Understanding the effect of vibration on heat pipe performance is important in the design of systems where they are to be employed. Most current and proposed Air Force applications for heat pipes are in dynamic mechanical systems. These dynamic systems are invariably subjected to vibration during their operation. Satellites undergo station-keeping and orbit change maneuvers where thruster firings cause vibration, not to mention the launch environment. Engine turbines obviously are exposed to vibration during their operation. High speed aircraft will see a wide variety of vibration both internally generated and due to external inputs such as turbulence or taxiing on a rough runway. It is important to know how these vibration environments effect heat pipe

performance. A heat pipe that provides adequate heat transfer under static conditions may perform quite differently while subjected to vibration. This difference, if any, must be incorporated into the design of the system where the heat pipe is proposed for use.

*Previous Vibration Experiments.* A literature search and interviews with Dr. Jerry Beam of the Wright Laboratory, Power and Technology Branch, and with Major W. Jerry Bowman, Department of Aeronautics and Astronautics, Air Force Institute of Technology, Air University, revealed that little research has been done on the effects of vibration on heat pipe performance. While there have been experiments done to validate entire systems in a vibration environment, little has been done to treat the subject of how vibration affects heat pipe operation in general. What results are published tend to describe the vibration testing done on a satellite, for example, but do not quantify how the heat pipe performed, or even if it was operating at the time of the test.

Two works were reviewed that do indeed investigate this more general question. The first was a report by J. E. Deverall on work done at Los Alamos Scientific Laboratory (2:1-7). This report describes an experiment designed to evaluate the effect of vibration on a heat pipe. The heat pipe used was a stainless steel pipe with a wrapped screen wick and water as a working fluid. The test consisted of operating the heat pipe at an equilibrium temperature and

then subjecting the pipe to sinusoidal and random vibration at various levels. During the test, pipe wall temperatures were monitored along the length of the pipe. The objective was to note any change in pipe operating temperature due to vibration. Another experiment was conducted during which the vibration frequency was held constant at 60 cycles per second (cps) and the angle of inclination was varied from 0 to 40 degrees. Here again, the data observed was the pipe wall temperature at various locations along the length of the pipe. The conclusion of this report is that "sinusoidal and random vibration, within the spectrum tested, are not detrimental to heat pipe performance" (2:7). The second work addressing this subject was a report by Richardson et al. on research performed at Louisiana State University (6:249-265). They investigated the effect of longitudinal vibration on heat pipe performance. The testing was performed on a stainless steel heat pipe with a rigid porous metal wicking structure and water as a working fluid. The experimenters used time to evaporator dryout as the criterion of performance (6:255). Testing was done at 32°, 35°, and 38° inclination and at frequencies of 60, 120, 240, and 580 cps. They concluded that longitudinal vibration has a detrimental effect on the maximum heat transfer capability of a heat pipe constructed in the same manner as the one in the experiment (6:265). It was reported that the effect is greater at lower frequencies and higher amplitudes. The authors indicated that "the most pressing need is for an

investigation providing information on actual maximum heat transfer capability" and that "An investigation should be made of the effect of transverse vibration" (6:265).

### *Objective*

The objective of this thesis is to determine the effect of transverse vibration on the capillary limit of a wrapped screen wick copper/water heat pipe. This is a logical extension of the work described in the reports mentioned above and will address an area of concern to the Air Force.

### *Approach*

To attain this objective, an experimental heat pipe and apparatus were designed and built. This enabled test runs at a defined pipe inclination angle, vibration frequency, and vibration level. The pipe operating temperature was also adjustable. The requirement was to be able to determine what the power throughput of the heat pipe was at any given time. The criterion of performance for this experiment was maximum heat transport through the pipe.

The static performance of the pipe was first measured through a series of tests with no vibration input. These tests provided a baseline of maximum heat transport for the pipe over a range of heat pipe operating temperatures. Once this baseline performance was established, tests were run with vibration input perpendicular to the longitudinal axis of the pipe. These runs were made at three vibration frequencies and three vibration levels. This was intended

to determine if there was any change in performance which could be associated with a particular frequency or level of vibration. The results from the vibration test runs were compared to those from the static baseline runs to determine if there was any effect on the maximum heat transport due to transverse vibration and to quantify that effect.

## II. Theory

### *Heat Pipe Operating Principles*

The particular design of heat pipes may vary greatly, but there are a few basic principles that determine how well a heat pipe works, or if it works at all. Since the heat pipe is a closed system that uses circulation of a working fluid to transport heat, that circulation is an important factor in how well the pipe works. "The maximum possible circulation is required to obtain the maximum heat transport capability of the heat pipe" (1:31). There are a number of limitations to this maximum heat transport capability. They are commonly known as the "sonic limit," the "entrainment limit," the "boiling limit," and the "capillary limit." Each limit is due to a particular physical phenomenon that occurs within the heat pipe when certain operating conditions are met. The following sections briefly explain each limit and its cause. For a more detailed explanation of the fundamentals behind heat pipe operation, the reader is directed to the works *Heat Pipe Theory and Practice* (1:1-242) by S. W. Chi and *Heat Pipes* (4:1-299) by Dunn and Reay. Both of these provide a comprehensive treatment of heat pipe operating principles.

*Sonic Limited Heat Transport.* Under certain pipe operating conditions, there is a choking of the vapor flow and the sonic limit of the pipe is reached (1:31). During operation of a heat pipe, the vapor stream is accelerated by

the addition of vapor in the evaporator section and decelerated by the removal of vapor in the condenser section (1:79). Depending upon the rate of heat input and heat rejection, the flow velocity can increase to the point where it becomes sonic at the end of the evaporator. At this point, the flow is choked and the heat transport capability of the evaporator section can not be increased. This condition is called the sonic limit of the heat pipe and it limits the "total power handling capability" (4:82) of the pipe. There is a closed form expression for the sonic limit based on one-dimensional flow theory. It assumes that the vapor properties follow the ideal gas law, that the flow is dominated by inertial effects, and that friction can be neglected. Chi explains that these assumptions are reasonable because "sonic limitation generally occurs when a heat pipe is operating at low vapor densities and high vapor velocities" (1:82). The equation for calculating the maximum sonic limited heat transport rate is found to be

$$Q_{s,max} = A_v \rho_v \lambda \left[ \frac{\gamma_v R_v T_v}{2(\gamma_v + 1)} \right]^{1/2} \quad (2.1)$$

where

- $Q_{s,max}$  = sonic limited heat transport rate (W)
- $A_v$  = cross-sectional area of vapor core (m<sup>2</sup>)
- $\rho_v$  = vapor density (kg/m<sup>3</sup>)
- $\lambda$  = latent heat of vaporization (J/kg)
- $\gamma_v$  = specific heat ratio
- $R_v$  = gas constant of the vapor (J/kg-K)
- $T_v$  = vapor stagnation temperature (K)

This equation was first proposed by an individual named Levy and is often referred to as "Levy's Equation" in much of the heat pipe literature (1:84).

*Entrainment Limited Heat Transport.* Another limit to the maximum heat transport capability of a heat pipe is the entrainment limit. It can be thought of as the limit due to the working fluid being torn from the surface of the wick structure by the passing high velocity vapor. As pointed out by Dunn and Reay, there is a shear force generated at the interface between the liquid and the vapor. The magnitude of this shear force is determined by the "vapor properties and velocity and its action will be to entrain droplets of liquid and transport them to the condenser end" (4:52). When enough liquid is being pulled from the wick surface, the continuous replenishment of the fluid in the evaporator is interrupted and the evaporator begins to dry out. Thus heat pipe performance is degraded. When this happens, the entrainment limit has been reached. Chi developed an expression which yields the maximum entrainment limited heat transfer rate for a heat pipe (1:87). It is as follows

$$Q_{e, \max} = A_v \lambda \left( \frac{\sigma \rho_v}{2 r_{h, s}} \right)^{1/2} \quad (2.2)$$

where

$Q_{e, \max}$  = entrainment limited heat transport rate (W)  
 $\sigma$  = surface tension coefficient (N/m)



$\rho_v$  = vapor density (kg/m<sup>3</sup>)  
 $r_{h,s}$  = surface pore hydraulic radius (m)

The surface pore hydraulic radius can be found with the following equation (1:87)

$$r_{h,s} = \frac{2A_s}{C_s} \quad (2.3)$$

where

$A_s$  = area of wick pore at wick-vapor interface (m<sup>2</sup>)  
 $C_s$  = wetted perimeter of wick pore at wick-vapor interface (m)

*Boiling Limited Heat Transport.* The boiling limit is reached when the heat flux in the evaporator section is such that vapor bubbles begin to form at the wick-pipe wall interface. This bubble formation is undesirable for a number of reasons. The bubbles tend to interrupt fluid flow throughout the evaporator and cause hot spots to develop (1:90). These effects have the result of degrading the radial heat flux into the pipe, and the heat transfer rate of the pipe is reduced. When these conditions occur it is known as the boiling limit. There is a significant difference between this and the other limits in that the "boiling limitation is a limitation of the radial heat flux density, while the other limitations are limitations of the axial heat flux" (1:90). As Chi points out, the analysis of this limitation requires the theory of nucleate boiling which is an in-depth subject in itself. The interested reader can find a discussion in either Chi's work or that by

Dunn and Reay. Chi does develop an expression for the maximum boiling limited heat transfer rate given by (1:91)

$$Q_{b,\max} = \frac{2\pi L_e k_e T_v}{\lambda \rho_v \ln\left(\frac{r_i}{r_v}\right)} \left( \frac{2\sigma}{r_n} - P_c \right) \quad (2.4)$$

where

- $Q_{b,\max}$  = boiling limited heat transfer rate (W)
- $L_e$  = length of the evaporator section (m)
- $k_e$  = effective thermal conductivity of liquid-saturated wick (W/m-K)
- $r_i$  = inner radius of pipe (m)
- $r_v$  = vapor core radius (m)
- $r_n$  = critical radius of nucleation (m)
- $P_c$  = capillary pressure (N/m<sup>2</sup>)

*Capillary Limited Heat Transport.* The capillary limit is possibly the most significant of the performance limits since it is typically the most restrictive limitation. The capillary limit is reached when the capillary pumping ability of the wick structure is no longer adequate to replenish the working fluid in the evaporator. The fluid is evaporated more quickly than it can be replaced and the evaporator section begins to dry out. The heat transport capability of the pipe is then degraded and the capillary limit has been reached. The capillary pumping ability of the wick is based on a pressure balance. Chi describes this pressure balance beginning with the pressure gradient within the vapor core due to vapor flow from the evaporator to the condenser. There is also a contribution due to liquid flow within the wick from the condenser to the evaporator. For

capillary pumping to take place, there must be a difference in pressure between the liquid side and the vapor side of the liquid-vapor interface "except at the point where the difference is minimum and is equal to zero" (1:33). Chi calls this pressure difference the capillary pressure and attributes it to the effect caused by menisci forming in the pores of the wick and being pushed into the wick structure by the greater pressure on the vapor side of the interface (1:33). After a fairly lengthy development, he derives a series of equations that may be used to calculate the capillary limited heat transport rate of a conventional heat pipe operating in heat pipe mode. As a preliminary step, the capillary limited heat transport factor,  $(QL)_{c,max}$ , is found. This factor is calculated using the equation (1:54)

$$(QL)_{c,max} = \frac{\frac{2\sigma}{r_c} - \Delta P_l - \rho_l g L_t \sin \psi}{F_l + F_v} \quad (2.5)$$

where

- $(QL)_{c,max}$  = capillary limitation on the heat transport factor (W-m)
- $r_c$  = effective capillary radius (m)
- $\Delta P_l$  = normal hydrostatic pressure (N/m<sup>2</sup>)
- $\rho_l$  = liquid density (kg/m<sup>3</sup>)
- $g$  = force of gravity (m/s<sup>2</sup>)
- $L_t$  = total length of heat pipe (m)
- $\psi$  = heat pipe inclination (°)
- $F_l$  = liquid frictional coefficient [(N/m<sup>2</sup>)/(W-m)]
- $F_v$  = vapor frictional coefficient [(N/m<sup>2</sup>)/(W-m)]

The effective capillary radius for a wire screen wick is found using the following equation (1:35)

$$r_c = \frac{w+d}{2} = \frac{1}{2N} \quad (2.6)$$

where

$$\begin{aligned} w &= \text{wire spacing (m)} \\ d &= \text{wire diameter (m)} \\ N &= \text{screen mesh number (m}^{-1}\text{)} \end{aligned}$$

The liquid frictional coefficient may be found using (1:39)

$$F_l = \frac{\mu_l}{KA_w \rho_l \lambda} \quad (2.7)$$

where

$$\begin{aligned} \mu_l &= \text{liquid viscosity (kg/m-sec)} \\ K &= \text{wick permeability (m}^2\text{)} \\ A_w &= \text{cross-sectional area of wick (m}^2\text{)} \end{aligned}$$

For a wrapped screen wick, the wick permeability is computed using (1:42)

$$K = \frac{d^2 \epsilon^3}{122 (1-\epsilon)^2} \quad (2.8)$$

where

$$\epsilon = \text{wick porosity}$$

Wick porosity is calculated using (1:42)

$$\epsilon = 1 - \frac{1.05 \pi N d}{4} \quad (2.9)$$

Similarly, the vapor frictional coefficient can be found using the following equation (1:44)

$$F_v = \frac{(f_v Re_v) \mu_v}{2 r_{h,v}^2 A_v \rho_v \lambda} \quad (2.10)$$

where

- $f_v$  = drag coefficient for vapor flow
- $Re_v$  = vapor flow Reynolds number
- $\mu_v$  = vapor viscosity (kg/m<sup>3</sup>)
- $r_{h,v}$  = vapor core hydraulic radius (m)

The quantity  $(f_v Re_v)$  is often referred to as the drag coefficient, and has been shown to be approximately equal to 16 for circular vapor flow passages when assuming incompressible, laminar flow (1:45). The vapor core hydraulic radius is simply the radius of the vapor core when considering circular annular flow passages. Once the capillary heat transport factor has been calculated, the capillary heat transport limit may be found. This is accomplished using the equation (1:59)

$$Q_{c,max} = \frac{(QL)_{c,max}}{\frac{1}{2}L_c + L_a + \frac{1}{2}L_e} \quad (2.11)$$

where

- $Q_{c,max}$  = capillary limited heat transport rate (W)
- $L_c$  = length of heat pipe condenser (m)
- $L_a$  = length of heat pipe adiabatic section (m)

### *Temperature Drop Along Heat Pipe Operating in Heat Pipe Mode*

A heat pipe operating in heat pipe mode has a predictable temperature drop. By definition, if the pipe is

operating in the heat pipe mode, it is operating within the limits discussed in the preceding sections. This being the case, the difference between the pipe wall temperature at the evaporator and the pipe wall temperature at the condenser can be calculated. This calculation entails finding the temperature drops during each step of heat transfer in the pipe, and then summing them to get a total temperature drop along the pipe. Knowing this quantity is useful during experimentation because it provides a clue as to whether the pipe is operating in heat pipe mode, or if it has reached one of the limits. The basic equation used in this calculation is Fourier's law of heat conduction (1:69)

$$Q = \frac{1}{R} (T_1 - T_2) \quad (2.12)$$

where

- Q = heat transfer rate (W)
- R = thermal resistance (K/W)
- T<sub>1</sub> = temperature at location 1 (K)
- T<sub>2</sub> = temperature at location 2 (K)

As Chi points out, the significant heat transfer mechanisms in a heat pipe are conduction across the heat pipe wall and through the liquid saturated wick. This happens in the evaporator section and then again in the condenser section. The other small temperature drops associated with evaporation and condensation at the vapor-liquid interface and with the convective heat transfer as the vapor travels down the pipe are typically small in comparison (1:69). The

calculation presented here assumes that these small temperature drops are insignificant compared to the conduction terms. With this assumption in mind, the total temperature drop can be found by summing the temperature drops through the evaporator pipe wall, through the liquid saturated wick in the evaporator, through the liquid saturated wick in the condenser, and through the pipe wall in the condenser. These different surfaces within the pipe can be seen in Figure 2.1. In a basic heat pipe of annular construction, all these surfaces are cylindrical. The thermal resistance for a cylindrical wall can be calculated using (1:70)

$$R = \frac{\ln\left(\frac{r_2}{r_1}\right)}{2\pi Lk} \quad (2.13)$$

where

- $r_2$  = outer radius (m)
- $r_1$  = inner radius (m)
- $L$  = cylinder length (m)
- $k$  = thermal conductivity of the material [W/(m-K)]

First, the temperature drop across the evaporator pipe wall is calculated as

$$T_{p,e} - T_{pw,e} = \frac{Q \ln\left(\frac{r_o}{r_i}\right)}{2\pi L_e k_p} \quad (2.14)$$

where

- $T_{p,e}$  = temperature of evaporator pipe wall (K)

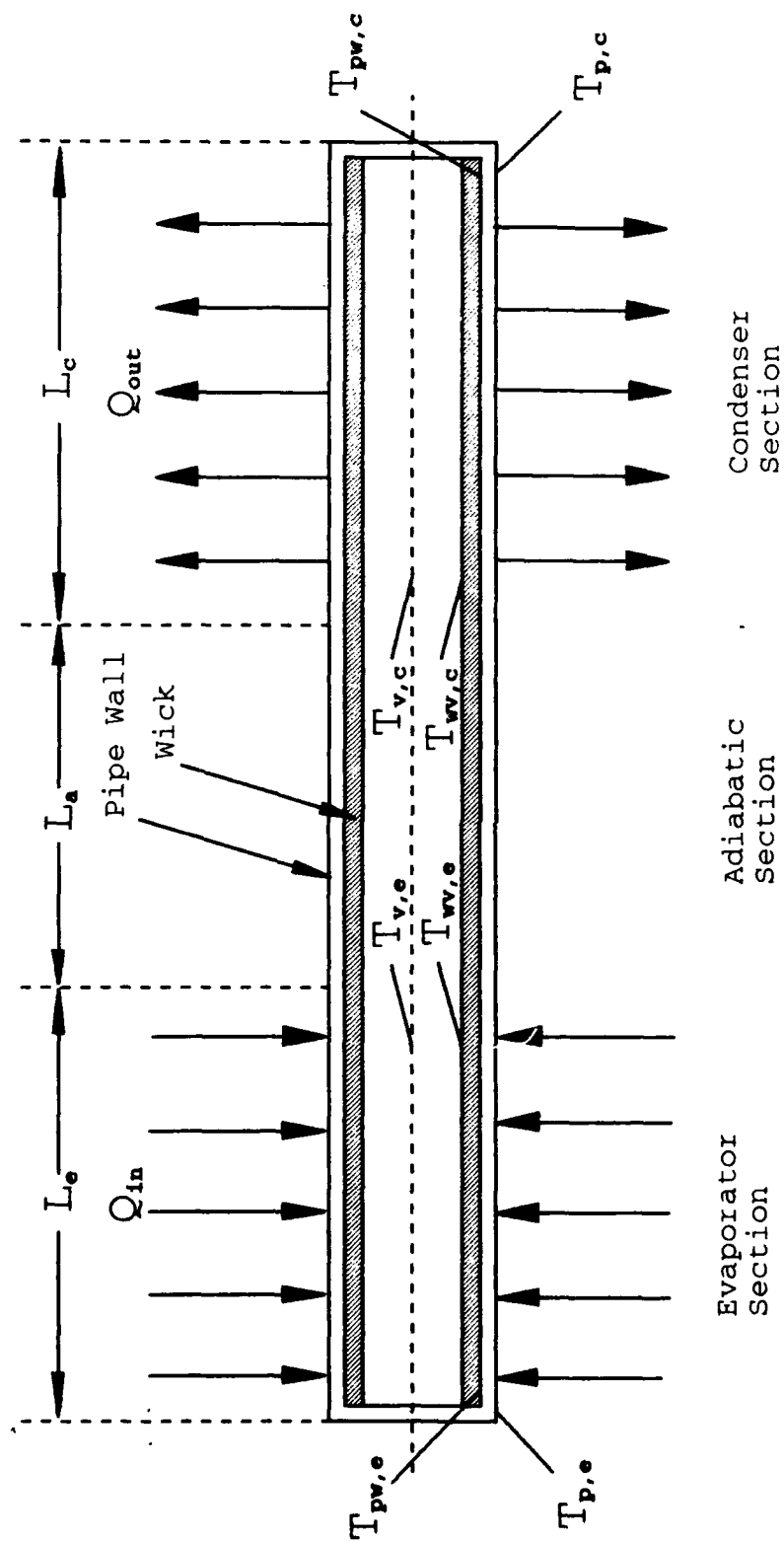


Figure 2.1 Heat Flow Path Through a Heat Pipe (1:70)



- $T_{pw,e}$  = temperature of pipe-wick interface in evaporator section (K)  
 $r_o$  = outside radius of pipe (m)  
 $k_p$  = thermal conductivity of pipe material [W/(m-K)]

Next, calculate the temperature drop across the saturated wick in the evaporator section

$$T_{p,e} - T_{wv,e} = \frac{Q \ln\left(\frac{r_i}{r_v}\right)}{2\pi L_e k_{e,e}} \quad (2.15)$$

where

- $T_{wv,e}$  = temperature at wick-vapor interface in evaporator section (K)  
 $k_{e,e}$  = effective thermal conductivity of liquid saturated wick at evaporator (W/m-K)

For a tightly wrapped screen wick, the effective thermal conductivity,  $k_{e,e}$ , can be calculated using (1:50)

$$k_{e,e} = \frac{k_l [(k_l + k_w) - (1-\epsilon)(k_l - k_w)]}{[(k_l + k_w) + (1-\epsilon)(k_l - k_w)]} \quad (2.16)$$

where

- $k_l$  = thermal conductivity of liquid (W/m-K)  
 $k_w$  = thermal conductivity of wick material (W/m-K)

Wick porosity for a tightly wrapped screen wick may be calculated using Eq (2.9). Again, it is assumed that the temperature drop from the wick-vapor interface to the vapor in the evaporator section is small relative to the conduction terms. This assumption yields

$$T_{wv,e} - T_{v,e} = 0 \quad (2.17)$$

where

$T_{v,e}$  = temperature of vapor in evaporator section  
(K)

It is also assumed that the temperature drop during the passage of vapor from the evaporator to the condenser is small, therefore

$$T_{v,e} - T_{v,c} = 0 \quad (2.18)$$

where

$T_{v,c}$  = temperature of vapor at condenser (K)

Similar to the assumption leading to Eq (2.17), the temperature drop from the vapor in the condenser section to the wick-vapor interface is assumed to be small resulting in

$$T_{v,c} - T_{wv,c} = 0 \quad (2.19)$$

where

$T_{wv,c}$  = temperature at wick-vapor interface at condenser (K)

Next calculate the temperature drop through the liquid saturated wick at the condenser end of the pipe

$$T_{wv,c} - T_{pw,c} = \frac{Q \ln\left(\frac{r_i}{r_v}\right)}{2\pi L_c k_{e,c}} \quad (2.20)$$

where

- $T_{pw,c}$  = condenser temperature at pipe-wick interface (K)  
 $k_{e,c}$  = effective thermal conductivity of liquid saturated wick at condenser

Since the wick material and working fluid are identical at the condenser and evaporator,  $k_{e,c}$  is equal to  $k_{e,e}$  and can be found using Eq (2.16). Finally, the temperature drop across the pipe wall in the condenser section is found using

$$T_{pw,c} - T_{p,c} = \frac{Q \ln\left(\frac{r_o}{r_i}\right)}{2\pi L_c k_p} \quad (2.21)$$

where

- $T_{p,c}$  = condenser pipe wall temperature (K)

Now, each of these contributions may be summed to yield the total temperature drop across the heat pipe

$$\begin{aligned} T_{p,e} - T_{p,c} = & (T_{p,e} - T_{pw,e}) + (T_{pw,e} - T_{wv,e}) + (T_{wv,e} - T_{v,e}) \\ & + (T_{v,e} - T_{v,c}) + (T_{v,c} - T_{wv,c}) \\ & + (T_{wv,c} - T_{pw,c}) + (T_{pw,c} - T_{p,c}) \end{aligned} \quad (2.22)$$

#### *Temperature Gradient Along Evaporator Section Assuming Pure Conduction*

In contrast to the preceding section, the opposite situation may be evaluated where the evaporator has completely dried out. In this case the only significant heat transfer mechanism is pure conduction down the wall of

the pipe. The temperature gradient may be calculated as a function of distance from the end of the pipe. This information is useful as a second means of determining whether or not the pipe is operating in the heat pipe mode, or if it has reached one of the limits. To simplify this analysis several assumptions are made. First, that the heat transfer is one-dimensional down the longitudinal axis of the pipe. Second, assume uniform heat flux throughout the heater section, in other words uniform heating. These assumptions have a varying degree of validity depending upon the construction of the pipe, and the type of heater used. Figure 2.2 is a graphical depiction of a section of a simple heat pipe and the heat transfer mechanisms at work in this situation. Considering the assumptions above, an energy rate balance can be defined

$$\dot{E}_{in} + \dot{E}_g - \dot{E}_{out} = \dot{E}_{st} \quad (2.23)$$

where

- $\dot{E}_{in}$  = rate of energy transfer into evaporator (W)
- $\dot{E}_g$  = rate of energy generation within evaporator (W)
- $\dot{E}_{out}$  = rate of energy transfer out of evaporator (W)
- $\dot{E}_{st}$  = rate of energy storage within evaporator (W)

Assuming there is no energy storage or generation within the heat pipe, the above equation reduces to

$$\dot{E}_{in} = \dot{E}_{out} \quad (2.24)$$

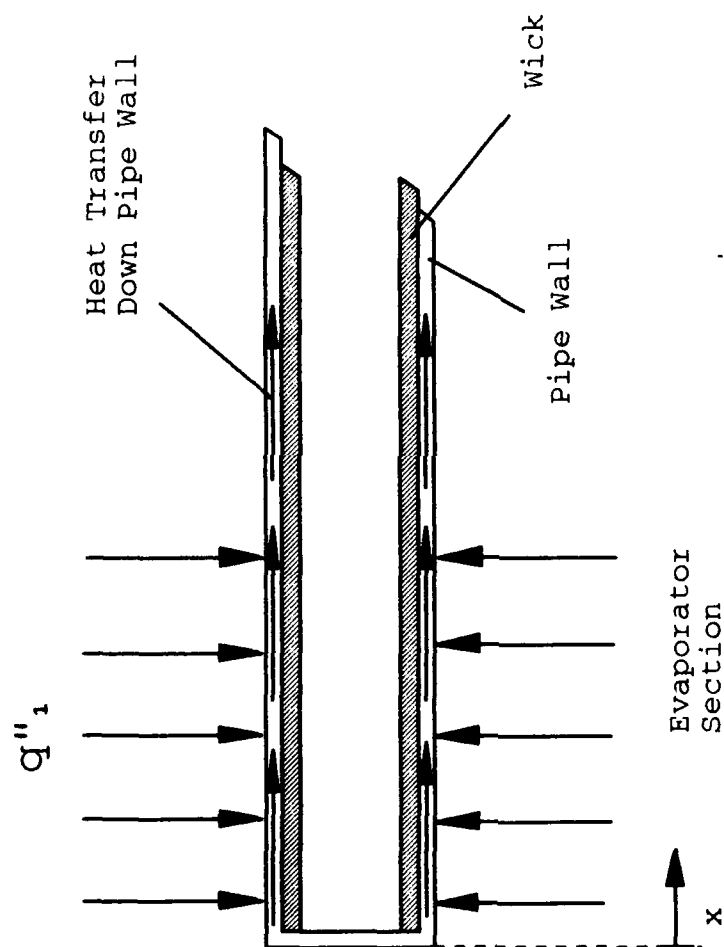


Figure 2.2 Heat Flow Path During Pure Conduction

A cylindrical control volume may be defined which encompasses the surface of the evaporator section that is in contact with the heater. One end of the cylindrical control volume coincides with the evaporator end of the pipe, and the other end is located at a distance  $x$  measured from the evaporator end of the pipe as depicted in Figure 2.2. The rate of energy transfer into this volume is calculated to be

$$\dot{E}_{in} = q''_1 A_s \quad (2.25)$$

where

$$\begin{aligned} q''_1 &= \text{power density of the heater (W/m}^2\text{)} \\ A_s &= \text{surface area in contact with heater (m}^2\text{)} \end{aligned}$$

This surface area may be calculated as

$$A_s = 2\pi r_o x \quad (2.26)$$

where

$$x = \text{distance from evaporator end of pipe (m)}$$

Substitution of Eq (2.26) into Eq (2.25) yields

$$\dot{E}_{in} = 2q''_1 \pi r_o x \quad (2.27)$$

In a state of pure conduction, all the energy entering the pipe will travel down the pipe wall. Therefore, all energy entering the control volume will exit the volume through the cross sectional area of the pipe wall at distance  $x$  from the

evaporator end. The energy transfer out of the control volume may be calculated using

$$\dot{E}_{out} = q''_2 A_c \quad (2.28)$$

where

$$\begin{aligned} q''_2 &= \text{conduction heat flux down pipe wall (W/m}^2\text{)} \\ A_c &= \text{cross-sectional area of pipe wall (m}^2\text{)} \end{aligned}$$

The heat flux due to one-dimensional conduction can be calculated using Fourier's equation

$$q''_2 = -k \frac{\partial T}{\partial x} \quad (2.29)$$

where

$$T = \text{pipe wall temperature at location } x \text{ (K)}$$

The cross-sectional area of the pipe is found using

$$A_c = \frac{\pi}{4} (d_o^2 - d_i^2) \quad (2.30)$$

where

$$\begin{aligned} d_i &= \text{inner pipe diameter (m)} \\ d_o &= \text{outer pipe diameter (m)} \end{aligned}$$

Equations (2.29) and (2.30) may now be substituted into Eq (2.28) to get the expression

$$\dot{E}_{out} = -k \frac{\partial T}{\partial x} \left( \frac{\pi}{4} \right) (d_o^2 - d_i^2) \quad (2.31)$$

Now substituting Eqs (2.27) and (2.31) into Eq (2.24) and solving for  $\partial T/\partial x$  yields an expression for the change in pipe wall temperature with change in distance from the evaporator end of the pipe. This expression is

$$\frac{\partial T}{\partial x} = - \frac{4q''_1 d_o x}{k(d_o^2 - d_i^2)} \quad (2.32)$$

where

$\partial T/\partial x$  = change in pipe wall temperature with change in distance from the evaporator end of the pipe (K/m)

From the preceding section, it is clear that a heat pipe operating in heat pipe mode will have a temperature drop of only a few degrees along the entire length of the pipe. Equation (2.32) reveals that the temperature gradient along the pipe wall will be large once the pipe begins to operate in a pure conduction mode. An observation of this gradient should, therefore, be a key piece of data in determining when the evaporator section has dried out and the pipe is no longer operating in the heat pipe mode.

#### *Temperature Gradient Along Adiabatic Section Assuming Pure Conduction*

This final section deals with the calculation of the pipe wall temperature gradient in the adiabatic section assuming that the evaporator is completely dried out and pure one-dimensional conduction down the pipe wall is the



only heat transfer mechanism at work. This is a necessary calculation due to the fact that an imperfect heater will not provide uniform heat flux throughout the evaporator section. As a result, the temperature gradient found in the previous section may be hard to observe depending on the instrumentation used in the experiment. For the adiabatic section the calculation is similar to that done for the heater section, only now the heat flux into the pipe is based on the entire surface area of the evaporator, a constant. The basic equation is again Eq (2.24),  $\dot{E}_{in} = \dot{E}_{out}$ . A similar development to that in the last section uses a cylindrical control volume which encloses the entire evaporator section of the pipe. The energy transfer rate into the control volume is calculated using the evaporator section length,  $L_e$ , in the determination of the surface area in contact with the heater. The calculation of the energy transfer out of the control volume again uses the cross-sectional area of the pipe wall, only in this case the area is determined at  $x = L_e$ . Solving for the change in heat pipe wall temperature with change in distance from the evaporator end of the pipe yields

$$\frac{\partial T}{\partial x} = -\frac{q}{kA_c} \quad (2.33)$$

where

$q$  = heat transfer rate into evaporator (W)

The cross-sectional area is computed using Eq (2.30).

This expression is valid for locations along the adiabatic section of the pipe. As was determined for the evaporator section, Eq (2.33) indicates a large temperature gradient along the adiabatic section pipe wall once the pipe is operating in a pure conduction mode. This large gradient should be easy to observe relative to the smaller temperature drop associated with operation in the heat pipe mode. It can be used as an indication that the evaporator section has dried out and the pipe is no longer operating in heat pipe mode.

### *III. Experiment Design*

In order to achieve the objective of this thesis, it was first necessary to design an experiment that would allow the collection of pertinent data which could later be used to draw a meaningful conclusion. The following sections describe the hardware, data acquisition system, and the test procedure used in the experiment.

#### *Heat Pipe Design*

Non-hazardous materials were used in the heat pipe design to simplify construction and subsequent experimentation. In addition to this criteria, cost, availability, and workability of materials were prime considerations. Taking these factors into account the following design was developed.

*Operating Conditions.* The first step in the design process was the choice of the desired pipe operating conditions. The heat pipe was designed to operate at moderate temperatures so as not to require special equipment or materials such as those necessary for pipes using liquid metal or cryogenic liquids for working fluids. This simplified the task somewhat by allowing the use of standard materials and easily implemented heating and cooling techniques. The heat pipe was designed for an operating temperature of 100° C and a maximum heat transport capability of at least 100 W.

*Physical Dimensions.* The next step was choosing the physical dimensions of the heat pipe. A consideration here was the ability to mount the heat pipe to the shaker system used for vibration input. The dimensions had to physically allow for mounting on the shaker while providing the rigidity and structural integrity required for the testing. The shaker was limited with respect to the mass that it could drive to the desired vibration level, and this was a factor in sizing the pipe. Workability and ease of instrumentation were also considered. Finally, and most importantly, the pipe dimensions had to be adequate to support the objective of the experiment. That is, the size of the pipe had to allow for proper operation and the collection of pertinent data. After weighing all the above considerations, and reviewing the heat pipe designs used in similar experiments, a heat pipe working length of  $L_w = 3.048 \times 10^{-1} \text{ m}$  (12 in) was chosen. The pipe had an evaporator length of  $L_e = 1.016 \times 10^{-1} \text{ m}$  (4 in), an adiabatic length of  $L_a = 9.208 \times 10^{-2} \text{ m}$  (3.625 in), and a condenser length of  $L_c = 1.111 \times 10^{-1} \text{ m}$  (4.375 in). The outside diameter of the pipe was  $d_o = 2.223 \times 10^{-2} \text{ m}$  (0.875 in) with an inside diameter of  $d_i = 1.892 \times 10^{-2} \text{ m}$  (0.745 in). The endcaps were machined to a minimum wall thickness of  $3.175 \times 10^{-3} \text{ m}$  (0.125 in). These dimensions are illustrated in Figure 3.1 and the mechanical integrity of the design is examined in the following sections.

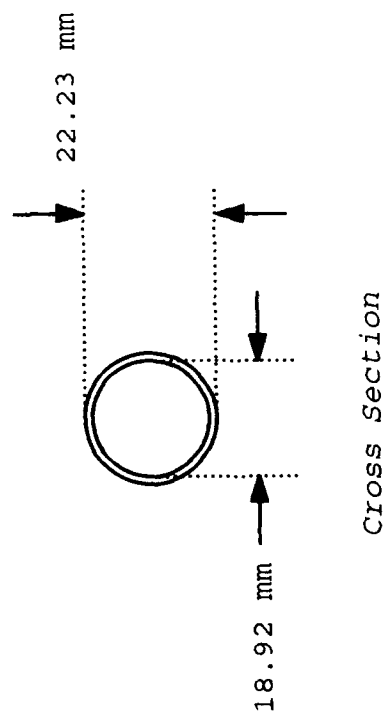
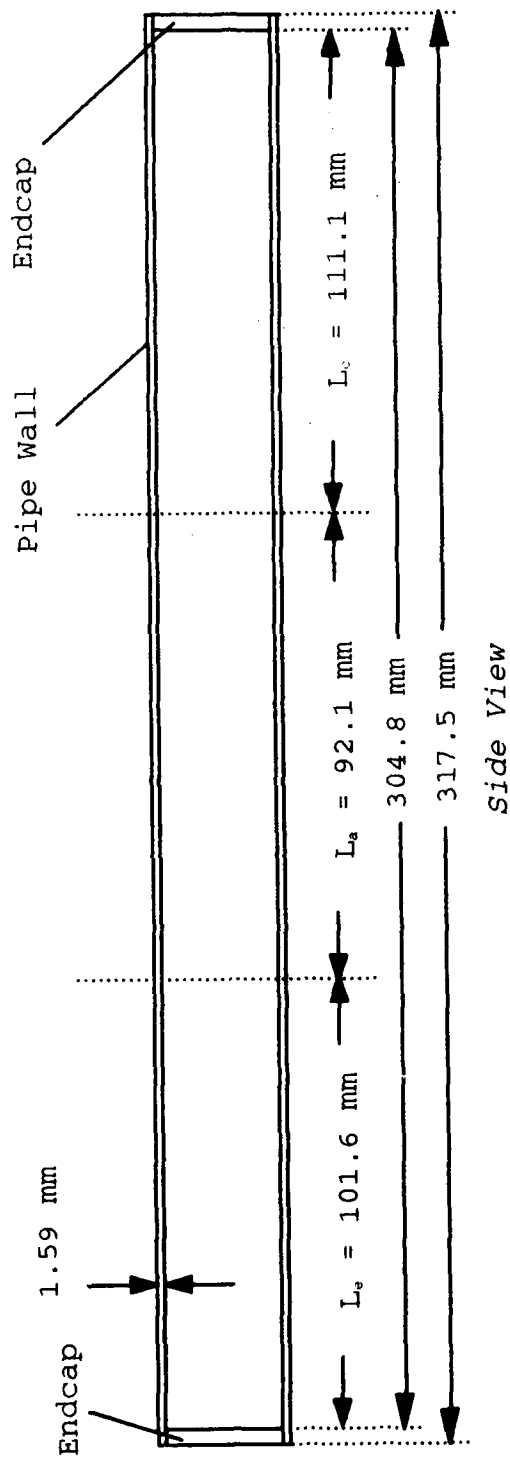


Figure 3.1 Heat Pipe Container Dimensions

*Choice of Structural Material.* Oxygen-free hard copper was chosen as the structural material for the pipe wall and the end caps. This material provides a higher tensile strength than soft copper and, since it is oxygen-free, has the added advantage of minimizing the contamination due to outgassing. In addition, it is readily available, can be machined and, while it is more expensive than soft copper, it is reasonably priced. Standard copper has an ultimate tensile strength (UTS) of approximately  $1.5 \times 10^8$  N/m<sup>2</sup> at 100° C (1:231). The UTS for oxygen-free hard copper is  $2.8 \times 10^8$  N/m<sup>2</sup> at 20° C and approximately  $2.4 \times 10^8$  N/m<sup>2</sup> at 100° C. As a conservative measure, the UTS for standard copper was used.

*Choice of Operating Fluid.* The choice of an operating fluid took into account the desired operating conditions and the pipe material. The fluid chosen had to be both compatible with copper, and have a useful temperature range that encompassed the design operating temperature of 100° C. There are a number of prospective fluids that can be used at this temperature, but few satisfy the material compatibility concerns and also satisfy the general criteria for this design. For instance, water, methanol, and acetone all cover this temperature range, but of the three, only water meets the other criteria (4:89). Methanol and acetone are difficult to work with, and can be considered hazardous under certain conditions. Water satisfies all the criteria, and has been proven compatible with copper through testing

and past usage (1:164). Therefore deionized, demineralized water was selected as the working fluid.

*Wick Design.* The design of the wick for this pipe was driven by the objective of the thesis, material compatibility, ease of manufacture, and the design operating conditions. By virtue of the thesis objective, a wrapped screen wick was chosen. Copper was used for the wick material so that there would be no compatibility concerns with the working fluid or the pipe material. Due to its use in similar experiments and its availability, 100 mesh copper screen was chosen as a candidate. This screen has 3937 wires/meter (100 wires/in) and a measured wire diameter of  $d = 1.067 \times 10^{-4} \text{ m}$  (.0042 in). The screen thickness ( $t_w$ ) was measured to be  $2.54 \times 10^{-4} \text{ m}$  (.010 in).

The next step in the development of the wick design was the evaluation of the wicking ability of the 100 mesh screen. This evaluation was based on the capillary pumping ability required to overcome a hydrostatic pressure that was determined using (1:183)

$$P_g = \rho_l g (d_i \cos \psi + L_t \sin \psi) \quad (3.1)$$

where

$$P_g = \text{hydrostatic pressure (N/m}^2\text{)}$$

From Table A.1, which is a subset of the thermophysical properties of saturated water located in Appendix A, at 100° C  $\rho_l = 9.5785 \times 10^2 \text{ kg/m}^3$ . Substituting this and the pipe

dimensions into Eq (3.1), and using a pipe inclination of  $\psi = 0^\circ$  yields a hydrostatic pressure of  $P_g = 1.780 \times 10^2 \text{ N/m}^2$  that had to be overcome by the capillary pumping ability of the wick. As a rule of thumb, the wick capillary pressure should be greater than or equal to twice the hydrostatic pressure as calculated above (1:183). The capillary pressure was determined using

$$P_c = \frac{2\sigma}{r_c} \quad (3.2)$$

where

$$P_c = \text{capillary pressure (N/m}^2\text{)}$$

For 100 mesh screen,  $N = 3.937 \times 10^3 \text{ m}^{-1}$ , and the effective capillary radius was found by solving Eq (2.6) to get  $r_c = 1.270 \times 10^{-4} \text{ m}$ . From Table A.1,  $\sigma = 5.890 \times 10^{-2} \text{ N/m}$  and Eq (3.2) was used to find the capillary pressure,  $P_c = 9.276 \times 10^2 \text{ N/m}^2$ . With a  $P_c \approx 5P_g$ , this choice of wick material was confirmed to have more than adequate capillary pressure.

Proceeding with the wick design, an iterative process was used to determine the actual number of screen wraps required to meet the design heat transport capability of 100 W. This involved assuming a number of wraps, and thereby a wick thickness, and using this assumed wick thickness to calculate the capillary limited heat transport factor. A slightly altered form of Eq (2.5) was used to calculate this factor (1:183)



$$(QL)_{c,max} = \frac{P_c - P_g}{F_v + F_l} \quad (3.3)$$

Having already determined  $P_c$  and  $P_g$ ,  $F_l$  and  $F_v$  remained to be solved for. Before these could be calculated however, the wick porosity and its permeability were determined using Eqs (2.8) and (2.9). The wick porosity was found to be  $\epsilon = 6.536 \times 10^{-1}$  and the permeability was  $K = 2.171 \times 10^{-10} \text{ m}^2$ . For an assumed number of screen wraps, the cross-sectional area of the wick could be calculated using

$$A_w = \frac{\pi}{4} (d_i^2 - d_v^2) \quad (3.4)$$

where

$d_v$  = vapor core diameter (m)

As the final step in this iterative process, a wick consisting of two screen wraps was evaluated. In this case the wick thickness was twice the screen thickness, and was determined to be  $t_w = 5.080 \times 10^{-4} \text{ m}$ . The vapor core diameter was found by subtracting twice the wick thickness from the inner diameter of the pipe. This calculation assumes the tightly wrapped screen does not have any space between it and the pipe wall or between the screen wraps. The vapor core diameter was calculated to be  $d_v = 1.788 \times 10^{-2} \text{ m}$ . Substituting into Eq (3.4) gave a wick cross-sectional area of  $A_w = 2.946 \times 10^{-5} \text{ m}^2$ . Looking up the remaining thermophysical properties in Table A.1, the liquid

frictional coefficient was calculated using Eq (2.7) and found to be  $F_1 = 2.018 \times 10^1 [(N/m^2)/(W-m)]$ . Likewise, the vapor frictional coefficient was found to be  $F_v = 3.564 \times 10^{-3} [(N/m^2)/(W-m)]$  using Eq (2.10). At this point, with all the pieces in hand, the heat transport factor could be calculated using Eq (3.1) and was found to be  $(QL)_{c,max} = 3.714 \times 10^1 W-m$ . The final step in the evaluation of this choice of wick material and the number of screen wraps was the solution of Eq (2.11) for the capillary limited heat transport rate. This rate was found to be  $Q_{c,max} = 1.871 \times 10^2 W$ , which well exceeded the minimum design criteria of 100 W. Therefore, the wick was designed to be two wraps of 100 mesh copper screen and to have a length equal to that of the total pipe operating length,  $L_t$ .

*Analysis of Material Properties Versus Stress.* Now that the dimensions and material of the pipe itself had been determined, as well as the design of the wick, an analysis of the pipe material properties versus expected stresses was accomplished to insure adequate strength of the pipe wall and endcaps during operation. This evaluation looked primarily at the stress in the pipe wall and end caps due to pressurization of the pipe during heating. The concern being that the ultimate tensile strength (UTS) of the copper would be exceeded and the pipe would leak or burst when operating at an elevated temperature. This analysis uses the UTS of standard copper as a conservative measure. As stated earlier, this value is  $UTS = 1.5 \times 10^8 N/m^2$  at  $100^\circ$

C. The maximum hoop stress in the pipe wall ( $f_{max}$ ) can be determined using (1:172)

$$f_{max} = \frac{Pd_o}{2t} \quad (3.5)$$

where

$$\begin{aligned} f_{max} &= \text{maximum hoop stress in pipe wall (N/m}^2\text{)} \\ P &= \text{pressure differential across wall (N/m}^2\text{)} \\ t &= \text{pipe wall thickness (m)} \end{aligned}$$

The maximum stress in a flat circular endcap equals (1:173)

$$f_{max} = \frac{Pd_o^2}{8t^2} \quad (3.6)$$

where

$$\begin{aligned} f_{max} &= \text{maximum stress in flat circular endcap (N/m}^2\text{)} \\ P &= \text{pressure differential across endcap (N/m}^2\text{)} \\ d_o &= \text{endcap diameter (m)} \\ t &= \text{end cap thickness (m)} \end{aligned}$$

In both of these expressions, the pressure differential can be approximated by the vapor pressure of working fluid since it is typically much larger than the ambient pressure (1:173). With the chosen pipe dimensions, the pipe wall thickness is  $1.651 \times 10^{-3}$  m and the pipe outer diameter is  $d_o = 2.223 \times 10^{-2}$  m. The vapor pressure of water at  $100^\circ$  C is  $P = 1.0133 \times 10^5$  N/m<sup>2</sup> (5:A22). Substituting these values into Eq (3.5) yields a maximum hoop stress of  $f_{max} = 6.822 \times 10^5$  N/m<sup>2</sup>. According to Chi, heat pipe containers are typically designed in accordance with the American Society of Mechanical Engineers (ASME) code which "specifies that the maximum allowable stress at any temperature be one-

quarter of the material's ultimate tensile strength at that temperature" (1:172). It is clear that this pipe design is well within this standard. Next the endcaps are evaluated using Eq (3.6). The endcap thickness is  $t = 3.175 \times 10^{-3}$  m, the endcap diameter is taken to be equal to the inside diameter of the pipe or  $1.892 \times 10^{-2}$  m. These values may be substituted along with the vapor pressure into Eq (3.6) to get a maximum stress in the cap of  $f_{max} = 4.498 \times 10^5$  N/m<sup>2</sup>. This is once again well within the one-quarter of UTS criteria. Therefore, both the wall thickness and the endcap thickness chosen should be more than adequate for the vapor pressures at temperatures near the expected pipe operating temperature.

Evaluating both the maximum allowable hoop stress for the pipe wall and the maximum allowable stress for the endcaps, the maximum allowable operating temperature was calculated to be approximately 250° C. With anticipated pipe operating temperatures below 100° C, the design was considered very conservative from a material strength standpoint. This is especially true given the fact that the maximum stress experienced at this temperature is only 25% of the ultimate tensile strength of the material at this temperature.

*Predicted Sonic Limit.* The previous sections describe the preliminary design of the pipe. Given the physical dimensions and the wick design chosen, the other heat pipe limits had to be predicted to determine which would be the

limiting factor to the overall heat pipe performance. The predicted sonic limit of the pipe was calculated using Eq (2.1). For this heat pipe  $A_v = 2.511 \times 10^{-4} \text{ m}^2$ . At  $100^\circ \text{ C}$ , the vapor density is  $\rho_v = 5.956 \times 10^{-1} \text{ kg/m}^3$ ,  $\lambda = 2.257 \times 10^6 \text{ J/kg}$ , and  $T_v = 373.15 \text{ K}$ . For water,  $R_v = 462 \text{ J/(kg-K)}$ , and the vapor specific heat ratio is  $4/3$  (1:86). Substituting these values into Eq (2.1) yields a sonic limited heat transport rate of  $Q_{s,max} = 7.491 \times 10^4 \text{ W}$ . This limit was clearly much higher than the capillary limit calculated for the wick in the previous section, and therefore was not expected to be a concern.

*Predicted Entrainment Limit.* The next limitation evaluated for this pipe was the entrainment limit. This was calculated using Eq (2.2). The cross-sectional area of the vapor core for this pipe is  $A_v = 2.511 \times 10^{-4} \text{ m}^2$ , and the surface pore hydraulic radius was calculated using a modified form of Eq (2.3)

$$r_{h,s} = \frac{1}{2N} - \frac{d}{2} \quad (3.7)$$

With  $N = 3.937 \times 10^3 \text{ m}^{-1}$  and  $d = 1.067 \times 10^{-4} \text{ m}$ , this radius was calculated to be  $7.365 \times 10^{-5} \text{ m}$ . From Table A.1,  $\rho_v = 5.956 \times 10^{-1} \text{ kg/m}^3$ ,  $\lambda = 2.257 \times 10^6 \text{ J/kg}$ , and  $\sigma = 5.890 \times 10^{-2} \text{ N/m}$ . Substituting these values into Eq (2.2) yields the entrainment limited maximum heat transport rate of  $Q_{e,max} = 8.746 \times 10^3 \text{ W}$ . Like the sonic limit, this value was much

less restrictive than the capillary limit, and was not expected to impact the performance of the pipe.

*Predicted Boiling Limit.* The boiling limited heat transfer rate was calculated using Eq (2.4). For this design,  $L_e = 1.016 \times 10^{-1} \text{ m}$ ,  $r_i = 9.462 \times 10^{-3} \text{ m}$ , and  $r_v = 8.954 \times 10^{-3} \text{ m}$ . In a conventional heat pipe, the critical radius of nucleation is typically  $2.540 \times 10^{-7} \text{ m}$  (1:92). From Table A.1,  $\rho_v = 5.956 \times 10^{-1} \text{ kg/m}^3$ ,  $\lambda = 2.257 \times 10^6 \text{ J/kg}$ , and  $\sigma = 5.890 \times 10^{-2} \text{ N/m}$  at this operating temperature. The vapor temperature is assumed to be equal to the design operating temperature or  $T_v = 373.15 \text{ K}$ . The next variable,  $k_s$ , was calculated using Eq (2.16). At  $100^\circ \text{ C}$ ,  $k_1 = 6.800 \times 10^{-1} \text{ W/(m-K)}$  (5:A22) and  $k_w = 400 \text{ W/(m-K)}$  (5:A3). The wick porosity was found to be  $\epsilon = 6.536 \times 10^{-1}$  using Eq (2.9). Substituting these values into Eq (2.16) yields  $k_s = 1.397 \text{ W/(m-K)}$ . The capillary pressure was calculated to be  $9.276 \times 10^2 \text{ N/m}^2$  using Eq (3.2). Next, the boiling limited heat transfer rate could be calculated by substituting all of these values into Eq (2.4) to get  $Q_{b,max} = 2.076 \times 10^3 \text{ W}$ . This limit was well above the capillary limited heat transport and therefore was not expected to limit the pipe performance.

*Predicted Capillary Limit.* It was clear after evaluating the wick design and the other predicted limits that the capillary limit would be the most restrictive and would bound the performance of this pipe. Therefore the

design was determined to be adequate to satisfy the objective of the experiment.

Once this was determined, a series of calculations were done to build a curve of predicted maximum capillary limited heat transfer rates as a function of pipe operating temperature ( $T_{op}$ ). The calculation to find these points is the same as that for the capillary limited heat transfer rate done in the analysis of the wick design. The thermophysical properties were changed for each calculation to reflect the operating temperature of interest. Since the capillary limit was the most restrictive limit for this pipe, this curve represents the theoretical maximum throughput of the pipe in terms of heat transfer rate, or power. Figure 3.2 is an illustration of the  $Q_{c,max}$  versus  $T_{op}$  curve.

#### *Heat Pipe Construction*

Once the specific heat pipe design was complete, the pipe had to be built. This included not only the construction of the heat pipe container, but the determination of the correct working fluid volume, and the filling of the pipe. The following sections describe this process.

*Manufacture of the Pipe.* The heat pipe was constructed of oxygen-free hard copper. It consisted of a section of pipe that was  $3.175 \times 10^{-1}$  m (12.50 in) in length to allow for a  $3.048 \times 10^{-1}$  m (12.00 in) total working length after

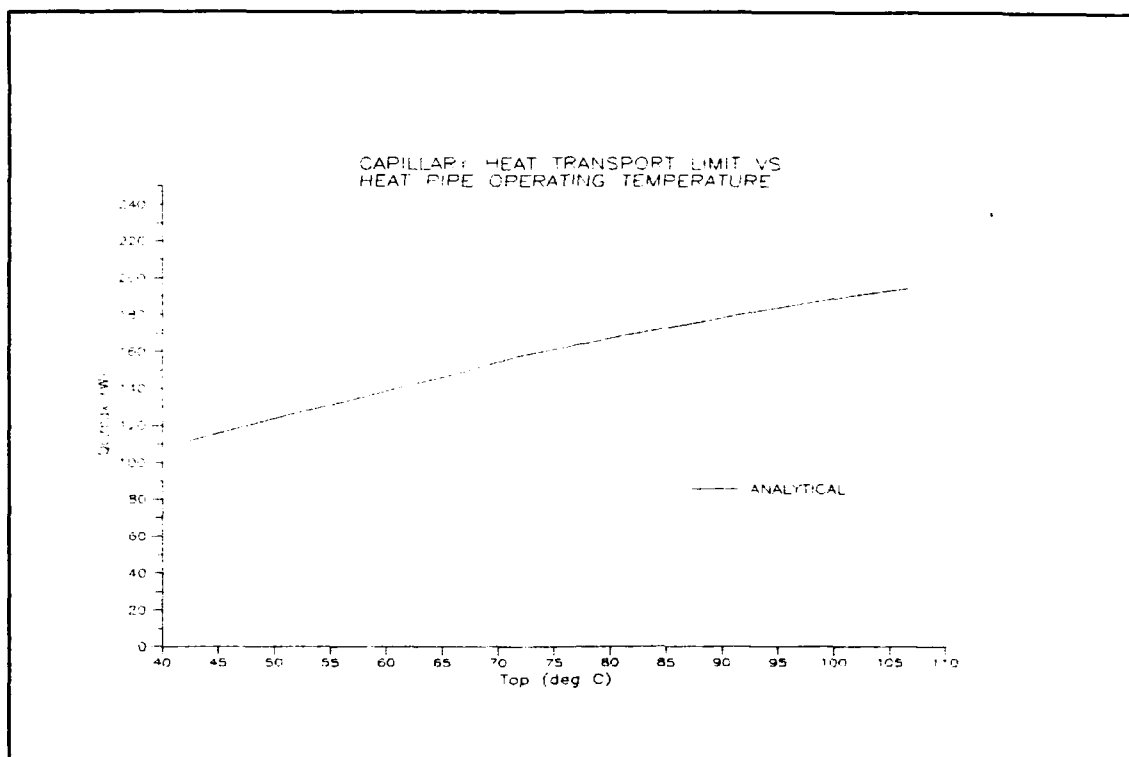


Figure 3.2 Analytical  $Q_{c,max}$  Versus  $T_{op}$

installation of the endcaps, each of which had a total depth of  $6.350 \times 10^{-3}$  m (0.25 in). The outside diameter of the pipe was  $d_o = 2.223 \times 10^{-2}$  m (.875 in) and the inside diameter was  $d_i = 1.892 \times 10^{-2}$  m (.745 in). The wall thickness was  $t = 1.651 \times 10^{-3}$  m (.065 in). It had a condenser section of length  $L_c = 1.111 \times 10^{-1}$  m, an adiabatic section of length  $L_a = 9.210 \times 10^{-2}$  m, and the evaporator section had length  $L_e = 1.016 \times 10^{-1}$  m. Figure 3.3 gives an illustration of the overall construction of the pipe.

The ends of the pipe were counterbored to a depth of  $6.350 \times 10^{-3}$  m to provide a step in the interior surface of the pipe for the endcaps to butt up against. The endcaps



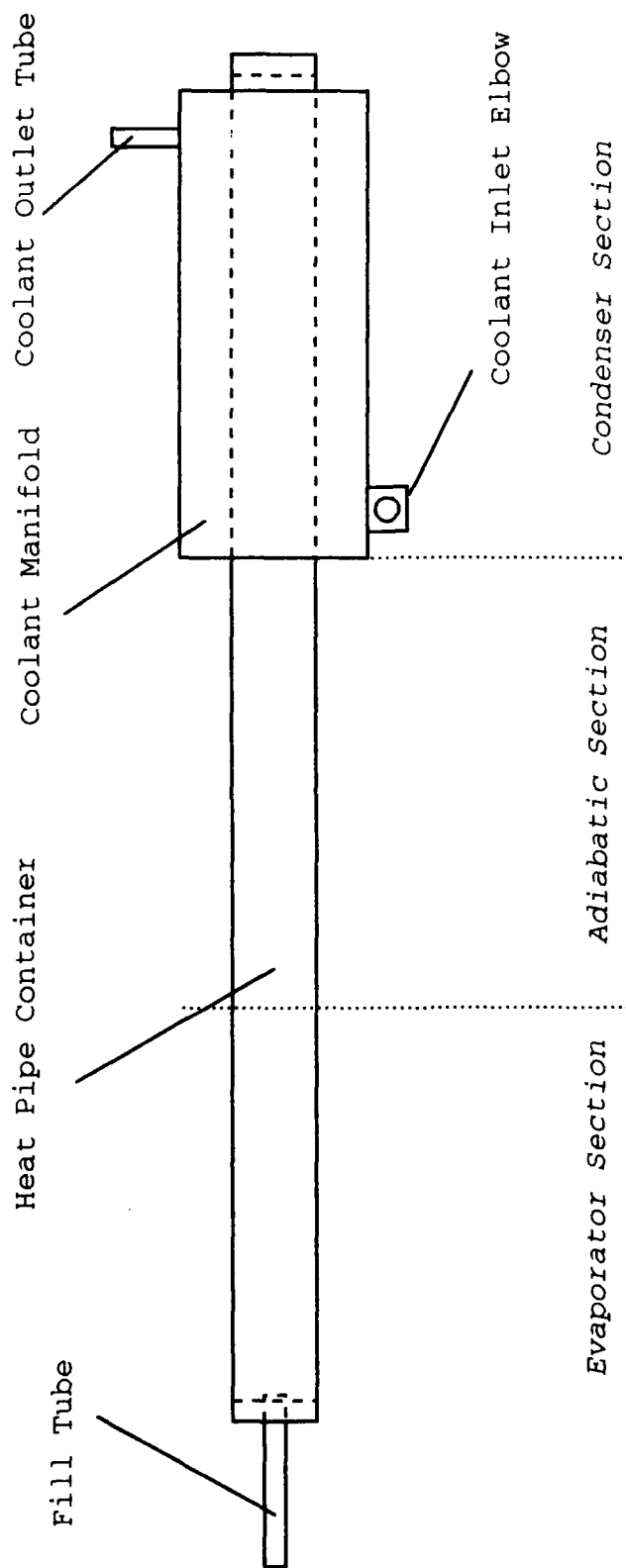
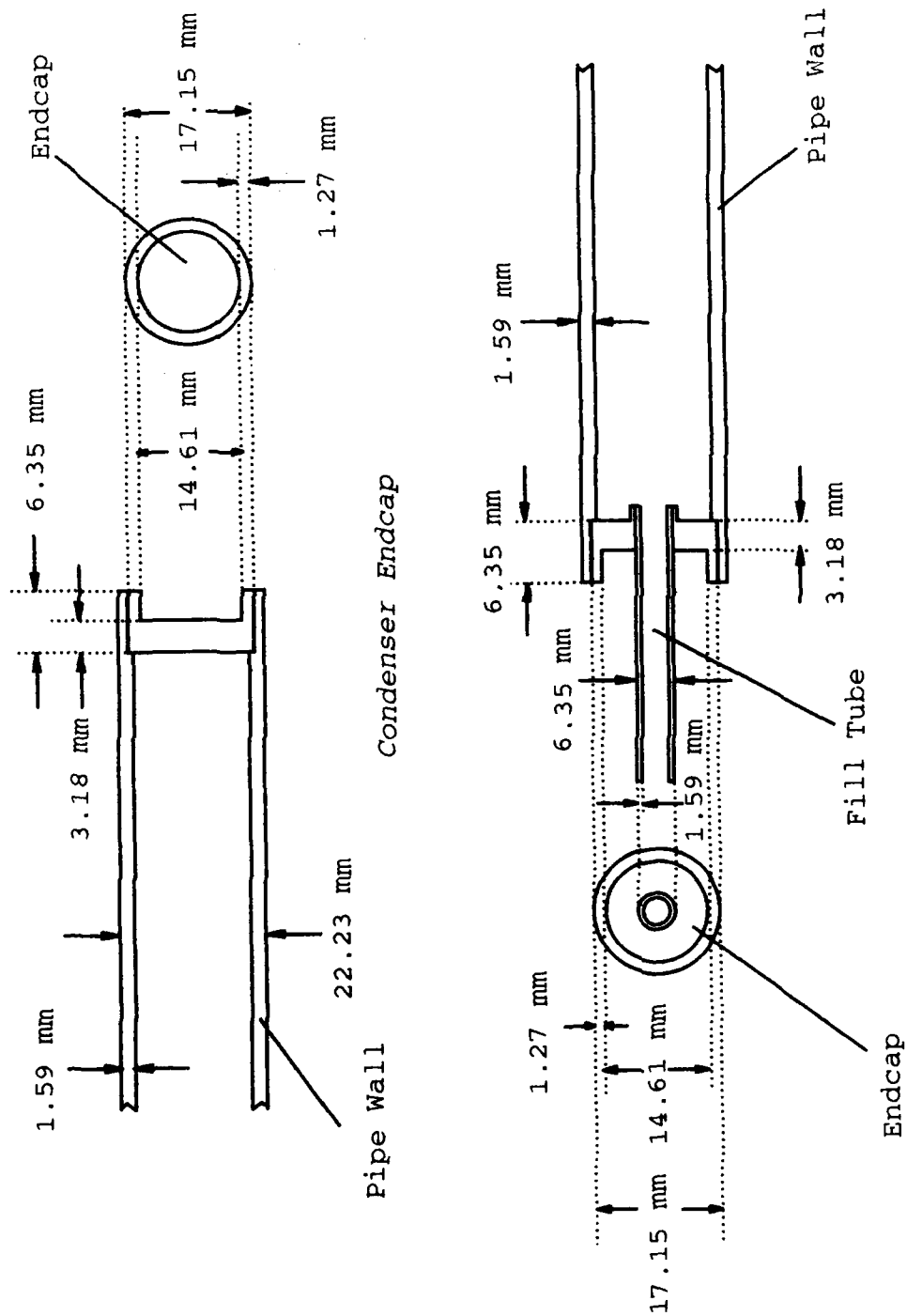


Figure 3.3 Experimental Heat Pipe

were  $1.715 \times 10^{-2}$  m in diameter and  $6.350 \times 10^{-3}$  m deep. The centers were machined to give a minimum endcap thickness of  $3.175 \times 10^{-3}$  m. The evaporator section endcap was center-drilled to accept a fill tube and had a raised lip on the inside surface to provide material to weld the fill tube in place. Figure 3.4 illustrates the endcap construction and dimensions. The fill tube was made of  $6.350 \times 10^{-3}$  m outside diameter copper tubing with a  $8.890 \times 10^{-4}$  m wall. A manifold was silver soldered to the pipe wall over the condenser section to allow coolant flow over the condenser. This manifold was constructed of copper pipe and was  $1.016 \times 10^{-1}$  m in length, had an outside diameter of  $4.122 \times 10^{-2}$  m, and a  $1.588 \times 10^{-3}$  m wall thickness. The ends of the manifold were machined from  $1.588 \times 10^{-3}$  m thick copper plate. The manifold pipe section was silver soldered to the manifold ends and they were in turn soldered to the heat pipe wall. The end of the manifold nearest the condenser end of the pipe was attached at a distance of  $1.175 \times 10^{-1}$  m from that end of the heat pipe. The part of the condenser that was not covered by the manifold allowed the mounting of a thermocouple on the pipe wall at a point not obstructed on the interior by the endcap. A 90° brass elbow was soldered into the manifold at the location shown in Figure 3.3 for coolant inlet and a straight coolant outlet tube was soldered in place at the other end of the manifold as shown.

Prior to the assembly of any portion of the pipe, all the copper parts were put through a stringent cleaning



Evaporator Endcap

Figure 3.4 Endcap Construction

process, and care was taken to make certain that the parts remained uncontaminated. Obviously, activities such as silver soldering are inherently contamination producing processes, and the parts needed to be recleaned following these activities. The parts were given a final cleaning before assembly and closing of the pipe.

The cleaning process consisted of a number of steps. First, the parts were given an acetone rinse to remove any oils on the surface, followed by an acid dip in a hydroxy-acetic/phosphoric acid solution to eliminate any oxidation of the surface. This acid dip was followed by a water rinse using deionized/demineralized water to wash away the residual acid. As a last step, the parts were immediately given a methanol rinse to help them dry quickly in order to minimize any new oxidation of the surface.

Following the initial cleaning of all the parts, the next step in the construction of the heat pipe was the insertion of the endcap at the condenser end. This was done in an argon atmosphere inside a dry box. The endcap was welded in place using tungsten inert gas (TIG) welding. This technique results in a clean weld, and a vacuum tight seal of the pipe end. The argon atmosphere provides an inert environment to prevent contamination of the material surface. The pipe was then removed from the dry box and the wick was installed.

The wick was constructed of 100 mesh copper screen. It had a length of  $3.048 \times 10^{-1}$  m and a width of  $1.191 \times 10^{-1}$  m

to allow for two complete wraps of screen and the extra that would be bent into a tang by the wrapping tool. The wick was wrapped using a two piece mandrel-type wrapping tool. The inner piece consisted of a solid center rod with a groove cut along its length. The outer piece was a section of pipe with an inside diameter equal to that of the heat pipe itself and with a slot cut along its length. The edge of the screen was threaded into the groove of the rod and then the rod was inserted into the slit pipe with the screen feeding through the slot. The center rod was then turned, pulling the screen through the slot and wrapping it tightly about the center rod. This device allowed the screen to be wrapped very tightly and at the correct radius of curvature so that it fit properly against the inner wall of the heat pipe. Once the entire length of screen was wound into the slit pipe, it was butted against the end of the heat pipe and the center rod was pushed into the heat pipe, pulling the wrapped screen with it. Once inserted into the heat pipe, the center rod was turned in the opposite direction to "back-wrap" the screen against the inside of the pipe, and to release the tool. Then the center rod was withdrawn, leaving the screen wound tightly against the interior surface of the heat pipe.

The final step in the construction of the heat pipe container was the installation of the evaporator end endcap. First, the fill tube was TIG welded into the endcap and then a vacuum valve was silver soldered to the other end of the

fill tube. This valve provided a means of temporarily closing the pipe to the environment once the endcap was installed. After cleaning the parts, they were put back into the dry box. Then the endcap was placed against the step of the counterbore and TIG welded in place with the fill tube and valve protruding from the end. The valve was now closed to prevent the ambient atmosphere from entering the pipe when it was removed from the dry box. This concluded the manufacture of the heat pipe container.

*Heat Pipe Working Fluid Inventory.* The working fluid inventory had to be calculated based on the dimensions of the heat pipe container and wick, as well as the anticipated operating conditions. The following equation was used to make this calculation (1:206)

$$m = A_v L_t \rho_v + A_w L_t \epsilon \rho_l \quad (3.8)$$

where

$m$  = fluid inventory mass (kg)

The working fluid mass was determined using  $A_v = 2.511 \times 10^{-4} \text{ m}^2$ ,  $L_t = 3.048 \times 10^{-1} \text{ m}$ ,  $A_w = 2.946 \times 10^{-5} \text{ m}^2$ , and a wick porosity of  $\epsilon = 6.536 \times 10^{-1}$ . From Table A.1,  $\rho_l = 9.579 \times 10^2 \text{ kg/m}^3$  and  $\rho_v = 5.956 \times 10^{-1} \text{ kg/m}^3$ . Substituting these values into Eq (3.8) yields a working fluid mass of  $m = 5.669 \times 10^{-3} \text{ kg}$  or  $m = 5.669 \text{ g}$ . According to Chi, this method of fluid inventory calculation results in a slight overfill of the pipe. This is due to the fact that this

method neglects the effect of meniscus recession occurring in the wick pores (1:206).

*Heat Pipe Fill Procedure and Apparatus.* Once the heat pipe container was built and the desired working fluid was determined, the pipe had to be filled. The first step in this process involved pulling a vacuum on the heat pipe container. This accomplished two principle objectives. First, it insured that the container was capable of holding the necessary vacuum and, second, it eliminated any remaining liquid and noncondensable gases that may have been left in the pipe during the manufacturing process. This included any gas that may have been impregnated into the surface of the copper while it was exposed to the ambient atmosphere. The fill tube of the heat pipe was attached to a vacuum pump and the pump was used to pull the atmosphere inside the pipe container down to a pressure of approximately  $1.3 \times 10^{-3} \text{ N/m}^2$  ( $1 \times 10^{-5} \text{ torr}$ ). To insure that the pipe was able to hold a vacuum, the valve on the fill tube was closed for a period of time, and then opened while observing the vacuum gauge. Any rise in the internal pressure of the pipe that occurred while the pipe was isolated from the pump indicated a leak, or that outgassing was still going on. This sequence of pumping the pipe atmosphere down and then checking the pressure over time was continued until no increase in pipe pressure was observed while the pipe was isolated from the pump. At this point it was assumed that the pipe was capable of holding a vacuum,

and that all but a negligible amount of the noncondensable gases and other contaminants had been evacuated from the container and wick. The pipe was now ready to be filled with the working fluid.

The filling apparatus was a system of valves, tubing, and fluid containers. Figure 3.5 is an illustration of this fill system. Prior to filling the heat pipe, it's empty mass was measured using a Metler balance. The heat pipe fill tube was hooked into the system, and the fill system, up to the valve on the pipe fill tube (A), was evacuated using a vacuum pump to remove any atmosphere. The valve to the vacuum pump (B) was then closed sealing the fill system with a vacuum inside. The beaker was filled with the deionized, demineralized water to be used as the working fluid. At this point the pipe was under vacuum with its valve (A) closed, and the fill system was under vacuum and sealed. The valve above the beaker (C) was then opened allowing fluid to enter the system and rise up in the pipette. The pipette would eventually be used to measure the volume of fluid entering the pipe from the fill system. Once an adequate volume of fluid had entered the system, the valve above the beaker (C) was closed. At this point the pipe was sealed and under vacuum, and the fill system was filled with fluid up to the pipe fill tube valve (A). The valve above the column of water in the pipette (D) was then opened to atmospheric pressure so that positive pressure would exist above the column of water during the filling of



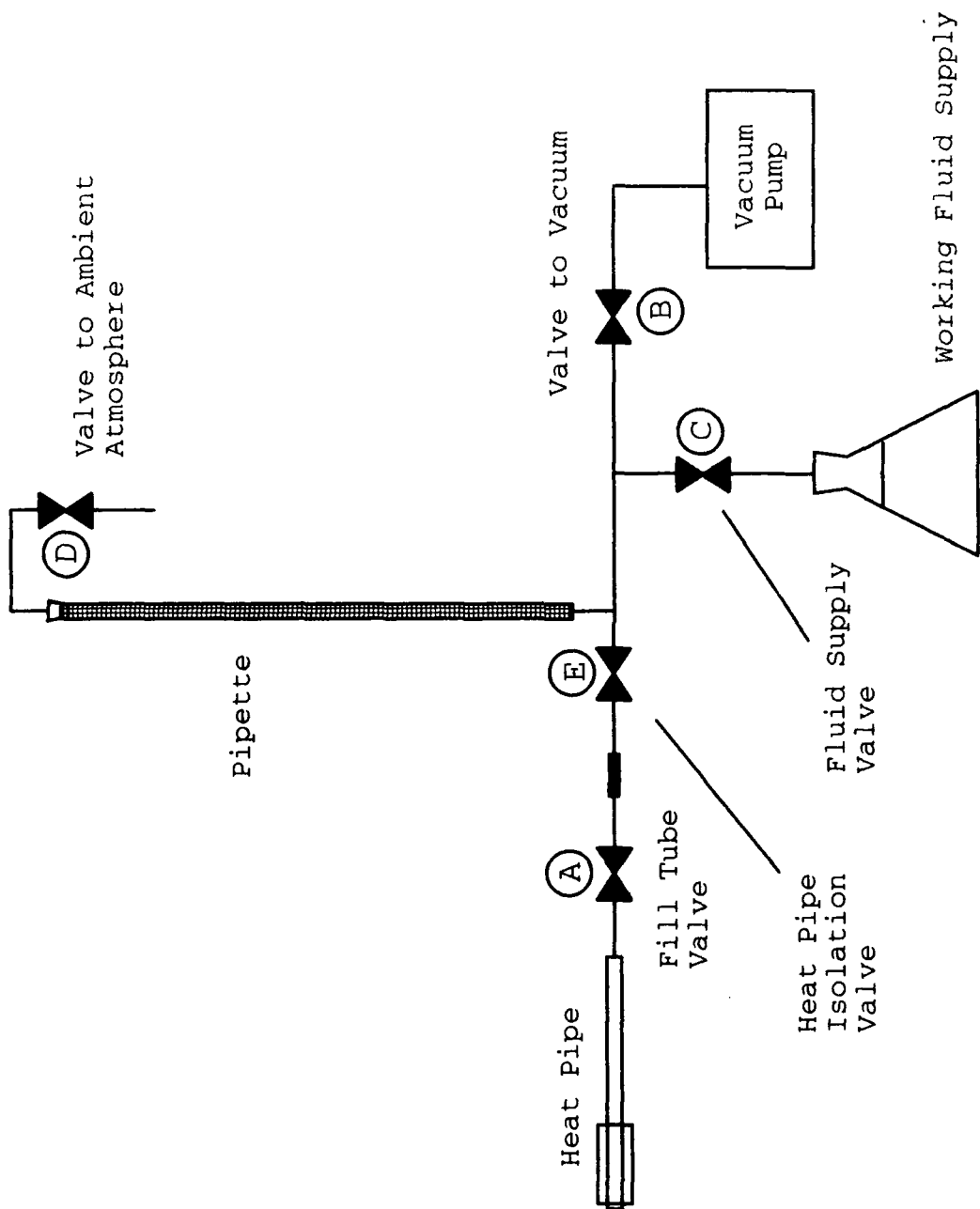


Figure 3.5 Fill Station Apparatus

the pipe. Next, the reading on the pipette was noted as a reference volume. The calculation in the preceding section yielded a desired mass of working fluid, 5.669 g. To be able to measure the proper inventory of fluid using the pipette, a volume was needed. The temperature of the water in the fill system was approximately 25° C, and at that temperature 5.669 g of water corresponds to approximately 5.7 cc of water. Having calculated the desired fill volume, and the noting the reference volume on the pipette, the valve on the pipe fill tube (A) was slowly opened and the fluid was pulled from the fill system into the pipe by the vacuum in the pipe. The desired volume of fluid was measured by watching the fluid column in the pipette drop. When the correct fluid volume had been let into the pipe, the valve on the pipe fill tube (A) was closed, once again sealing the pipe. The heat pipe was then removed from the fill system and its mass was measured using a Metler balance to confirm that the correct fluid inventory had been added. Once this was confirmed, the pipe was given a crude evaluation to insure that it operated in the heat pipe mode. This was done by using a tape heater to apply heat to the evaporator end while checking the temperature of the condenser end. Once it was confirmed that it was operating as a heat pipe, the fill tube was given a double crimp using a crimping tool to provide a vacuum tight seal, and the valve was removed from the fill tube. The fill tube was given a permanent seal by TIG welding the end of the tube

closed. At this point the pipe was filled and ready for operation and testing.

### *Heating Apparatus*

The heating apparatus chosen had to meet a number of requirements. It had to be capable of supplying a sufficient power density, and had to be able to withstand the vibration to which it would be subjected while in contact with the pipe. After evaluating several heating schemes, a flexible tape heater was chosen. This type of heater had the advantages of being low cost, relatively high power density, and the ability to be shaped to fit the contour of the pipe wall. It also had a relatively small mass, which was important due to the mass constraints on the shaker system to be used. The particular heater used in this experiment was manufactured by Omegalux corporation. It was a model STH051-060, Flexible Electric Heating Tape that consisted of nichrome heating wire covered with a high temperature, non-electrically conductive insulation braiding called Samox. This heater had a length of 1.829 m (6 ft) and a width of  $1.270 \times 10^{-2}$  m (0.5 in). The maximum power of the heater was 470 W at 120 volts and it had a power density of  $2.015 \times 10^4$  W/m<sup>2</sup> (13 W/in<sup>2</sup>). With an evaporator section length of only  $1.016 \times 10^{-1}$  m (4 in), the heater was wrapped in layers in order to get sufficient power density to run the experiment. To minimize the loss of heat to the environment, the heater was covered with two layers of

fiberfax insulation, a ceramic fiber-based batting material. This in turn was covered with an aluminum foil adhesive tape to hold the batting together during vibration. The electrical power input to the heater was monitored using a voltmeter and an ammeter. The power could be calculated using  $P = I \times V$ , where  $P$  is the power in watts,  $I$  is the current in amps, and  $V$  is the voltage in volts. The power input was controlled through the use of a signal conditioning rectifier (SCR) that allowed the power to be varied in small, measurable increments. The actual power into the heater was not critical since the true losses to the environment were not known. The measurement of the heater input power was important to insure that power was increased at the same rate from experiment to experiment.

#### *Coolant Control System*

A coolant control system was necessary for this experiment in order to allow the controlled variation of heat pipe operating temperature. This ability was required in order to operate the pipe at various points along the  $Q_{c,max}$  versus  $T_{op}$  curve. While the pipe was operating in the heat pipe mode, the pipe operating temperature could be varied by varying the condenser temperature. This was accomplished by changing the coolant flow rate. Normal tap water was used as a coolant in this experiment and it was run through the manifold surrounding the condenser section of the heat pipe. The coolant inlet temperature was not

controlled and was determined by the temperature of the water in the building plumbing. The flow rate was controlled using a valve at the source water pipe. The flow rate was measured using two methods. First, the water flowed through a rotameter on the way from the source water pipe to the manifold, and second, it was measured using a graduated cylinder upon exiting the manifold. The rotameter gave a rough indication of what the flow rate was for purposes of adjustment with the valve. The graduated cylinder was used to get an accurate flow rate by measuring the volume of water collected per unit time.

#### *Vibration Input Apparatus*

An apparatus had to be designed to allow the controlled input of vibration into the heat pipe. Since data was to be taken at several different frequencies, and several different amplitudes, the system would have to support this requirement. The following sections describe the shaker system itself, and the fixture designed to mate the heat pipe to the vibration actuator.

*Shaker System.* An Unholtz-Dickie model 5PM shaker was used for this experiment. This is a benchtop style electromagnetic shaker with a  $5.080 \times 10^{-2}$  m (2 in) actuator surface. It was driven by an Unholtz-Dickie model TA-30 250 W amplifier, and the signal was generated using an Unholtz-Dickie model OSP-4 oscillator-servo programmer. A control accelerometer mounted on the vibration fixture provided a

feedback signal to the OSP-4. The OSP-4 used this signal to maintain the designated vibration frequency and amplitude. The shaker was placed on vibration isolation blocks to provide a steady surface and the fixture was mounted to the actuator surface.

*Vibration Fixture.* A fixture had to be designed to mount the heat pipe to the shaker actuator surface. The fixture had to both mate the pipe to the shaker, and provide structural support to maintain the rigidity of the pipe during vibration. As with the rest of the hardware design, keeping the mass at a minimum was important due to the mass limits of the shaker. The model 5PM shaker is capable of driving approximately 2.3 kg at 30 Hz and 5.0 g. Therefore, the combined mass of everything to be attached to the shaker actuator had to be less than 2.3 kg. To satisfy this constraint while minimizing the flexing of the unsupported portions of the pipe, the fixture was designed to support the pipe at two points along its length. The support points broke the length into three equal sections. This was a compromise between supporting the pipe along its entire length, with the corresponding mass penalty, and supporting it only at its ends, leaving a long unsupported length in between. Figure 3.6 is an illustration of the fixture and how the pipe mounts to it. The heat pipe was thermally insulated from the fixture using rings of phenolic. This provided a rigid, non-thermally conductive support to the pipe. The caps on the fixture could be removed by loosening

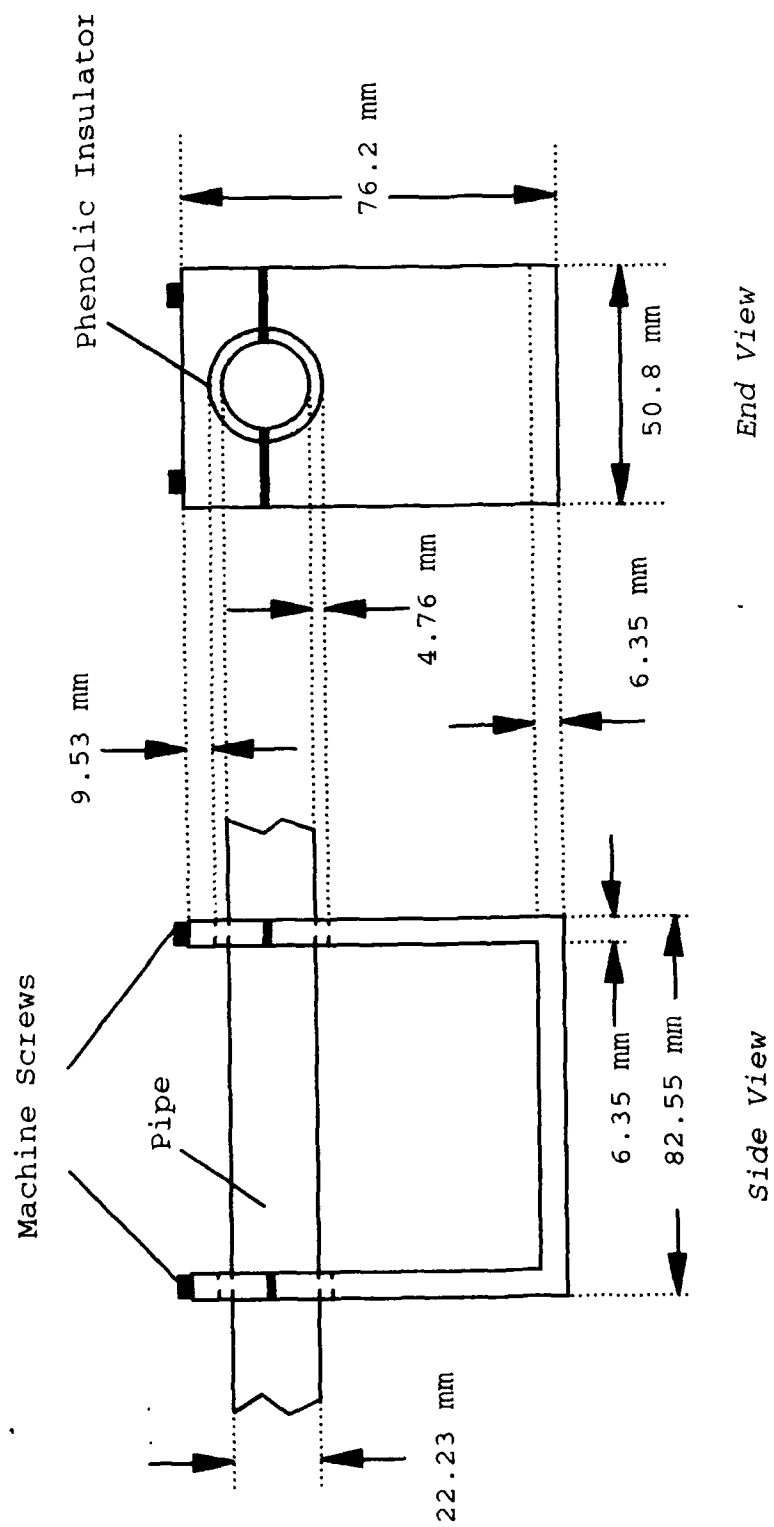


Figure 3.6 Vibration Fixture

the two allen head screws which secured each cap. The insulator rings were also split so that the pipe could easily be removed from the fixture while leaving all the instrumentation intact. The fixture was constructed of aluminum.

#### *Data Acquisition System*

The data acquisition system for this experiment had to be capable of reading and storing a variety of information. During a given test, there were vibration frequency and amplitude data, temperature data, heater power data, and coolant flow rate data to be monitored and recorded. The following sections describe the system designed to accomplish this.

*Vibration Data Acquisition.* The vibration data was measured using accelerometers. The vibration in the actuator axis direction was the control variable for the experiment, so it was at a known frequency and amplitude. The vibration frequency and amplitude in the other two directions were measured using single axis accelerometers aligned with these axes and mounted on the vibration fixture as shown in Figure 3.7. The output from the control accelerometer was fed back to the oscillator-servo programmer and used to maintain the desired signal. The output from the "off-axis" accelerometers was routed through a Kistler Piezotron Coupler, model 5124A, and then into a Tektronix 2246 100 MHz oscilloscope for display. The



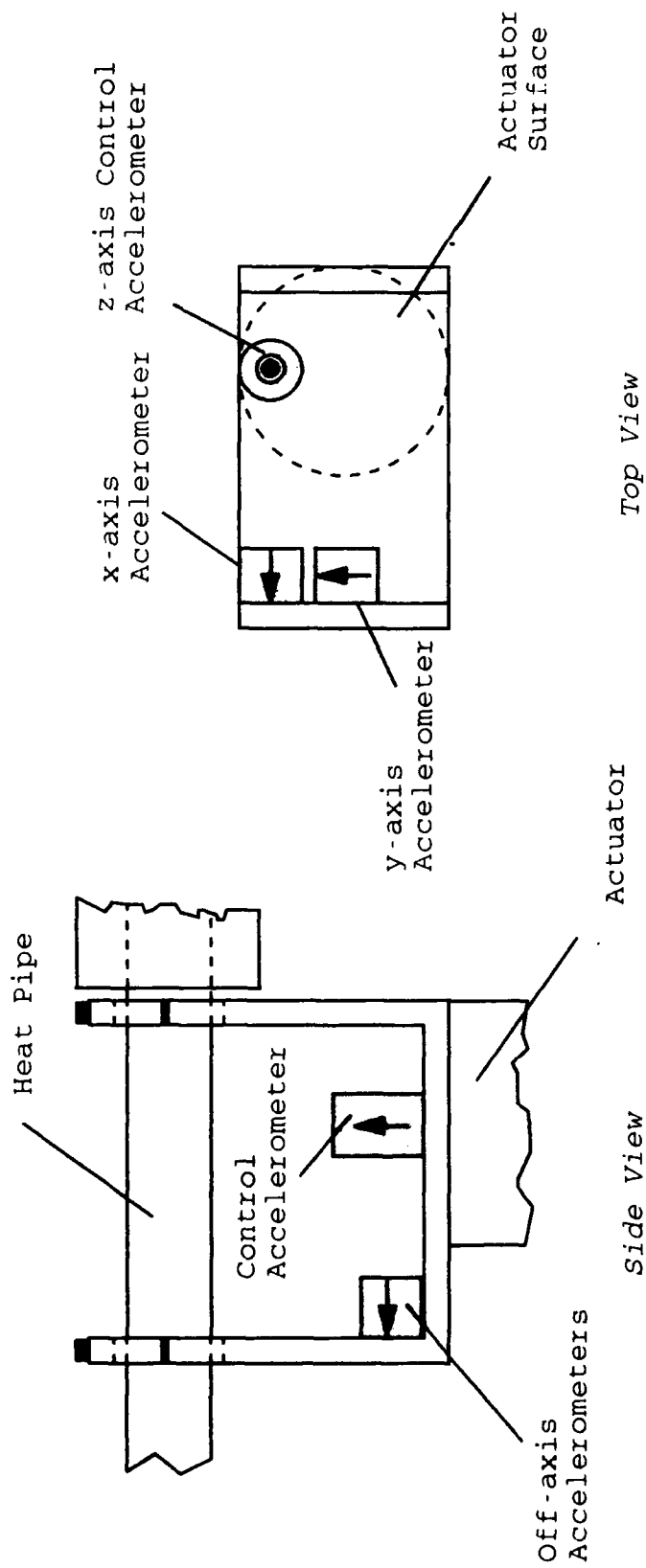


Figure 3.7 Accelerometer Locations

readings for the off-axis vibration amplitudes were taken manually using the oscilloscope.

*Temperature Data Acquisition.* There were many temperatures to be monitored and recorded during this experiment. Pipe wall temperatures, ambient air temperature, and coolant inlet and outlet temperatures were all recorded.

*Temperature Measurement.* The temperature measurements were taken using thermocouples. Omega model 5TC-GG-T-730-72 T-type copper/constantan thermocouples with a  $2.54 \times 10^{-4}$  m (.010 in) diameter bead were used. The leads were 1.829 m in length and had glass/glass insulation. The 10 thermocouples used to measure temperatures were mounted as shown in Figure 3.8. Defining  $x$  as the distance from the inside surface of the evaporator end endcap, there were three thermocouples under the heater. The first thermocouple (TC) was located at  $x = 5.0$  mm, another at  $x = 72.5$  mm and the final TC under the heater was located at  $x = 95.0$  mm. Three TCs were located along the adiabatic section at  $x = 125$  mm,  $x = 155$  mm, and  $x = 185$  mm. One TC was used measure the condenser wall temperature and it was located at  $x = 300.0$  mm, 5 mm from the inside surface of the condenser end endcap. One TC was used to record ambient air temperature and two were used to measure the temperature of the coolant flowing into and out of the manifold around the condenser section. These last two were mounted in custom made fittings as depicted in Figure 3.9. The thermocouples

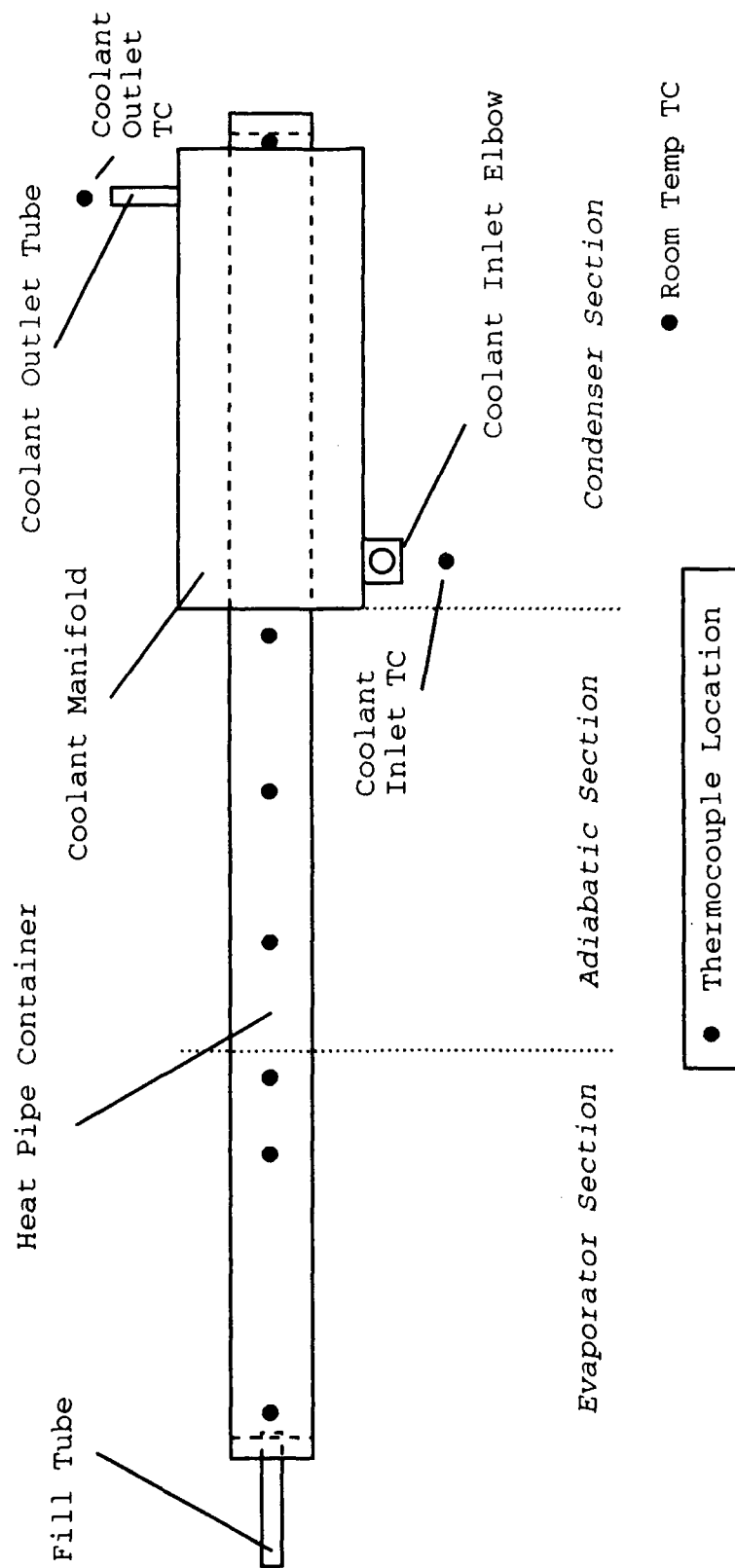


Figure 3.8 Thermocouple Locations

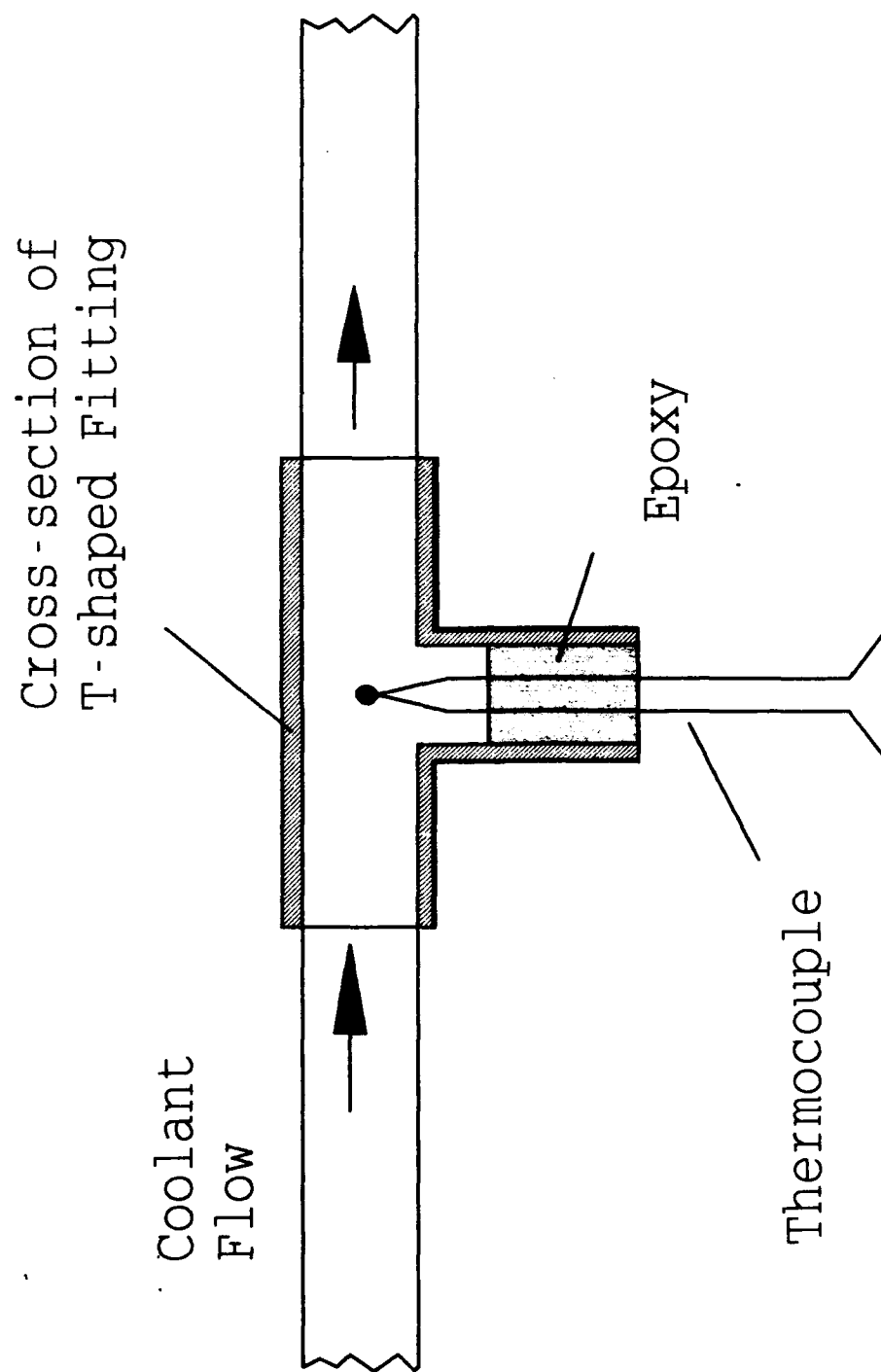


Figure 3.9 Coolant Thermocouple

measuring pipe wall temperatures were mounted using nichrome heater wire. This wire was wound tightly around the pipe and over the TC leads just behind the bead of the TC. The thermocouples in contact with the pipe wall, but not under the heater, were covered with a thermally conductive grease to insure good contact with the surface. This grease had a flash point of 210° C, so it could not be used under the heater. The TC leads were supported along the pipe length with plastic wire ties and routed to a point near the vibration fixture where they were brought off together at a single point in a bundle. This bundle was anchored to the shaker chassis to provide support and strain relief.

*Temperature Recording.* The center of the temperature data acquisition system was the Keithley Metrabyte DAS-8 data acquisition board which was installed into a Zenith Z-248 personal computer. This board allowed the sampling of up to sixteen data channels. It was programmed to sample the channels for a user-definable period of time, and then write an average value to a text file on disk. For this application, each of the ten TC channels described above was sampled 1000 times over a period of 5 seconds and the average reading was written to the text file on disk. This was a short enough duration to see any meaningful trends in the temperature data while keeping the data files at a manageable size for each test run.

### *Experimental Test Procedure*

The experimental test procedure used in this experiment was developed over a series of preliminary runs and was designed to provide repeatability and accurate data collection from test run to test run. Figure 3.10 gives an illustration of the overall experimental setup, and this may be a helpful reference during the explanation of the test procedure. The first step in the procedure was to insure that the heat pipe was at room temperature. The pipe was then tilted to an angle of approximately  $45^\circ$ . This insured that the wick was completely wet all the way to the evaporator end of the pipe. While inclined  $45^\circ$ , the heater power was set at 100 W. As the evaporator section heated up, the pipe began to operate in the heat pipe mode, albeit gravity assisted due to the inclination. This was done to guarantee that the pipe was starting in the heat pipe mode. This mode of operation was maintained until the heat pipe operating temperature reached  $35^\circ\text{C}$ . The heat pipe operating temperature was taken to be the same as the pipe wall temperature in the adiabatic section. This temperature was calculated by taking the average of the readings from the two TCs in the adiabatic section located closest to the evaporator section. In theory this section of the pipe should be nearly isothermal and these TCs consistently displayed temperatures within  $1^\circ\text{C}$  of one another. The third adiabatic section TC was only 5 mm from the end of the condenser section, and was typically at a temperature  $3^\circ\text{C}$

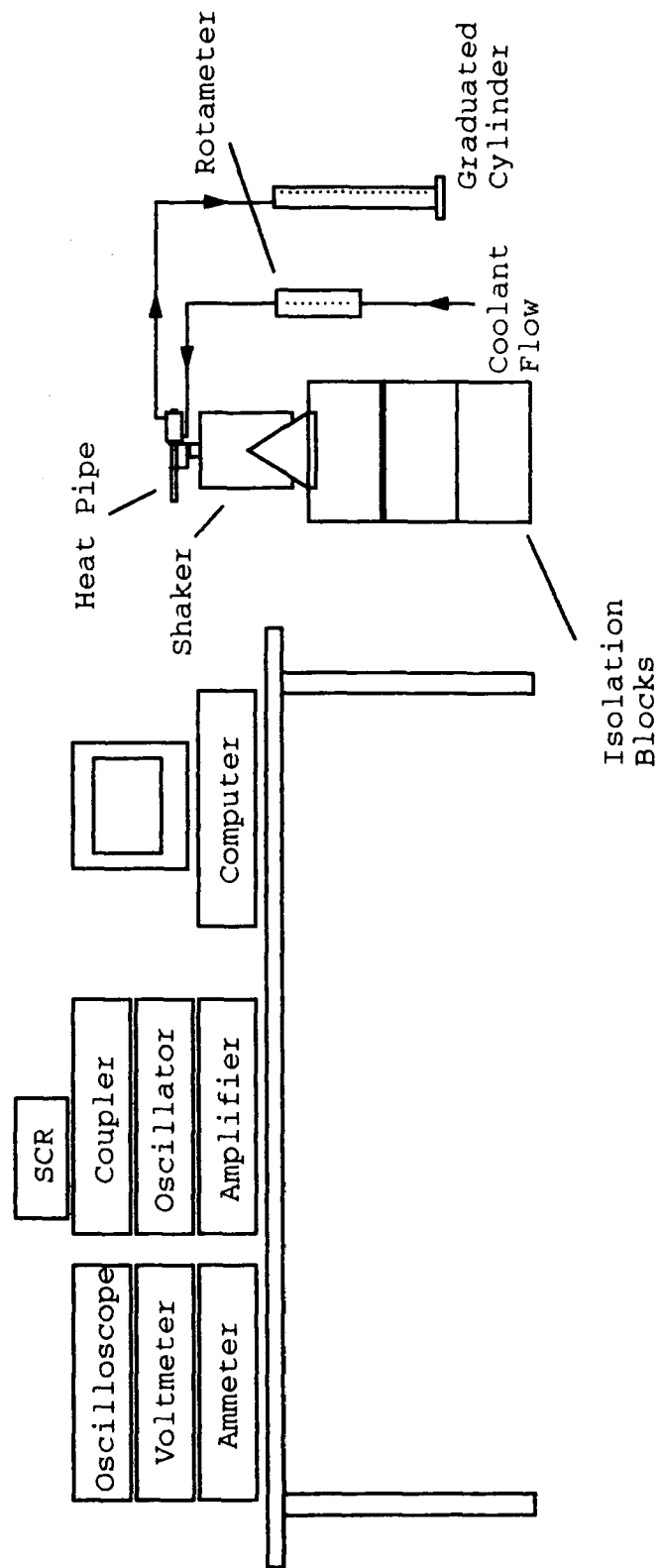


Figure 3.10 Experimental Setup

to 5° C lower than the other two. Due to this, it was not included in the operating temperature determination. Once an operating temperature of 35° C was reached, the pipe was leveled and the vibration level for that test run was set. The pipe was allowed to come to steady operation under this condition. The heater power was then increased in increments of 5 W until the evaporator section began to dry out. The heater power was only increased after the TC at the evaporator end of the pipe had been at a constant temperature for five time steps, or 25 seconds. Evaporator dryout was indicated by a rapid increase in the temperature at the evaporator end of the pipe, and this was considered the failure condition for the test run. When this indication was observed, the vibration amplitude in all three axis directions was noted as well as the coolant flow rate. The adiabatic section temperatures and coolant inlet and outlet temperatures were recorded by the DAS-8 and written to the data file.

The critical data points for each test run were the vibration frequency and amplitude, the heat pipe operating temperature, the coolant flow rate, and the coolant inlet and outlet temperatures. These were used to determine the maximum heat transfer rate at that pipe operating temperature and for the vibration condition imposed during that test. The expression used to calculate this maximum was



$$Q_{\max} = \dot{m}c_{p,1}\Delta T$$

(3.9)

where

- $Q_{\max}$  = maximum heat transfer rate (W)
- $\dot{m}$  = mass flow rate of coolant (kg/s)
- $c_{p,1}$  = specific heat of coolant [J/(kg-K)]
- $\Delta T$  = change in coolant temperature (K)

#### IV. Experiment Analysis

The design of the experiment was discussed in detail in Chapter 3. This chapter examines the actual implementation of the design, and the resulting experimental error. Each part of the data acquisition process is evaluated, and a determination of the accumulated experimental error is made.

##### *Temperature Measurements*

*Method.* T-type thermocouples were used to measure the various temperatures of interest during the experiment. These were attached using the various methods described in Chapter 3. The signals generated by the thermocouples were sampled for a five second period, averaged, rounded to the nearest integer value, and then written to a data file using the Keithley Metrabyte DAS-8 data acquisition board.

Before using the thermocouples, the calibration of each was checked to insure that it was operating properly and an accurate reading could be expected. This was accomplished using a portable thermocouple calibrator manufactured by Omega. This device had several functions including a self-calibration routine to insure that the unit itself was in calibration, and a mode in which it could be used to send a calibration signal to another device. Additionally, up to two thermocouples could be connected to the device and a reading could be displayed from each. It is this last mode that was used to check the thermocouples used in this

experiment. Since the thermocouples came assembled from the manufacturer, it was expected that they would be more accurate than thermocouples produced in the lab. To check the bias of each thermocouple, it was connected to the calibrator along with a previously calibrated thermocouple, and the temperature readings were compared. The reading given by the previously calibrated thermocouple was assumed to be the true temperature. By taking the difference between the reading given by the thermocouple whose bias was being checked and the calibrated thermocouple, the bias was determined.

The Keithley Metrabyte DAS-8 was also calibrated before use. The DAS-8 has a user adjustable ice-point built into the board in the form of a thermistor to compensate for the ambient temperature. In order to calibrate the board, the calibration mode on the Omega thermocouple calibrator was used to provide a known signal to the board. The ice-point was then adjusted using the appropriate potentiometer on the board until the output of the DAS-8 corresponded to the signal input by the calibrator. To insure that the ice-point was set correctly, a temperature reading was taken with a given thermocouple using the Omega calibrator, and then this same thermocouple was connected to one channel of the DAS-8 and used to take the same measurement. When the temperature magnitude indicated by each of these methods was identical, the ice-point setting was regarded as being correct.

*Experimental Error.* The calibration procedure used to check the thermocouples yielded no surprises. The entire set of thermocouples to be used in the experiment demonstrated a bias of  $0^{\circ}\text{C}$  as compared to the calibration thermocouple when compared at room temperature. It was assumed that the bias would not vary significantly across the range of temperatures seen during testing. Therefore the thermocouples were considered to be accurate to within the display capability of the calibrator, which was  $0.1^{\circ}\text{C}$ , and to have a negligible contribution to the overall system error. The other error associated with the thermocouples was due to the mounting procedures used. The pipe wall temperatures were measured using thermocouples wired to the surface as described in Chapter 3. This method of attachment does not provide as accurate a reading of the pipe wall temperature as some other methods of attachment, such as spot welding the thermocouples to the surface. For this experiment, however, a true magnitude was not critical for many of the temperature measurements, and this method of attachment provided flexibility in the movement or replacement of the thermocouples if necessary. Since the criteria for ending a test run was a rapid increase in temperature at the end of the evaporator section, a capability to observe this trend was all that was needed. The adiabatic section temperatures were somewhat more critical since they were used to determine the pipe operating temperature for a given test run. The mounting of

these thermocouples was given special attention to insure good contact of the thermocouple bead with the pipe wall. Thermally conductive grease was used on these thermocouples to further aid in making good contact and in minimizing convective heat transfer from the thermocouple bead to the environment. These measures were expected to provide for accurate temperature measurement in this section, and the error due to thermocouple mounting was assumed to be small. Finally, the accuracy of the coolant temperatures was the most critical. To measure these temperatures, the thermocouple bead was inserted directly into the coolant flow as illustrated in Figure 3.9, and therefore the error due to the mounting procedure was negligible.

The DAS-8 accuracy was stated by the manufacturer to be  $\pm 2^{\circ}$  C. This error is due to variations in the ambient environment, and their effect on the thermistor that provides the ice-point calibration for the board. Therefore, all the temperature readings recorded by the DAS-8 were taken to have an error of  $\pm 2^{\circ}$  C, relative to the true temperature. Since all the channels use the same thermistor as their ice-point, they were all assumed to have identical errors relative to the true temperature. Based on this assumption, the error was considered to be negligible when taking the difference between two measured temperatures.

The chosen method of displaying and recording temperatures had an error associated with it as well. Due

to noise on the data acquisition system, the first decimal place in the displayed temperature readings was very unsteady. To compensate for this unsteadiness, the temperature readings were rounded to the nearest integer value. Since the measured temperature was rounded to the nearest integer value, there was an error contribution due to rounding. The recorded value could be  $\pm .5^{\circ}$  C of the measured value, and this would figure into the accumulative experimental error.

#### *Vibration Data*

*Method.* Accelerometers were used to collect vibration data during the experiment. The principle axis of interest was the vibration actuator axis, which was vertical and normal to the longitudinal axis of the heat pipe. The control accelerometer was mounted with its measurement axis aligned with the actuator axis, allowing the OSP-4 vibration controller to use the accelerometer output in a feedback control loop to maintain the desired vibration level. The other two right-handed axes were normal to the actuator axis, and were instrumented with accelerometers aligned with these axes. These two axes point in what were termed the "off-axis" directions. All three accelerometers were mounted to the base of the vibration fixture and their locations are represented in figure 3.7. The output from the "off-axis" accelerometers was input to the oscilloscope and the vibration level was determined from the voltage

displayed. The frequency and level in the actuator axis direction were read directly from the OSP-4 display.

Before the accelerometers were mounted to the fixture, they were calibrated. This process involved mounting the accelerometer to be calibrated on top of an accelerometer that had already been calibrated, which was in turn mounted to the actuator surface of a shaker. The previously calibrated accelerometer was known as a calibration standard. The output from the accelerometer to be calibrated was routed through the charge amplifier or coupler that would be used with that accelerometer during the experiment. The standard accelerometer had its own calibrated charge amplifier, and the output from both accelerometers was read using a voltmeter. Since the standard accelerometer had a known voltage per g output, it was used to adjust the shaker to provide a 100 Hz, 1.0 g vibration input to the accelerometers. The output of the accelerometer being calibrated was then recorded, and this provided the voltage per g output of that accelerometer at the 1.0 g level. It was assumed that the accelerometer would be operated in its linear region, and that the change in output with frequency was negligible. This process was repeated for each of the three accelerometers to be used in the experiment. Since the OSP-4 was to be used as the signal generator and vibration controller, its accelerometer charge amp was adjusted via a potentiometer on the rear

panel of the unit so that the display indicated 1.0 g during the calibration.

*Experimental Error.* While there was undoubtedly some error associated with the accelerations measured using this method, it was regarded as inconsequential to the results of the experiment. There was error associated with the fact that the accelerometers were mounted to the fixture instead of the pipe itself, and there was error associated with measuring the vibration only near the center of the pipe. The objective of the experiment was to examine the effect on pipe performance of vibration normal to the longitudinal axis of the pipe. To accomplish this, the effect on pipe performance was evaluated at vibration levels within certain vibration "regimes" as opposed to specific levels and frequencies. Therefore, the off-axis accelerometers were used to make a qualitative assessment that the vibration input to the pipe was principally in the transverse direction, and that minimal vibration was experienced in the longitudinal direction. Likewise, the vibration input in the direction of the actuator axis was intended to be approximately the same as the level that was set on the OSP-4. With the objective being to analyze how transverse vibration in general affects the pipe capillary limit, it was not necessary to input exactly 5.0 g. An input of 4.9 g or 5.1 g would be accurate enough to distinguish any difference in effect between this vibration level and an input near 1.0 g. Therefore, the error in measuring the



exact vibration input to the pipe was considered to be insignificant to the results of the experiment. If the experiment had been an examination of a particular pipe design destined for a particular application, the exact determination of vibration input would be more important. That was not the case in this experiment.

#### *Coolant Flow Measurement*

*Method.* The measurement of the mass flow rate of the coolant was a critical piece of data for this experiment. This measurement would be one of several used to determine the power transported by the heat pipe, and its accurate recording was important to reduce the error in this power determination. Two methods were used to get a flow rate. The first measurement was taken using a rotameter. This device was used to get a rough estimate of the flow rate for purposes of adjusting the rate at the water supply valve. Although this was a useful device in setting up the experimental operating conditions, it was not very accurate due to the nonlinearities in the device itself and the difficulty in getting an accurate reading off of the scale. The second measurement, and the one used to determining the power transport, was taken using a 500 ml graduated cylinder and a stopwatch. Upon exiting the coolant manifold, the flow was collected in the graduated cylinder for a measured time interval. The volume collected was then divided by this time interval to calculate the actual fluid flow rate.

*Experimental Error.* The error in the measurements taken with the rotameter was very large, and these were not used to make any calculations. Therefore, they did not enter into the calculation of the experimental error. The error that impacted the results of the experiment was the error involved in using the graduated cylinder to measure flow rate. The time interval was measured using a stopwatch that displayed elapsed time in hundredths of a second. Therefore, the error in reading the time interval measurement was determined to be very small. The cylinder was graduated in increments of 5 ml, and it was assumed that a reading could be taken to within  $\pm 2.5$  ml of the actual level. Therefore, with the error in the time measurement being insignificant, the contribution to the experimental error was the  $\pm 2.5$  cc error in the volume measurement. To minimize the impact of this error on the accumulated experimental error, the time interval was made as large as was practical given the size of the cylinder and the flow rate.

#### *Heat Pipe Inclination Measurement*

*Method.* The heat pipe tilt angle is an important factor in the heat transfer capability of a heat pipe. For this experiment, no scale existed against which to measure the actual tilt of the pipe, although great care was taken to insure that this angle of inclination was the same from test to test. The intent was to make the pipe level so that

the static test results would be close to the analytically predicted results. A small level was used to check the pipe inclination at the point in the test procedure where the pipe was leveled. This level was placed on the coolant manifold and aligned with the longitudinal axis of the pipe. For each test, the angle of the pipe was set so that the level reading was the same as for the previous tests.

*Experimental Error.* There was no measurement of the actual angle of inclination of the heat pipe. Therefore, it was assumed that the difference in angle from test to test could be kept small by using the level and a great deal of care to insure that the bubble in the level was at the same position for each test. Given the care taken in leveling the pipe, and the lack of an accurate angle measurement, the error was assumed to be small and was not figured into the accumulated experimental error.

#### *Determination of Accumulated Experimental Error*

*Error Bar Calculation.* Knowing the error contribution of each system component as described above, the overall accumulated experimental error was determined. These component errors were considered to be uncertainties in the measurements as opposed to absolute errors. This distinction is made so that the calculation of the accumulated error yields an uncertainty in the final result, not a maximum absolute error. This uncertainty was

calculated using the following formula for the root-sum square (rss) error (3:63)

$$E_{rss} = \left[ \left( \Delta u_1 \frac{\partial f}{\partial u_1} \right)^2 + \left( \Delta u_2 \frac{\partial f}{\partial u_2} \right)^2 + \dots + \left( \Delta u_n \frac{\partial f}{\partial u_n} \right)^2 \right]^{\frac{1}{2}} \quad (4.1)$$

where

- $E_{rss}$  = root-sum square error
- $f$  = function of independent measurements
- $u_1$  = first independent measurement
- $u_2$  = second independent measurement
- $u_n$  = nth independent measurement
- $\Delta u_1$  = error in first independent measurement
- $\Delta u_2$  = error in second independent measurement
- $\Delta u_n$  = error in nth independent measurement

In this experiment, the accumulative experimental error was calculated for the maximum heat transport rate of the pipe which is given by Eq (3.9). Equation (4.1) takes the following form for this calculation

$$\Delta Q = \left\{ \left( \Delta \dot{m} \frac{\partial Q}{\partial \dot{m}} \right)^2 + \left( \Delta c_{p,1} \frac{\partial Q}{\partial c_{p,1}} \right)^2 + \left[ \Delta (\Delta T) \frac{\partial Q}{\partial \Delta T} \right]^2 \right\}^{\frac{1}{2}} \quad (4.2)$$

where

- $\Delta Q$  = rss error in the maximum power transport (W)
- $\dot{m}$  = coolant mass flow rate (kg/sec)
- $\Delta \dot{m}$  = error in coolant mass flow rate (kg/sec)
- $c_{p,1}$  = specific heat of coolant (J/kg-K)
- $\Delta c_{p,1}$  = error in specific heat of coolant (J/kg-K)
- $\Delta T$  = temperature change of coolant across condenser (K)
- $\Delta(\Delta T)$  = error in temperature change of coolant across condenser (K)

The value for the specific heat of water was found in Table A.1, and the error in this value was considered negligible. With  $\Delta c_{p,1} \approx 0$ , the second term of the above expression is approximately zero, and Eq (4.2) can be written

$$\Delta Q = \{ (c_{p,1} \Delta T \Delta \dot{m})^2 + [\dot{m} c_{p,1} \Delta (\Delta T)]^2 \}^{\frac{1}{2}} \quad (4.3)$$

The coolant flow rate was calculated using  $\dot{m} = m/t$ , where  $m$  is the mass of the coolant collected expressed in kg and  $t$  is the interval over which it is collected in sec. The error in the coolant flow rate measurement was found using

$$\begin{aligned} \Delta \dot{m} &= \left[ \left( \Delta m \frac{\partial \dot{m}}{\partial m} \right)^2 + \left( \Delta t \frac{\partial \dot{m}}{\partial t} \right)^2 \right]^{\frac{1}{2}} \\ &= \left( \frac{\Delta m^2}{t^2} + \frac{m^2 \Delta t^2}{t^4} \right)^{\frac{1}{2}} \end{aligned} \quad (4.4)$$

where

$m$  = mass of coolant collected (kg)  
 $t$  = time interval of coolant collection (sec)  
 $\Delta m$  = error in coolant mass measurement (kg)  
 $\Delta t$  = error in time measurement (sec)

The error in the time measurement was considered to be negligible, and with  $\Delta t \approx 0$ , the second term in Eq (4.4) is approximately equal to zero yielding

$$\Delta \dot{m} = \frac{\Delta m}{t} \quad (4.5)$$

The temperature change,  $\Delta T$ , is the difference between the coolant temperature leaving the manifold and the temperature of the coolant when it entered the manifold. Given this definition of  $\Delta T$ , the error in the measurement of this temperature difference was calculated using

$$\begin{aligned}\Delta(\Delta T) &= \left[ \left( \Delta T_{out} \frac{\partial \Delta T}{\partial T_{out}} \right)^2 + \left( \Delta T_{in} \frac{\partial \Delta T}{\partial T_{in}} \right)^2 \right]^{\frac{1}{2}} \\ &= (\Delta T_{out}^2 - \Delta T_{in}^2)^{\frac{1}{2}}\end{aligned}\quad (4.6)$$

where

$$\begin{aligned}T_{out} &= \text{coolant temperature leaving manifold (K)} \\ T_{in} &= \text{coolant temperature entering manifold (K)} \\ \Delta T_{out} &= \text{error in temperature leaving manifold (K)} \\ \Delta T_{in} &= \text{error in temperature entering manifold (K)}\end{aligned}$$

As described in the earlier sections, the uncertainty in the coolant mass measurement was  $\pm 2.5$  g. Substituting this value for  $\Delta m$  in Eq (4.5) yields  $\Delta \dot{m} = 2.5 \times 10^{-3}/t$  kg/sec. The uncertainty in the measurement of  $\Delta T$  was due only to the rounding of  $T_{in}$  and  $T_{out}$ . Therefore,  $\Delta T_{out} = 5.0 \times 10^{-1}$  K and  $\Delta T_{in} = 5.0 \times 10^{-1}$  K. Substituting these values into Eq. (4.6) yields  $\Delta(\Delta T) = 7.071 \times 10^{-1}$  K. The expressions for  $\Delta \dot{m}$  and  $\Delta(\Delta T)$  were then substituted into Eq. (4.5) to give

$$\Delta Q = \left[ \left( 2.5 \times 10^{-3} \frac{c_{p,l} \Delta T}{t} \right)^2 + (7.071 \times 10^{-1} \dot{m} c_{p,l})^2 \right]^{\frac{1}{2}} \quad (4.7)$$

This expression is the accumulative experimental error in the maximum heat transport rate of the heat pipe. For a given test run, the  $c_{p,1}$  in J/kg-K corresponding to  $T_{in}$ ,  $\dot{m}$  in kg/sec, and the measured  $\Delta T$  of the coolant in degrees K were substituted into Eq (4.7) to find the uncertainty in the calculated maximum heat transfer rate. This heat transfer rate was then reported as  $Q \pm \Delta Q$  W.

*Other Sources of Error.* There are a number error sources that were assumed small or otherwise disregarded in this analysis. While an attempt was made to address the significant contributions to the accumulated experimental error, the following are some of the error sources that may under certain conditions impact the results of the experiment. First of all, the error analysis in the preceding section uses a root-sum square error calculation. A calculation of the absolute error would yield significantly larger error bars. This was not considered desirable since it implies that the errors of the individual system components all happen to have the same sign, and they happen to be at a maximum. Therefore, when they are summed to get the accumulated error, the magnitude is the maximum possible if everything is at its worst. This was regarded as unlikely, so the rss method was used. It takes into account the likelihood that some errors will be positive and some will be negative, and that it is unlikely that the absolute error scenario would occur. Again, that is why  $\Delta Q$  is an uncertainty in  $Q$ , and not an absolute error.

A second source of error that may be significant was in the measurement of the inclination angle. While this error was believed to be small, a change in angle from one test to another could cloud the interpretation of the results. A lower maximum heat transfer rate could then be due to either the vibration environment, or to a change in inclination of the pipe. While special care was taken to minimize this difference in angle, an improved angle measurement would have helped quantify this error.

A third source of error can be attributed to the manner in which the coolant temperatures were measured. The fittings holding the thermocouples that were used to measure the coolant temperatures were located approximately  $1.524 \times 10^{-1}$  m (6 in) from the inlet and outlet tubes on the manifold. This was necessary due to the motion of the pipe when undergoing vibration. As a result, some heat transfer took place through the coolant line wall as the coolant travelled from the manifold outlet to the measurement location. The coolant line was made of clear vinyl tubing, and this temperature drop between the manifold exit and the thermocouple fitting was believed to be small.

One other source of error in the results was due to fluctuations in the flow rate and temperature. While they were reasonably constant, there was some fluctuation in both the coolant flow rate and the coolant temperature due to the reliance on building plumbing for a supply of water. While fluctuations in the coolant temperature were small and



occurred gradually, the fluid flow rate could have sudden changes when there was a change in the building water pressure. Since the flow rate was figured as an average over time, this did not have much effect on the measured flow rate. A sudden change in flow rate could, however, cause an abrupt increase in cooling at the condenser, momentarily lowering the pipe operating temperature. If this occurred as the pipe was approaching its  $Q_{max}$ , it could potentially cause the pipe to dry out since  $Q_{max}$  is lower at lower operating temperatures. This momentary change in operating temperature might not have been recorded through the pipe wall due to the response time of the thermocouples, and the flow rate would be recorded at the averaged value, even though the instantaneous flow rate may have been higher. These changes would result in a larger uncertainty in the flow rate and  $c_{p,1}$  used to calculate the  $Q_{max}$  for that run.

## V. *Experimental Results*

The previous chapters have given an in-depth presentation of why this experiment was attempted, the theory behind heat pipes and their operating limits, the detailed experiment design, and the analysis of the error to be expected in the results. The following sections present these results with their corresponding uncertainties, and give an analysis of what the results mean.

### *Determination of Heat Pipe Performance With no Vibration*

In order to determine what effect the vibration of a heat pipe has on its performance, it is necessary to have a baseline with which to compare. One possibility is a comparison of vibration results with the analytically predicted static performance such as that illustrated in Figure 3.2. The drawback to this approach is that no real heat pipe will perform exactly as the analytical model predicts. Variations in cleanliness during assembly, the production technique, the true physical dimensions, and the tightness of the wick wrap are a few of the variables that impact the performance of the pipe. If a comparison is made to the analytical model, the cause of any performance difference is difficult, if not impossible, to determine. For this reason, the baseline for this experiment was defined to be actual performance data for the heat pipe while operating with no vibration input.

The capillary limited heat transport rate was determined through a series of 28 experimental test runs during which the pipe was level and held static. These static runs were made at a wide range of operating temperatures to encompass the entire spectrum of temperatures over which vibration data was expected to be taken. This range extended from 42° C to 102° C. The compilation of this static data represented a baseline to which performance data from the vibration runs could be compared with only a single variable, the vibration level.

The test run results for both the static runs and the vibration runs are tabulated in Table B.1 in Appendix B. These results were calculated using the data presented in Appendix C. The table gives the test run number, the vibration input for that test, the pipe operating temperature, and the calculated  $Q_{c,max}$  along with its uncertainty. The static run results are plotted in Figure 5.1 along with the analytically predicted static performance curve. As was expected, it is clear that it would not be very useful to compare the vibration data to the analytical model, given that even the static data varies from the analytical model by as much as 25% at  $T_{op} = 71^{\circ} \text{ C}$ . Therefore, the static performance data was used as the baseline for comparison.

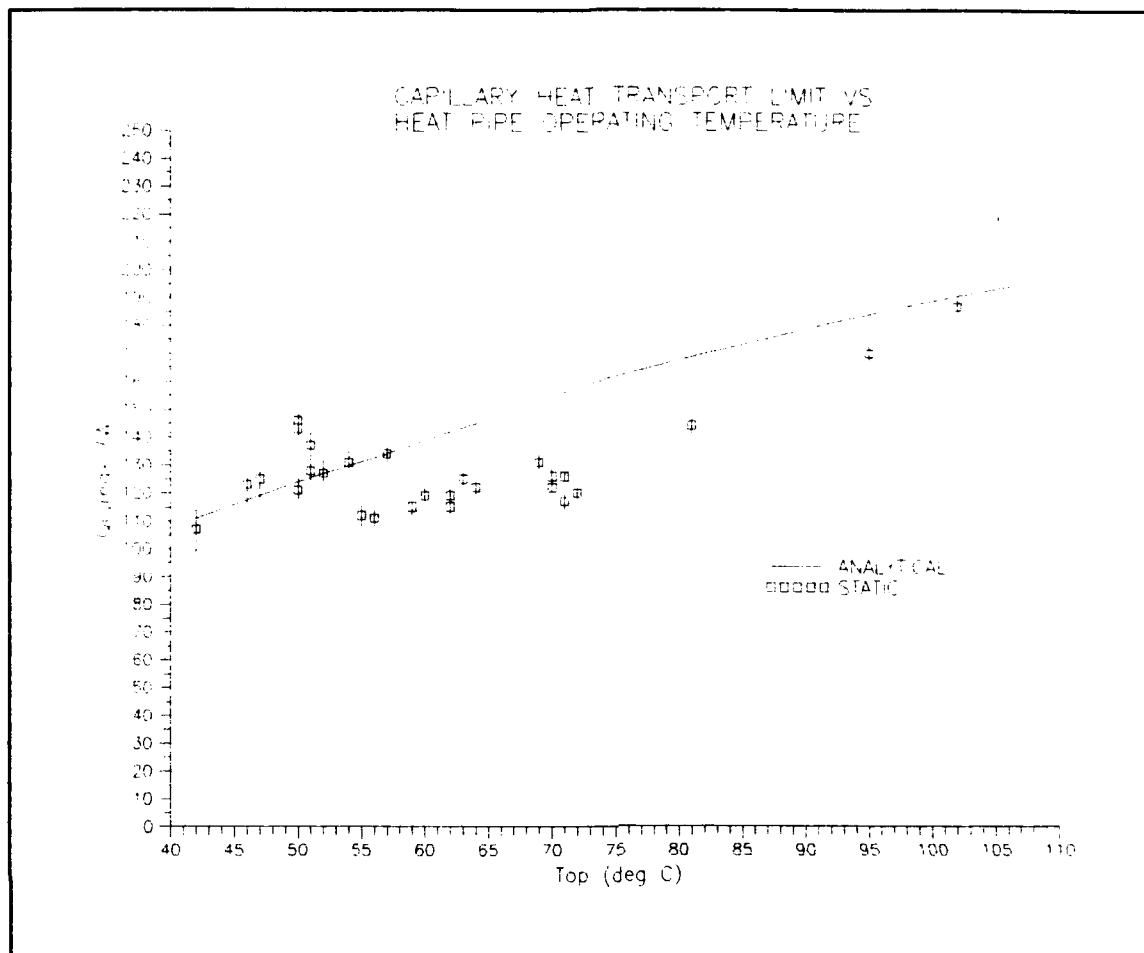


Figure 5.1  $Q_{c,max}$  vs.  $T_{op}$ : Static and Predicted

#### *Determination of Heat Pipe Performance During Transverse Vibration*

Having established the baseline performance with the 28 static test runs, the heat pipe performance in a vibration environment had to be determined. To address the general question of how transverse vibration affects the capillary limit, tests were run at three different frequencies and three different levels of vibration. This resulted in nine different combinations of vibration frequency and level, or

nine different vibration environments. Several test runs were made at each frequency and level combination to insure that the data collected was repeatable. This gave a higher degree of confidence in the results, and helped to quantify the "other" sources of error discussed earlier in Chapter 4.

The three frequencies chosen were 30 Hz, 250 Hz, and 1000 Hz. This range was intended to address both the lower frequencies often present in mechanical machinery and also the higher frequencies found in other dynamical systems such as spacecraft. The three frequencies were spaced far enough apart so as to represent three different vibration "regimes" that could be used to describe vibration effects at "low", "medium", and "high" frequencies.

The three vibration levels chosen were 1.0 g, 2.5 g, and 5.0 g. These again were chosen to represent likely loads to be experienced by a heat pipe as part of a system. The levels, like the frequencies, were intended to be far enough apart so as to be distinguishable from one another in terms of their effect on heat pipe performance.

A sinusoidal input was used for each of the vibration tests. The vibration of interest was in the direction normal to the longitudinal axis of the heat pipe. Measurement of the vibration level in the three orthogonal directions confirmed that vibration input to the pipe was primarily transverse vibration, with very little longitudinal vibration of the pipe. The level of vibration for each of the three axes was recorded during dryout, and

is found in Appendix C. Vibration level was typically an order of magnitude less severe along the pipe longitudinal axis than in the transverse direction. Therefore the results can be regarded as being the results of transverse vibration.

The results from the vibration runs are tabulated in Table B.1. Again, these results were calculated using the data found in Appendix C. They were then plotted along with the static data in order to make comparisons and determine what effect, if any, the transverse vibration had on the capillary limited heat transport rate of the pipe.

#### *Comparison of Vibration Data to Static Data*

Once the static and the vibration data were collected, they were plotted together in various combinations to analyze the results. To give an overview of what the results look like, Figure 5.2 illustrates all the vibration data and static data collected. From this graph it is clear that the majority of the data falls below the analytical model, but it follows the same basic curve as the prediction. From this illustration it can be seen that the vibration results fall within a narrower range of operating temperatures than do the analytical and static results. The remaining graphs were plotted over this narrower range of temperatures to give better resolution.

To be able to examine the effect of each vibration level and frequency on the  $Q_{c,max}$ , a separate plot of each was

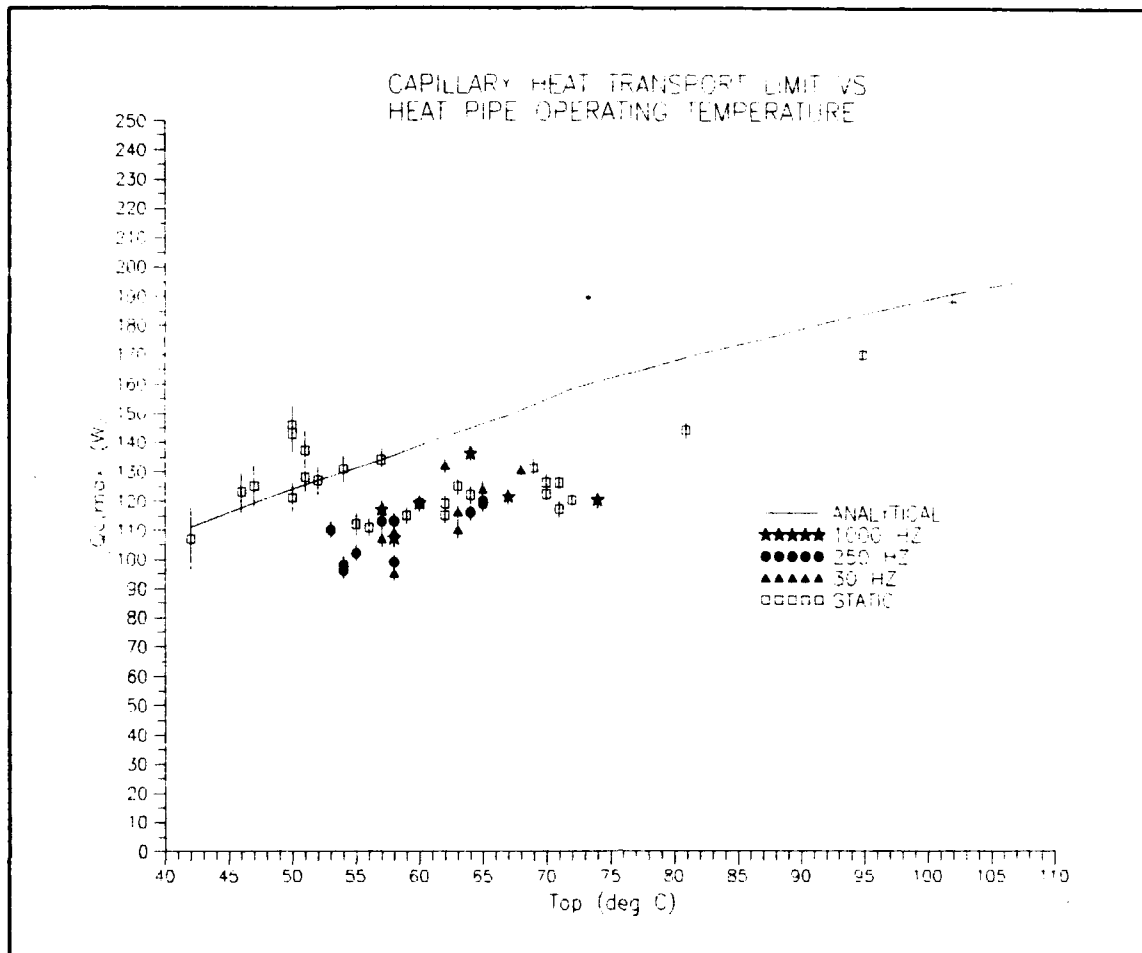


Figure 5.2  $Q_{c,max}$  vs.  $T_{op}$ : Static and Vibration Results

created. The first to be presented are the 1.0 g test runs. Figure 5.3 shows a plot of all the test run results obtained at the 1.0 g vibration level along with the static results. An examination of this plot revealed that there was no evident effect that could be attributed to the vibration at this level. While a few of the data points were low compared to static points at similar temperatures, the majority were near or even above corresponding static results. Therefore, there was no general trend in this data to indicate that the vibration had an effect.

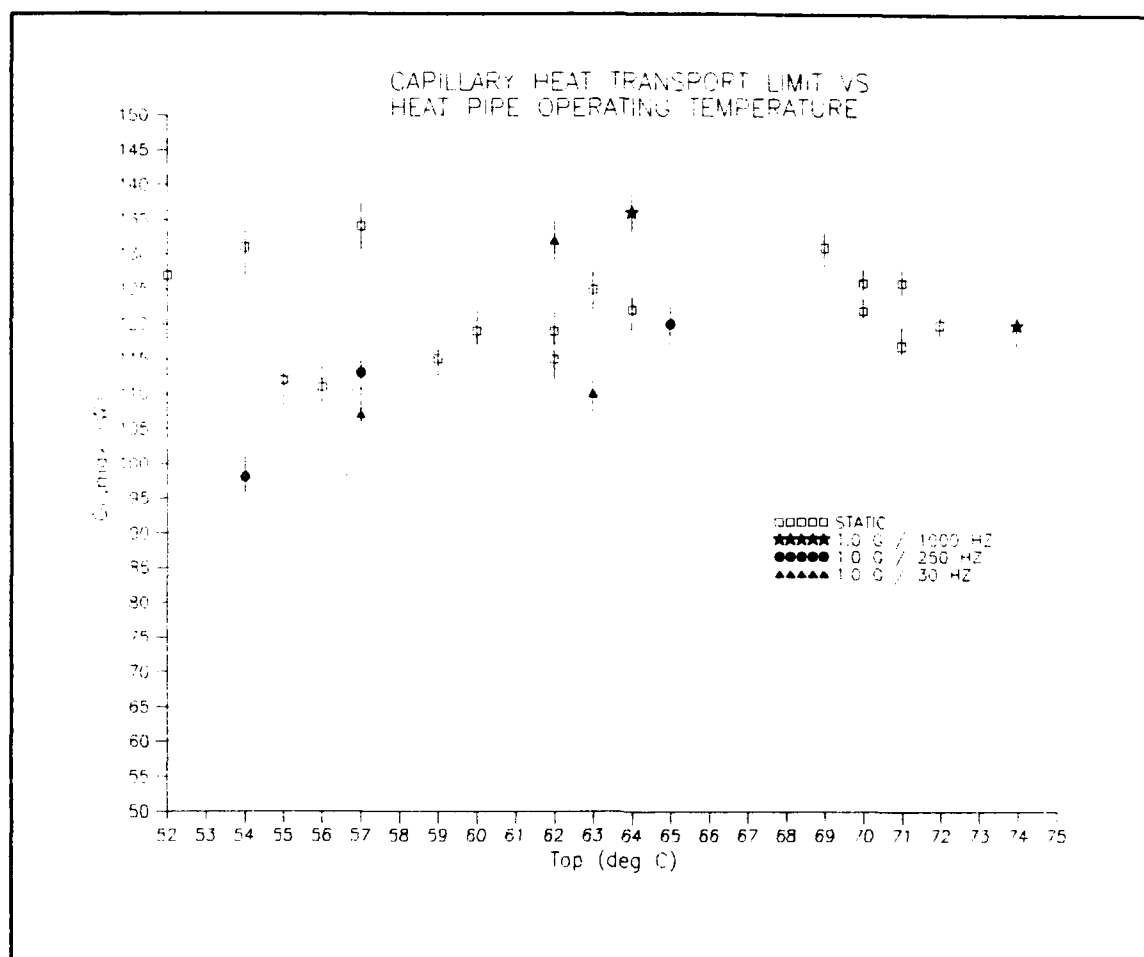


Figure 5.3  $Q_{c,max}$  vs.  $T_{op}$ : Vibration at 1.0 g

Examining the higher level vibration runs next, the results from the 2.5 g tests were plotted as shown in Figure 5.4. This display of the 2.5 g results had more data points that appeared to be low compared to the corresponding static results, but still no general trend. Two of the runs at  $T_{op} = 58^{\circ} C$  demonstrated what appeared to be low values of  $Q_{c,max}$  relative to the static results, but with the majority of the results very close to the static performance, the presence of any effect due to vibration was inconclusive.



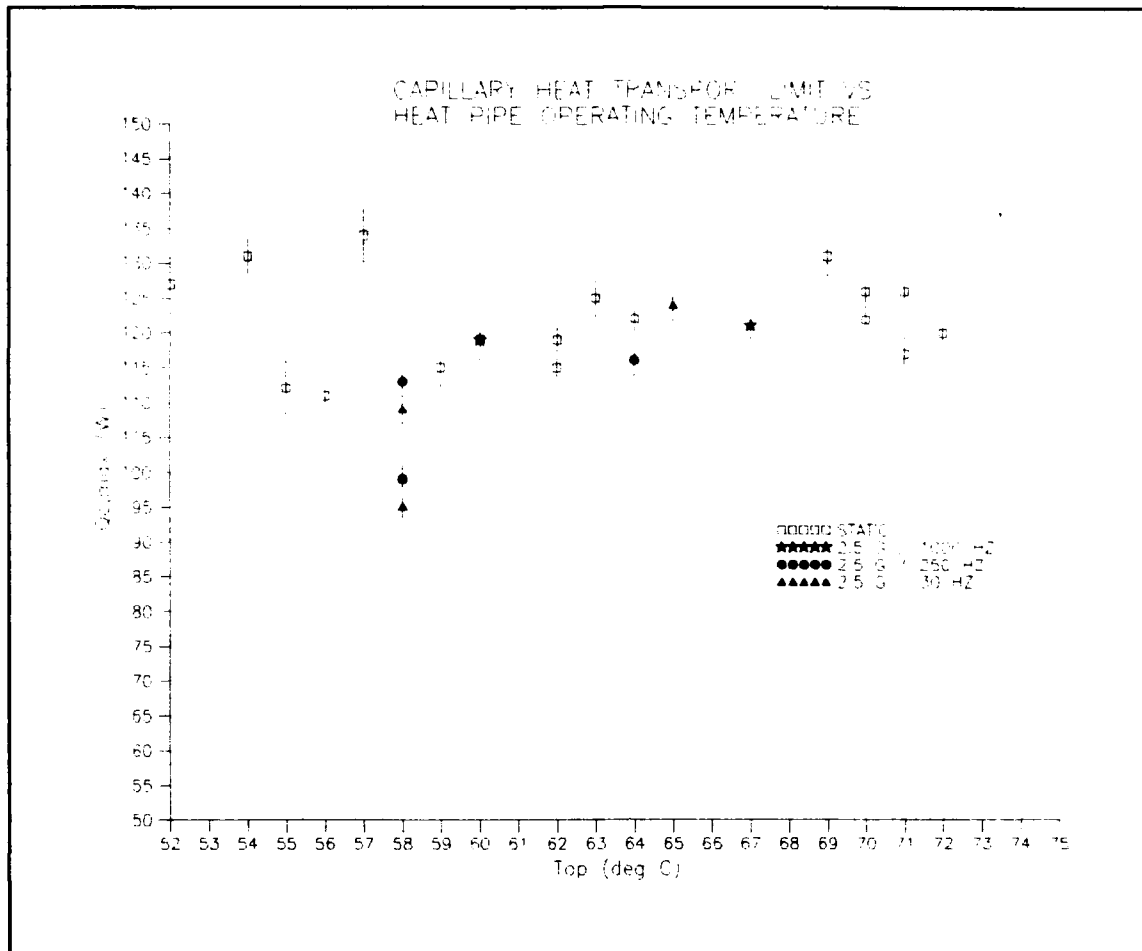


Figure 5.4  $Q_{c,max}$  vs.  $T_{op}$ : Vibration at 2.5 g

The results from the highest level runs were plotted next and can be seen in Figure 5.5 below. Here again, there were several points that appeared to be lower than the static results at the same temperature. The group as a whole, however, did not display any tendency either higher or lower. Therefore, no effect was seen due to vibration at the 5.0 g level.

After evaluating the results according to vibration level, they were next plotted according to frequency of vibration.

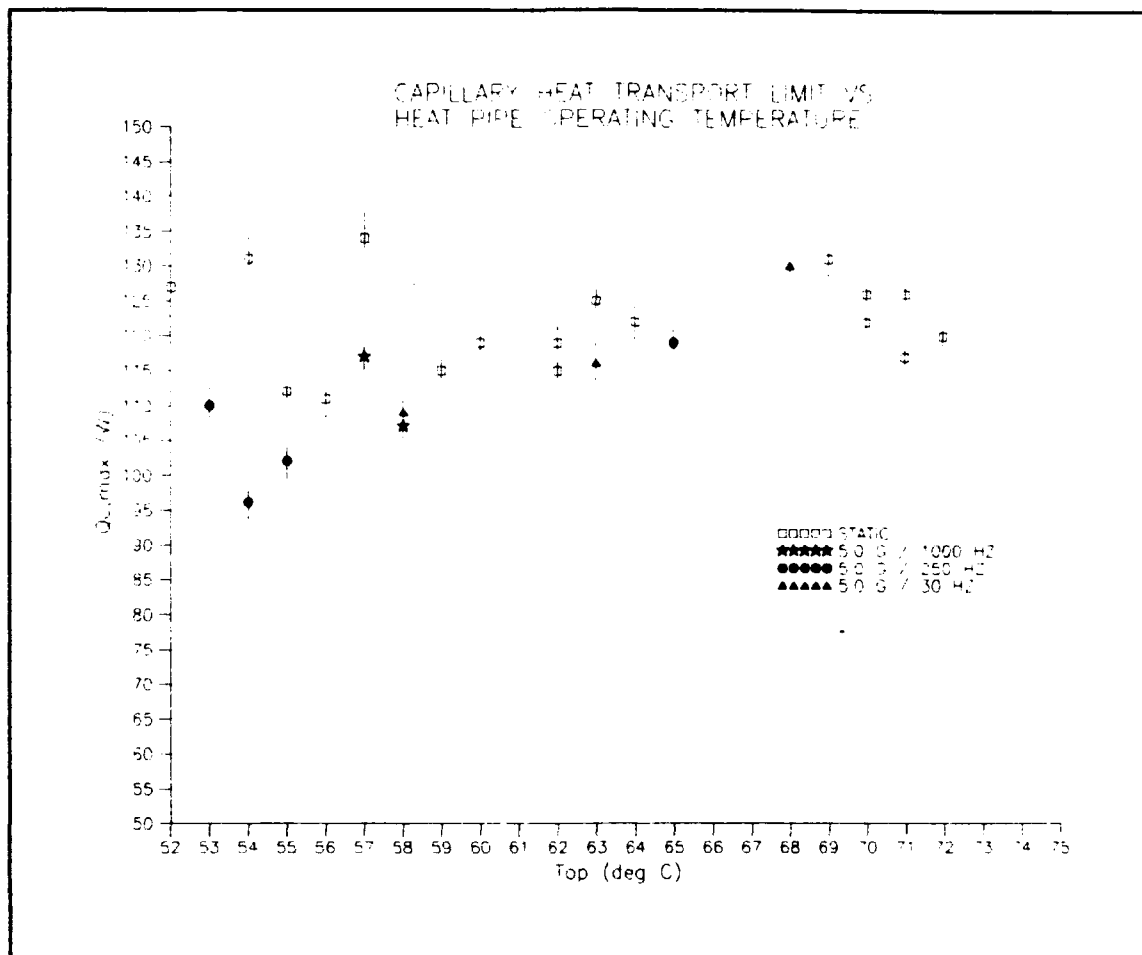


Figure 5.5  $Q_{c,max}$  vs.  $T_{op}$ : Vibration at 5.0 g

Figure 5.6 illustrates the results obtained from all of the 30 Hz test runs versus the static results. This representation of the results again gave several points where  $Q_{c,max}$  was lower than the corresponding static results. Here again, as with all of the runs plotted according to level, there is no trend that encompasses a majority of the points. Based on this, no effect due to vibration at 30 Hz was noted.

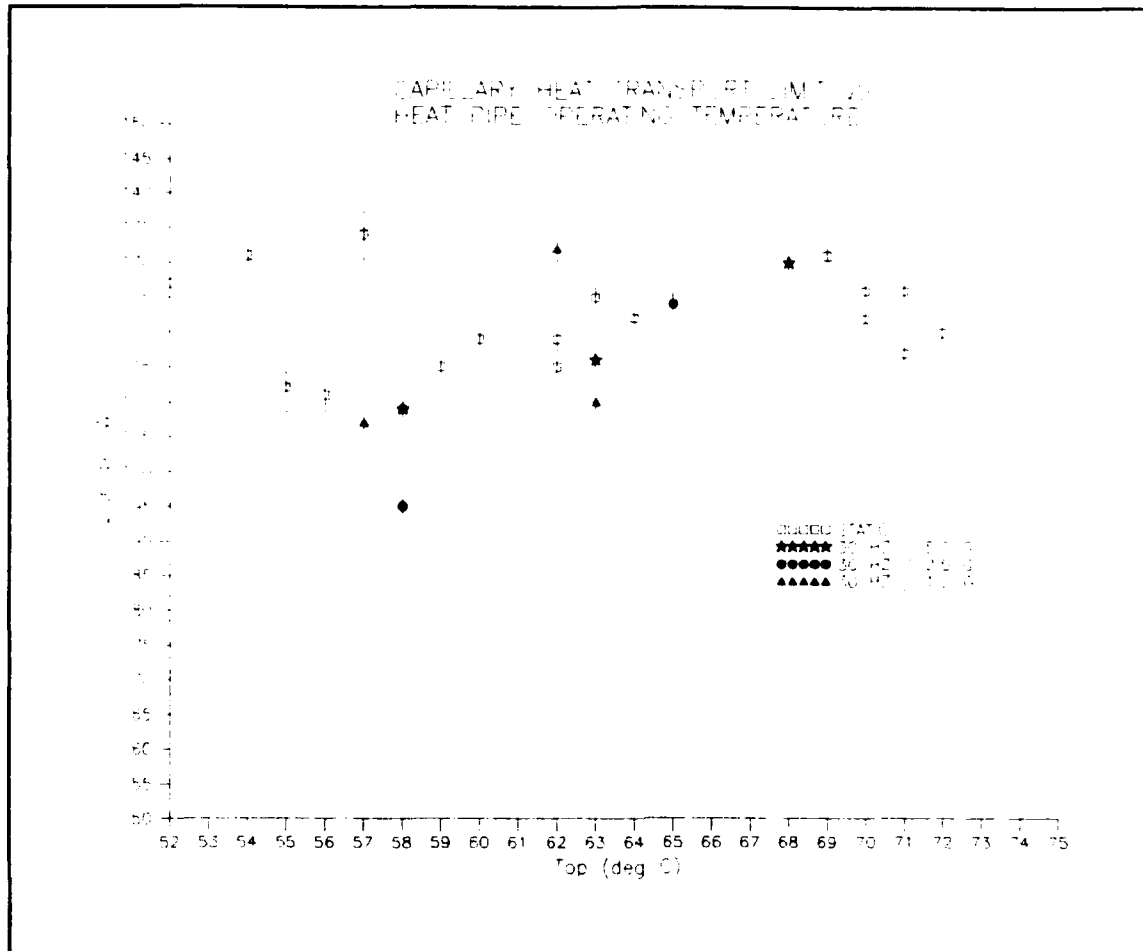


Figure 5.6  $Q_{c,max}$  vs.  $T_{op}$ : Vibration at 30 Hz

Moving to the next frequency, the results of the tests at 250 Hz were plotted as in Figure 5.7. This display of the results was the first to show a majority of the points at a lower  $Q_{c,max}$  than the static results at similar operating temperatures. While most of the points were only slightly lower, there were a number of points that were down significantly. With approximately half of the points still close to the level seen in the static testing, there was no definite degradation in the  $Q_{c,max}$  of the pipe. If these points did indeed represent a drop in the maximum heat

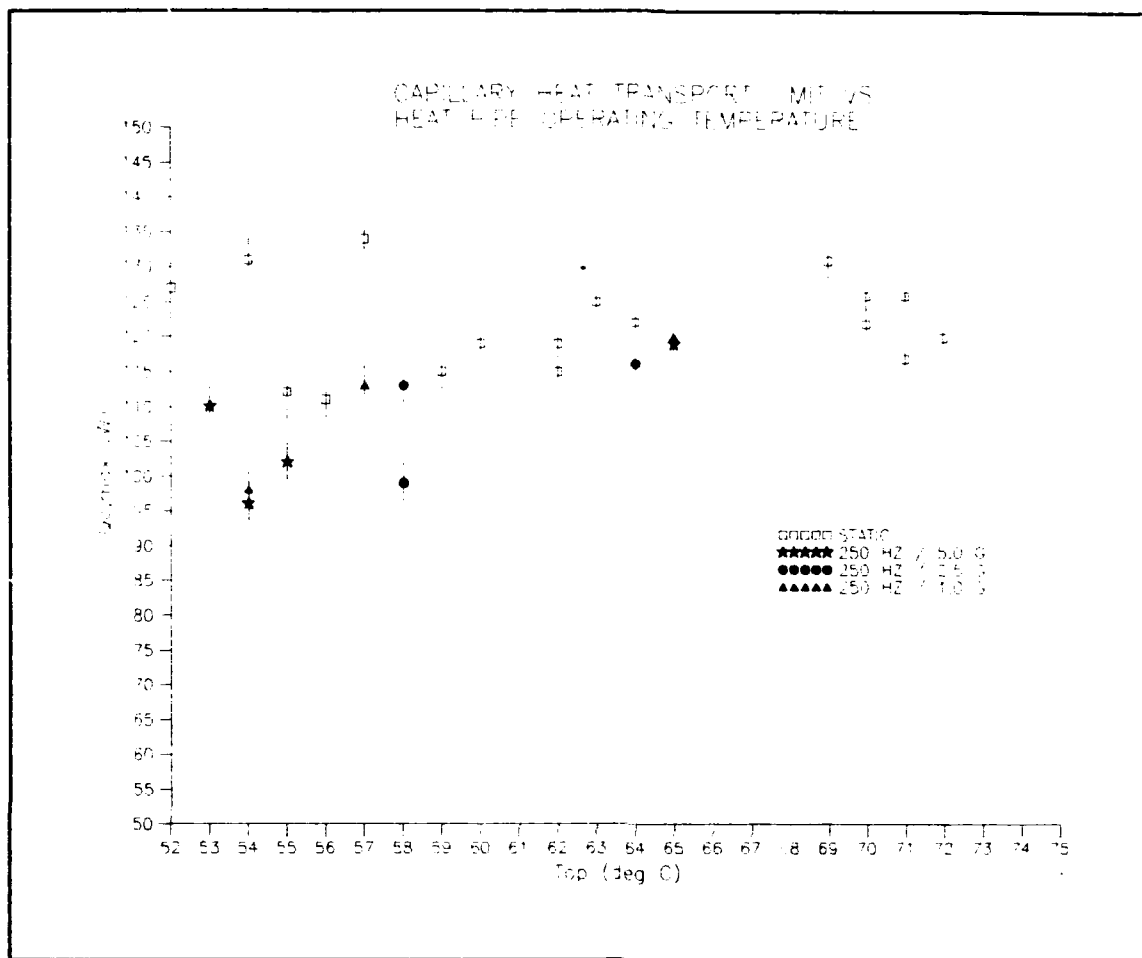


Figure 5.7  $Q_{c,max}$  vs.  $T_{op}$ : Vibration at 250 Hz

transfer rate capability of the pipe, it was a modest decrease.

The last display of the data was a plotting of all of the 1000 Hz runs against the static results. Figure 5.8 shows this representation. The results of the 1000 Hz fell very near the static results. As seen in Figure 5.8, there were a few points slightly above and a few slightly below the corresponding static results. Therefore, no discernable effect due to vibration at 1000 Hz was noted.

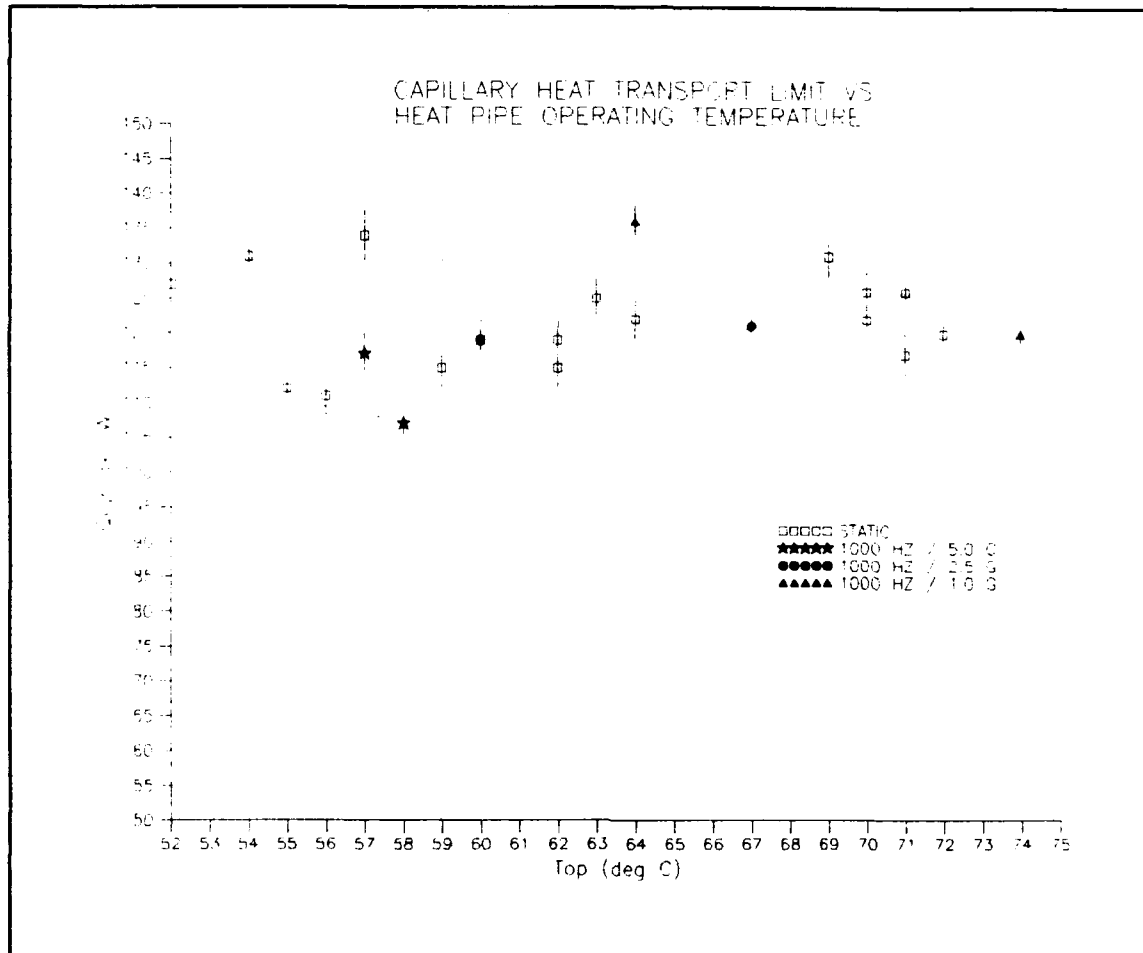


Figure 5.8  $Q_{c, max}$  vs.  $T_{op}$ : Vibration at 1000 Hz

From the preceding analysis of all the data collected, it was determined that the effect of transverse vibration on the capillary limited heat transport rate of this heat pipe was small or nonexistent. It was clear that there was no vibration level dependent effect on  $Q_{c, max}$  for the levels tested in this experiment. This was evident from the lack of any trend in the results when displayed according to vibration level. There was slightly more ambiguity in the results when plotted according to frequency. While it was fairly apparent from the results at 30 Hz and 1000 Hz that

there was no significant effect, the results from the 250 Hz runs were less clear. The fact that several tests at this frequency yielded a  $Q_{c,max}$  below that found during the static tests was cause for a closer look. Given that the remaining results at this frequency were very close to those from the static runs, there could be no conclusive determination that there was indeed an effect due to the vibration. Those results that were low relative to the static runs were low enough to be outside the error bars calculated for the test run. This lends credence to the argument that there is some effect due to vibration at this frequency. Even if there is an effect, the magnitude of the degradation is small, and would probably be much less than the uncertainty in the design process for someone designing a pipe for a particular application.

## VI. Conclusions and Recommendations

The analysis of the experiment design in Chapter 4 and the interpretation of the test results in Chapter 5 provide a basis upon which a conclusion may be drawn regarding the objective of this experiment. There are also a number of recommendations that can be made regarding further research in this area and the improved implementation of this or a similar experiment. The following sections elaborate on these subjects.

### *Conclusions*

For this experiment, a wrapped screen wick copper/water heat pipe was designed, constructed, and then tested to determine what effect transverse vibration would have on its capillary limited heat transport rate,  $Q_{c,max}$ . The heat pipe capillary limit was experimentally determined with no vibration input, and these static results were used as the baseline performance. The capillary limit was then reevaluated while the heat pipe was subjected to vibration normal to its longitudinal axis. The results of the vibration testing were compared to the results of the static testing to determine what effect the vibration had on the performance of the heat pipe. The pipe was tested at vibration frequencies of 30 Hz, 250 Hz, and 1000 Hz. The tests were run at vibration levels of 1.0 g, 2.5 g, and 5.0 g at each frequency.

The comparison of the results from the vibration testing with those from the static testing revealed that there was no significant effect on the capillary limit of the heat pipe due to transverse vibration. The 250 Hz test runs indicated what could be interpreted as a minimal degradation of the maximum heat transport rate, however this finding was inconclusive. While this conclusion can only be strictly applied to this pipe at the vibration frequencies and levels tested, it can also be expected to be applicable to pipes of similar construction at levels of vibration near to those evaluated here.

#### *Recommendations*

*Improvements to the Experiment.* While the conclusions drawn here are believed to be valid, several improvements could be made in the experiment design to reduce the uncertainty in the results. This would increase the repeatability of the data, and increase the confidence level of the conclusions drawn based on the data. In order to do this, the sources of error described in Chapter 4 need to be addressed. This includes both those that were figured into the accumulative experimental error calculated for this experiment, and those assumed to be small and insignificant.

One important improvement would be the measurement of the heat pipe inclination angle instead of assuming its variation is small from test to test. Another would be the minimization of the convection and radiation heat transfer



to the environment by insulating the entire length of the heat pipe. This would insure that the only heat loss from the pipe occurs in the condenser section. A reduction in the uncertainty in the capillary limit calculation would result from a more accurate measurement of the coolant inlet and outlet temperatures. This could be accomplished by taking the measurement at a location closer to the coolant manifold, or even within the manifold. Finally, a significant reduction in uncertainty could be realized with the use of a steady coolant supply. This would help by reducing the uncertainty in the coolant inlet temperature and the coolant flow rate. It would also eliminate the possibility of momentary fluctuations in the flow rate that might cause premature dryout, and therefore erroneous results.

*Other Areas of Investigation.* Research in this area should be continued to better quantify the effects of vibration on heat pipe performance. With the expanding set of environmental conditions under which heat pipes will undoubtedly be employed, it is important that these effects be well understood. While this experiment addressed the impact of transverse vibration on a heat pipe with a screen wick, its conclusion does not necessarily apply to vibration along the longitudinal axis of the pipe, or to heat pipes with different wick structures. The next topic to be investigated should be the effect of longitudinal vibration on heat pipe performance. While this topic has been

addressed to a limited degree by the engineering and scientific communities, few quantitative results exist. Once both transverse and longitudinal vibration effects for a particular heat pipe design have been evaluated, work will need to be done to determine the applicability of those results to heat pipes having a different design.

Appendix A: Thermophysical Properties of Saturated Water

TABLE A.1  
THERMOPHYSICAL PROPERTIES OF SATURATED WATER (5:A22)

TEMP (K)	SPECIFIC VOLUME (m <sup>3</sup> /kg)		HEAT OF VAPOR. (kJ/kg)	SPECIFIC HEAT (kJ/kg·K)	VISCOSITY (N·s/m <sup>2</sup> )		SURFACE TENSION (N/m)
T	$V_1 \cdot 10^3$	$V_v$	$\lambda$	$C_{p,1}$	$\mu_l \cdot 10^6$	$\mu_v \cdot 10^6$	$\sigma \cdot 10^3$
315	1.009	17.820	2402	4.179	631	9.69	69.2
320	1.011	13.980	2390	4.180	577	9.89	68.3
325	1.013	11.060	2378	4.182	528	10.09	67.5
330	1.016	8.820	2366	4.184	489	10.29	66.6
335	1.018	7.090	2354	4.186	453	10.49	65.8
340	1.021	5.740	2342	4.188	420	10.69	64.9
345	1.024	4.683	2329	4.191	389	10.89	64.1
350	1.027	3.846	2317	4.195	365	11.09	63.2
355	1.030	3.180	2304	4.199	343	11.29	62.3
360	1.034	2.645	2291	4.203	324	11.49	61.4
365	1.038	2.212	2278	4.209	306	11.69	60.5
370	1.041	1.861	2265	4.214	289	11.89	59.5
373	1.044	1.679	2257	4.217	279	12.02	58.9
375	1.045	1.574	2252	4.220	274	12.09	58.6
380	1.049	1.337	2239	4.226	260	12.29	57.6

*Appendix B: Table of Test Run Results*

TABLE B.1  
TEST RUN RESULTS

RUN #	VIBRATION FREQ/AMP (Hz/g)	T <sub>OP</sub> (deg C)	Q <sub>C,MAX</sub> (W)
1	STATIC	46	123 ± 7
2	STATIC	64	122 ± 3
3	STATIC	70	122 ± 2
4	STATIC	95	170 ± 3
5	STATIC	81	144 ± 3
6	STATIC	50	143 ± 7
7	STATIC	71	126 ± 2
8	STATIC	55	112 ± 4
9	STATIC	51	137 ± 7
10	STATIC	51	128 ± 5
11	STATIC	54	131 ± 5
12	STATIC	56	111 ± 3
13	STATIC	62	119 ± 3
14	STATIC	72	120 ± 2
15	STATIC	102	187 ± 4
16	STATIC	63	125 ± 3
17	STATIC	71	117 ± 3
18	STATIC	59	115 ± 3
19	STATIC	42	107 ± 11
20	1000 / 1.0	64	136 ± 3
21	1000 / 2.5	60	119 ± 3
22	1000 / 5.0	57	117 ± 3
23	250 / 1.0	57	113 ± 3
24	250 / 2.5	58	113 ± 3

25	250 / 5.0	53	110 ± 3
26	30 / 1.0	62	132 ± 3
27	30 / 2.5	58	109 ± 3
28	30 / 5.0	58	109 ± 3
29	STATIC	52	127 ± 5
30	STATIC	50	121 ± 5
31	STATIC	47	125 ± 7
32	250 / 5.0	55	102 ± 3
33	STATIC	50	146 ± 7
34	1000 / 1.0	74	120 ± 3
35	1000 / 2.5	67	121 ± 3
36	1000 / 5.0	58	107 ± 3
37	250 / 1.0	54	98 ± 3
38	250 / 2.5	58	99 ± 3
39	250 / 5.0	54	96 ± 3
40	30 / 1.0	63	110 ± 3
41	30 / 2.5	58	95 ± 3
42	30 / 5.0	63	116 ± 3
43	STATIC	57	134 ± 4
44	STATIC	60	119 ± 3
45	STATIC	69	131 ± 3
46	STATIC	70	126 ± 3
47	250 / 1.0	65	120 ± 3
48	250 / 2.5	64	116 ± 3
49	250 / 5.0	65	119 ± 3
50	30 / 1.0	57	107 ± 3
51	30 / 2.5	65	124 ± 3
52	30 / 5.0	68	130 ± 3
53	STATIC	62	115 ± 3

## *Appendix C: Reduced Test Run Data*

This appendix contains the reduced test run data for both the static and the vibration test runs. Each page contains the data taken just before and just after dryout for that particular run. While each test spanned a much larger time duration, this format presents the data during the most useful time period.

The header contains the date, run number, coolant flow rate, and the vibration parameters for that run. The vibration frequency and level listed are for the z axis. This is the shaker actuator axis and is normal to the longitudinal axis of the pipe. The levels in parentheses are the x and y axis values. The x axis is the transverse axis normal to the z axis, and the y axis is along the longitudinal axis of the pipe.

The first column contains elapsed time in seconds and the remaining columns display thermocouple data representing pipe wall temperatures. The thermocouples are numbered sequentially with position moving from the heater end of the pipe to the condenser end. Thermocouples T1 through T3 are heater section temperatures, T4 through T6 are adiabatic section temperatures, T7 is the condenser section temperature, T8 is the ambient room temperature, and T9 through T10 give coolant inlet and outlet temperatures respectively.

DATE: 09-19-1992 TIME: 16:13:11

RUN NUMBER: 1

FLOW RATE: 147 CC/MIN

VIBRATION: STATIC

TIME	T1	T2	T3	T4	T5	T6	T7	T8	T9	T10
660	94	93	78	45	44	40	34	22	20	31
665	94	94	78	45	44	40	34	22	20	31
670	95	94	78	45	44	40	34	22	20	31
675	95	94	78	45	44	40	34	22	20	31
680	95	94	78	45	44	40	34	22	20	31
685	95	94	77	45	44	40	34	22	20	31
690	96	95	79	45	44	40	34	22	20	31
695	96	95	79	45	44	40	33	22	20	31
700	96	96	79	45	44	40	34	22	20	31
705	96	96	79	45	44	40	34	22	20	31
710	96	96	79	46	44	40	34	22	20	31
715	97	96	80	45	44	40	34	22	20	31
720	97	96	80	45	44	41	33	22	20	31
725	97	97	80	46	44	40	33	22	20	31
730	97	97	80	45	44	40	33	22	20	32
735	98	97	80	46	45	40	33	22	20	32
740	98	98	81	46	45	41	34	22	20	32
745	99	98	81	46	45	40	34	22	20	32
750	99	98	81	46	45	40	34	22	20	32
755	100	99	82	46	45	40	35	22	20	32
760	100	99	81	46	45	40	35	22	20	32
765	100	99	82	46	45	40	35	22	20	32
770	100	99	82	46	45	40	35	22	20	32
775	101	100	82	46	45	40	35	22	21	32
780	101	100	82	46	45	41	36	22	21	32
785	102	100	82	46	45	41	36	22	20	32
790	103	100	82	46	45	40	35	22	20	32
795	104	101	82	46	45	40	36	22	20	32
800	105	101	83	46	45	40	36	22	21	32
805	106	101	83	46	45	41	36	22	20	32
810	107	101	83	46	45	41	35	22	20	32
815	108	101	83	46	45	40	35	22	20	32
820	109	102	83	46	45	41	35	22	20	32

DATE: 09-19-1992 TIME: 10:31:01

RUN NUMBER: 2

FLOW RATE: 53 CC/MIN

VIBRATION: STATIC

TIME	T1	T2	T3	T4	T5	T6	T7	T8	T9	T10
470	115	114	96	63	62	59	53	21	21	53
475	116	115	97	63	62	59	53	22	21	53
480	116	115	97	63	62	59	52	21	21	53
485	116	115	97	63	62	59	52	21	21	53
490	116	115	97	63	62	59	53	22	21	53
495	117	115	97	63	62	59	53	22	21	53
500	117	116	97	63	62	59	53	22	21	53
505	117	116	97	63	62	59	53	22	21	53
510	117	116	98	63	62	59	53	21	21	53
515	117	116	98	63	62	59	53	21	21	53
520	118	117	98	63	63	59	53	22	21	53
525	118	116	98	64	63	59	54	21	21	53
530	118	117	98	64	63	59	54	22	21	53
535	119	117	98	64	63	59	54	22	21	54
540	119	117	98	64	63	60	54	22	21	54
545	119	118	99	64	63	60	54	22	21	54
550	119	118	98	64	63	59	54	21	21	54
555	120	118	99	64	63	60	54	22	21	54
560	120	118	99	64	63	60	54	21	21	54
565	120	118	99	64	63	60	54	22	21	54
570	120	117	99	64	63	59	54	21	21	54
575	121	119	99	64	63	60	54	22	21	54
580	121	119	100	62	63	60	54	22	21	54
585	122	119	100	64	63	60	54	21	21	54
590	123	119	99	64	63	60	53	21	21	54
595	124	120	99	64	63	60	53	22	21	54
600	125	120	100	64	63	60	54	22	21	54
605	128	120	99	64	63	59	53	22	21	54
610	130	120	99	64	63	59	53	22	21	54
615	132	121	100	64	63	59	53	22	21	54
620	134	121	100	64	63	59	53	21	21	54
625	135	121	100	64	63	59	53	22	21	54
630	136	121	100	64	63	59	54	22	21	54



DATE: 09-19-1992 TIME: 11:16:29

RUN NUMBER: 3

FLOW RATE: 45 CC/MIN

VIBRATION: STATIC

TIME	T1	T2	T3	T4	T5	T6	T7	T8	T9	T10
0	119	120	99	67	66	62	59	22	21	57
5	119	120	100	67	66	62	59	22	21	57
10	120	121	100	67	66	62	59	21	21	57
15	120	121	100	68	66	62	59	22	21	57
20	120	121	99	68	67	63	59	22	21	57
25	121	122	100	68	67	63	59	22	21	57
30	121	122	100	68	67	63	60	21	21	57
35	121	122	101	68	67	63	60	22	21	57
40	121	122	101	68	67	63	60	22	21	57
45	121	122	101	69	67	63	60	22	21	58
50	121	122	101	69	67	64	60	22	21	58
55	122	122	101	69	67	64	60	22	21	58
60	122	123	101	69	68	64	60	21	21	58
65	123	123	102	69	68	64	60	22	21	58
70	123	123	102	69	68	64	60	22	21	58
75	123	124	102	69	68	64	60	22	21	58
80	124	125	103	69	68	64	59	22	21	59
85	124	125	102	69	68	64	60	22	21	58
90	124	125	103	70	68	65	60	22	21	58
95	124	125	103	70	68	65	60	22	21	59
100	125	126	103	70	69	65	61	22	21	59
105	125	126	103	70	69	65	61	21	21	59
110	126	126	103	70	69	65	61	22	21	59
115	127	127	103	70	69	65	61	22	21	59
120	127	127	103	70	69	65	60	22	21	59
125	128	127	104	70	69	65	60	21	21	60
130	130	127	104	70	69	65	60	22	21	59
135	131	127	104	71	69	66	60	22	21	59
140	133	127	104	70	69	66	60	22	21	59
145	134	127	104	70	69	66	60	22	21	60
150	135	127	104	70	69	66	61	22	21	60
155	136	128	104	71	69	66	61	22	21	60
160	137	128	105	71	70	66	61	22	21	60

DATE: 09-19-1992 TIME: 12:04:00

RUN NUMBER: 4

FLOW RATE: 40 CC/MIN

VIBRATION: STATIC

TIME	T1	T2	T3	T4	T5	T6	T7	T8	T9	T10
600	155	154	130	94	92	88	84	22	22	81
605	156	154	130	94	93	88	84	22	22	81
610	156	155	130	94	93	88	84	22	22	81
615	156	155	130	94	93	89	85	22	22	81
620	157	155	131	94	93	89	84	21	22	82
625	157	155	131	94	93	89	85	22	22	81
630	157	156	131	94	93	89	85	22	22	82
635	157	156	131	94	93	89	85	22	22	82
640	157	156	131	95	93	89	85	22	22	82
645	158	157	131	95	94	89	86	22	22	82
650	159	157	132	95	94	89	86	22	22	82
655	159	157	132	95	94	89	86	22	22	82
660	159	157	132	95	94	89	86	22	22	82
665	160	158	132	95	94	90	86	22	22	82
670	160	158	133	95	94	90	86	22	22	82
675	160	158	133	95	94	90	86	22	22	82
680	160	158	133	96	94	90	86	22	22	82
685	160	158	133	96	95	90	86	22	22	83
690	161	159	133	96	95	90	86	22	22	83
695	161	159	133	96	94	90	86	21	22	83
700	162	159	133	96	95	90	86	22	22	83
705	162	159	133	96	94	90	86	22	22	83
710	162	159	133	96	94	90	86	22	22	83
715	162	159	134	95	94	90	86	22	22	84
720	163	159	133	95	94	90	86	22	22	84
725	163	159	133	95	94	90	86	22	22	83
730	163	159	133	95	94	90	86	22	22	83
735	164	159	133	95	94	90	86	22	22	83
740	165	160	133	95	94	89	86	22	22	83
745	165	159	133	95	94	89	86	22	22	82
750	166	159	133	95	94	89	85	22	22	83
755	166	160	133	95	94	89	85	22	22	83
760	167	160	133	95	94	89	85	21	22	83

DATE: 09-19-1992 TIME: 13:51:45

RUN NUMBER: 5

FLOW RATE: 43 CC/MIN

VIBRATION: STATIC

TIME	T1	T2	T3	T4	T5	T6	T7	T8	T9	T10
190	135	135	114	78	77	74	68	21	22	67
195	135	135	114	78	78	74	68	22	22	67
200	135	136	114	79	78	74	68	22	22	67
205	135	136	114	79	78	74	68	21	22	67
210	136	135	115	79	78	74	69	22	22	68
215	136	136	115	79	78	74	69	21	22	68
220	136	137	115	79	78	74	69	22	22	68
225	136	137	115	79	78	74	69	22	22	68
230	136	137	115	79	78	74	69	21	22	68
235	137	137	116	80	79	74	70	22	22	68
240	137	138	116	80	79	75	70	22	22	68
245	137	138	116	79	79	75	70	21	22	68
250	138	138	116	79	78	75	70	21	22	68
255	138	139	116	80	79	75	70	21	22	69
260	138	139	116	80	79	75	71	21	22	69
265	139	139	117	80	79	75	70	22	22	69
270	139	140	117	80	79	75	71	21	22	69
275	139	140	117	81	80	76	71	22	22	69
280	140	140	118	81	80	76	71	22	22	69
285	140	140	117	81	80	76	71	21	22	69
290	140	141	118	81	80	76	71	22	22	69
295	140	141	118	81	80	76	71	22	22	69
300	141	141	118	81	80	76	71	22	22	70
305	142	142	118	81	79	76	71	22	22	70
310	143	142	118	81	79	75	71	22	22	70
315	145	143	118	80	80	76	71	22	22	70
320	146	143	119	81	80	76	71	22	22	70
325	147	143	118	81	80	76	71	22	22	70
330	149	143	119	81	80	76	71	22	22	70
335	153	144	119	81	80	76	71	22	22	70
340	156	144	119	81	79	76	71	22	22	70
345	158	145	119	81	80	76	71	22	22	70
350	160	146	119	80	79	76	71	21	22	70

DATE: 09-19-1992 TIME: 14:19:42

RUN NUMBER: 6

FLOW RATE: 146 CC/MIN

VIBRATION: STATIC

TIME	T1	T2	T3	T4	T5	T6	T7	T8	T9	T10
665	103	102	86	49	48	43	39	22	20	34
670	103	103	87	49	48	43	40	22	20	34
675	104	103	87	49	48	43	40	22	21	34
680	104	103	87	49	48	43	40	22	21	34
685	104	103	87	49	48	43	40	21	20	34
690	104	104	87	49	48	43	40	22	20	34
695	105	104	88	49	48	43	40	22	21	34
700	105	104	88	49	48	43	40	22	21	34
705	105	104	88	49	48	43	40	22	20	34
710	105	104	88	49	48	43	40	22	20	34
715	105	105	88	49	48	43	40	22	20	34
720	106	105	88	50	49	43	40	22	20	34
725	106	105	89	50	49	43	40	22	21	34
730	106	105	89	50	49	43	40	22	21	34
735	106	105	89	50	48	43	40	21	20	34
740	107	106	89	50	49	43	40	22	20	34
745	107	106	88	50	49	44	40	22	20	34
750	108	107	90	50	49	44	40	22	20	34
755	108	107	90	50	49	44	40	22	21	34
760	108	107	90	50	49	44	40	22	21	35
765	109	107	90	50	49	44	40	22	21	35
770	109	108	90	50	49	44	40	22	20	35
775	109	108	90	50	49	44	40	21	20	34
780	110	108	90	50	49	44	40	21	21	34
785	111	108	91	50	49	44	39	22	21	34
790	112	108	91	49	49	44	40	22	21	35
795	112	108	91	50	49	44	40	21	20	35
800	113	109	91	50	49	44	40	22	21	35
805	114	109	91	51	49	44	40	22	21	35
810	114	109	91	51	49	44	40	22	20	35
815	114	110	92	50	49	44	40	21	20	35
820	115	110	91	50	49	44	40	21	20	35
825	115	110	92	51	49	44	40	22	20	35

DATE: 09-19-1992 TIME: 15:07:06

RUN NUMBER: 7

FLOW RATE: 45 CC/MIN

VIBRATION: STATIC

TIME	T1	T2	T3	T4	T5	T6	T7	T8	T9	T10
355	124	123	102	70	68	65	60	22	21	60
360	125	124	102	70	69	65	60	22	21	60
365	125	124	102	70	69	66	60	22	21	60
370	125	124	102	70	69	66	60	22	21	60
375	126	124	103	70	69	66	60	22	21	60
380	126	125	103	70	69	66	59	22	21	60
385	126	125	103	70	69	66	60	22	21	60
390	127	125	103	70	69	66	60	22	21	60
395	127	125	103	70	69	66	61	22	21	61
400	127	126	104	70	69	66	61	22	21	61
405	128	126	104	71	69	66	61	22	21	61
410	128	127	104	71	70	66	61	22	21	61
415	129	127	104	71	70	66	61	22	21	61
420	129	127	104	71	70	66	61	22	21	61
425	130	127	105	71	70	67	62	22	21	61
430	130	128	105	71	70	67	61	22	21	61
435	131	128	105	71	70	67	62	22	21	61
440	132	128	105	71	70	67	62	22	21	61
445	132	128	105	71	70	67	62	22	21	61
450	133	128	105	71	70	67	63	22	21	61
455	133	129	105	71	70	67	63	22	21	61
460	134	129	105	71	70	67	62	22	21	61
465	135	129	105	71	70	67	61	22	21	61
470	136	129	106	71	70	67	61	22	21	61
475	137	130	106	71	71	67	61	22	21	61
480	137	130	106	71	71	67	61	22	21	61
485	138	131	106	71	71	67	62	22	21	62
490	139	132	106	71	71	67	62	22	21	62
495	140	132	106	72	71	67	62	22	21	61
500	141	132	106	72	71	67	61	22	21	62
505	143	132	107	72	71	67	61	22	21	62
510	145	133	107	72	71	67	61	22	21	62
515	147	133	107	71	71	67	61	22	21	62

DATE: 09-19-1992 TIME: 15:47:36

RUN NUMBER: 8

FLOW RATE: 67 CC/MIN

VIBRATION: STATIC

TIME	T1	T2	T3	T4	T5	T6	T7	T8	T9	T10
60	105	101	85	54	53	50	45	22	21	44
65	105	102	86	54	53	50	43	22	21	43
70	105	102	86	54	53	50	44	22	21	44
75	106	102	86	54	53	50	45	22	21	44
80	106	102	86	54	53	50	45	22	21	44
85	106	102	86	54	53	50	45	22	21	44
90	106	102	87	54	53	50	45	22	21	44
95	106	102	87	54	53	50	46	22	21	44
100	107	103	87	55	53	50	46	22	21	44
105	107	103	87	55	53	50	46	22	21	44
110	107	103	87	55	54	50	46	22	21	44
115	107	103	87	55	54	50	46	22	21	44
120	107	103	87	55	54	50	46	21	21	44
125	108	103	87	55	54	50	47	22	21	44
130	108	104	88	55	54	51	46	22	21	44
135	108	104	88	55	54	51	46	22	21	44
140	109	104	88	55	54	51	46	22	21	44
145	109	105	88	55	54	51	46	22	21	44
150	109	105	88	55	54	51	46	22	21	44
155	109	105	89	55	54	51	46	22	21	45
160	110	105	89	55	54	51	46	22	21	45
165	110	105	89	56	54	51	46	22	21	45
170	110	105	89	55	54	51	46	22	21	45
175	111	105	89	55	54	51	47	22	21	45
180	112	106	89	55	54	51	46	22	21	45
185	112	106	89	55	54	51	46	22	21	45
190	113	106	89	56	54	51	47	22	21	45
195	114	106	90	56	54	51	47	22	21	45
200	114	106	90	56	55	51	47	22	21	45
205	115	107	90	56	55	51	47	22	21	45
210	116	107	90	56	55	51	47	22	21	45
215	116	107	90	56	55	51	47	22	21	45
220	116	107	90	56	55	51	46	22	21	45

DATE: 09-21-1992 TIME: 10:05:22

RUN NUMBER: 9

FLOW RATE: 131 CC/MIN

VIBRATION: STATIC

TIME	T1	T2	T3	T4	T5	T6	T7	T8	T9	T10
685	102	100	85	50	48	43	39	21	21	35
690	102	101	85	50	49	43	39	22	21	35
695	102	101	85	50	49	43	39	21	21	35
700	103	101	86	50	49	44	39	22	21	35
705	103	101	86	50	49	44	39	21	21	35
710	103	102	86	50	49	44	39	21	21	35
715	103	102	86	50	49	44	39	21	21	35
720	103	102	86	50	49	44	39	21	21	35
725	104	102	86	50	49	44	39	21	21	35
730	104	102	87	50	49	44	39	22	21	35
735	104	103	87	50	49	44	40	22	21	36
740	105	103	87	50	49	44	40	21	21	35
745	105	103	87	50	49	45	39	22	21	36
750	105	103	87	50	49	45	39	22	21	36
755	105	104	88	50	49	45	39	22	21	35
760	105	105	88	50	49	45	39	22	21	36
765	106	105	88	50	49	45	40	22	22	36
770	106	106	89	51	50	45	40	22	21	36
775	106	106	89	50	50	44	40	21	21	36
780	107	106	89	51	50	45	40	22	21	36
785	107	106	90	51	50	45	40	22	21	36
790	108	107	90	51	50	45	40	22	21	36
795	108	107	90	51	50	45	39	22	21	36
800	109	107	90	51	50	45	39	22	21	36
805	110	108	90	51	50	45	39	22	21	36
810	111	108	90	51	50	45	39	22	21	36
815	111	108	90	51	50	45	40	22	21	36
820	111	108	91	51	50	45	39	22	21	36
825	112	108	91	51	50	45	39	22	21	36
830	112	109	91	51	50	45	39	22	21	36
835	113	109	91	51	50	45	39	22	21	36
840	113	109	91	51	50	45	40	21	21	36
845	114	109	91	51	51	45	40	22	21	36

DATE: 09-21-1992 TIME: 10:53:16

RUN NUMBER: 10

FLOW RATE: 108 CC/MIN

VIBRATION: STATIC

TIME	T1	T2	T3	T4	T5	T6	T7	T8	T9	T10
495	107	104	87	50	49	44	41	21	20	37
500	107	104	87	50	50	44	41	21	20	37
505	107	104	88	50	50	45	41	21	20	37
510	107	104	88	50	49	45	41	21	20	37
515	107	105	88	50	50	45	41	21	20	37
520	108	105	88	51	50	45	40	21	20	37
525	108	105	88	51	50	45	40	22	20	37
530	108	105	88	51	50	45	41	21	20	37
535	109	105	88	51	50	45	41	21	20	37
540	109	105	88	51	50	45	41	21	20	37
545	110	106	88	50	50	45	41	21	20	37
550	110	106	88	51	50	45	41	21	20	37
555	111	106	89	51	50	45	41	22	20	37
560	111	106	89	51	50	45	41	21	20	37
565	111	106	89	51	50	45	41	22	20	37
570	112	107	89	51	50	45	41	21	20	37
575	112	107	89	51	50	45	41	21	20	37
580	113	107	89	51	50	46	41	21	20	37
585	113	107	89	51	50	46	40	21	20	37
590	114	108	89	51	50	46	40	21	20	37
595	114	108	90	51	50	46	41	21	20	37
600	115	108	90	51	50	46	41	21	20	37
605	115	108	90	51	50	46	40	21	20	37
610	116	108	90	52	50	46	39	21	20	37
615	117	108	90	52	50	46	39	21	20	37
620	118	109	90	52	50	46	39	21	20	37
625	119	109	90	51	50	46	39	21	20	37
630	120	109	90	52	50	46	39	21	20	38
635	121	109	90	52	50	46	39	21	20	38
640	122	109	90	52	50	46	40	21	20	38
645	124	110	90	51	50	46	40	21	20	37
650	125	110	90	51	50	46	40	21	20	38
655	126	110	91	51	50	46	40	21	20	37



DATE: 09-21-1992 TIME: 12:15:43

RUN NUMBER: 11

FLOW RATE: 94 CC/MIN

VIBRATION: STATIC

TIME	T1	T2	T3	T4	T5	T6	T7	T8	T9	T10
100	109	109	91	53	52	48	41	22	21	41
105	109	109	91	53	52	48	41	22	21	40
110	110	109	92	53	52	48	42	22	21	40
115	110	110	92	53	52	48	41	22	21	40
120	110	110	92	53	52	48	40	21	21	40
125	110	110	92	53	52	48	40	21	21	41
130	111	110	92	53	52	49	40	21	21	40
135	111	110	92	54	52	49	40	21	21	41
140	111	111	92	54	52	49	40	21	21	41
145	112	111	92	54	52	49	40	21	20	41
150	112	111	93	54	52	49	40	21	21	41
155	113	111	93	54	53	49	41	21	21	41
160	113	111	93	54	52	49	40	21	21	41
165	113	111	93	54	52	49	40	21	21	41
170	114	112	93	54	53	49	41	21	21	41
175	114	112	93	54	53	49	41	21	21	41
180	114	112	93	54	53	49	41	21	21	41
185	114	112	93	54	53	49	41	21	21	41
190	114	112	93	54	53	49	41	21	21	41
195	115	112	93	54	53	49	40	21	21	41
200	115	112	94	54	53	49	41	21	21	41
205	115	113	94	54	53	49	41	21	20	41
210	116	113	94	54	53	49	40	21	21	41
215	117	113	94	54	53	49	40	22	21	41
220	118	113	94	54	53	49	40	21	21	41
225	118	113	94	54	53	49	40	21	20	41
230	119	113	94	54	53	49	40	21	20	41
235	119	114	94	54	53	49	40	21	21	41
240	119	114	94	54	53	49	40	21	21	42
245	120	114	95	54	53	49	41	22	21	41
250	121	115	95	54	53	49	41	21	21	41
255	121	115	95	54	53	50	40	21	21	42
260	122	115	95	54	53	50	40	21	21	41

DATE: 09-21-1992 TIME: 12:47:55

RUN NUMBER: 12

FLOW RATE: 61 CC/MIN

VIBRATION: STATIC

TIME	T1	T2	T3	T4	T5	T6	T7	T8	T9	T10
370	110	103	86	55	54	50	46	21	20	45
375	111	103	86	55	54	50	46	21	20	45
380	111	103	86	55	54	51	46	21	20	45
385	111	104	87	55	54	51	46	22	20	45
390	112	104	87	55	54	51	46	21	20	45
395	112	104	87	55	54	51	46	21	20	45
400	113	104	87	55	54	51	46	22	20	45
405	113	104	87	55	54	51	47	22	22	47
410	113	104	87	55	54	51	46	21	21	45
415	114	105	87	55	54	51	47	22	20	45
420	114	105	87	56	55	51	47	22	21	46
425	114	105	87	55	55	51	47	21	20	46
430	114	105	88	54	55	51	47	21	20	46
435	115	105	88	56	55	51	47	22	20	46
440	115	105	88	56	55	51	47	21	20	46
445	115	105	88	56	55	52	46	21	21	46
450	116	105	88	56	55	52	47	22	20	46
455	116	106	88	56	55	52	46	22	20	46
460	116	106	88	56	55	52	46	21	20	46
465	116	106	88	56	55	52	46	21	20	46
470	116	106	88	56	55	52	45	21	21	46
475	117	106	88	56	55	52	44	21	20	46
480	117	106	88	56	55	52	44	21	21	46
485	117	106	88	56	55	52	44	22	20	46
490	118	106	88	56	55	52	44	22	20	46
495	118	106	88	56	55	52	44	22	20	46
500	118	106	88	55	55	52	44	22	20	47
505	119	106	88	56	55	52	45	22	20	47
510	119	106	88	56	55	52	44	22	20	47
515	120	106	88	56	55	52	44	21	21	47
520	120	106	88	56	55	52	44	21	20	47
525	120	106	88	56	55	52	44	21	21	47
530	120	106	88	56	55	52	44	21	20	47

DATE: 09-21-1992 TIME: 13:55:53

RUN NUMBER: 13

FLOW RATE: 55 CC/MIN

VIBRATION: STATIC

TIME	T1	T2	T3	T4	T5	T6	T7	T8	T9	T10
290	111	110	93	60	59	56	51	22	21	50
295	112	110	93	60	59	56	51	22	21	50
300	112	111	94	60	59	55	51	21	21	50
305	112	111	94	60	59	56	51	22	21	50
310	112	111	94	60	60	56	51	22	21	50
315	113	111	94	60	59	56	52	21	21	50
320	113	111	94	60	59	56	52	21	21	50
325	113	112	95	60	60	56	52	22	21	50
330	114	112	95	61	60	56	53	22	21	50
335	114	112	95	59	60	56	52	21	21	50
340	114	112	95	61	60	57	53	22	21	51
345	114	112	95	61	60	57	53	22	21	51
350	114	113	95	61	60	57	53	21	21	50
355	115	113	96	61	60	57	53	22	21	51
360	115	113	96	61	60	57	53	22	21	51
365	115	114	96	61	61	57	53	22	21	51
370	116	114	96	62	61	57	53	22	21	51
375	116	114	97	62	61	57	53	22	21	51
380	116	114	97	62	61	58	53	22	21	51
385	117	115	97	62	61	58	53	22	21	51
390	117	115	97	62	61	57	54	21	21	51
395	117	115	97	62	61	58	54	22	21	51
400	117	115	98	62	61	57	54	21	21	51
405	118	115	98	62	61	57	54	21	21	51
410	119	116	98	62	61	58	54	22	21	52
415	121	116	98	62	62	58	54	22	21	52
420	121	116	98	62	62	58	54	22	21	52
425	122	116	98	63	62	58	53	21	21	52
430	123	117	98	63	62	58	54	22	21	52
435	123	117	98	63	62	58	54	22	21	52
440	124	117	98	63	62	58	54	22	21	52
445	126	117	98	63	62	58	53	22	21	52
450	127	118	98	63	62	58	53	21	21	52

DATE: 09-21-1992 TIME: 14:44:59

RUN NUMBER: 14

FLOW RATE: 41 CC/MIN

VIBRATION: STATIC

TIME	T1	T2	T3	T4	T5	T6	T7	T8	T9	T10
330	123	122	102	70	69	66	61	21	21	61
335	124	123	102	70	69	66	61	22	21	61
340	124	123	102	70	69	66	62	22	21	61
345	125	123	102	70	69	66	62	22	21	61
350	125	123	102	70	70	67	62	22	21	61
355	125	124	102	71	69	67	62	22	21	61
360	126	124	103	71	70	67	62	22	21	61
365	126	124	103	71	70	67	62	22	21	61
370	126	125	103	71	70	67	62	22	21	61
375	126	125	103	71	70	67	62	22	21	61
380	127	125	103	71	70	67	62	21	21	62
385	127	125	104	71	70	67	62	22	21	62
390	128	125	104	71	71	67	62	22	21	62
395	128	126	104	72	71	68	62	22	21	62
400	129	126	104	72	71	68	62	22	21	62
405	129	126	104	72	71	68	62	21	21	62
410	129	126	104	72	71	68	62	22	21	62
415	130	126	104	72	71	68	63	22	21	62
420	130	127	105	72	71	68	63	21	21	63
425	130	127	105	72	71	68	63	21	21	63
430	131	127	105	72	71	68	63	22	21	63
435	131	127	105	72	71	68	63	21	21	63
440	131	127	105	73	72	68	63	21	21	63
445	132	128	105	73	72	69	63	21	21	63
450	133	128	105	73	72	69	63	21	21	63
455	134	128	105	73	72	69	64	21	21	63
460	134	128	106	73	72	69	64	21	21	63
465	135	129	106	74	72	69	64	21	21	63
470	135	129	106	74	73	70	64	22	21	64
475	136	129	106	74	73	70	64	21	21	64
480	137	129	106	74	73	69	64	21	21	64
485	138	130	106	74	73	70	64	21	21	64
490	139	130	107	74	73	70	64	21	21	64

DATE: 09-21-1992 TIME: 15:49:55

RUN NUMBER: 15

FLOW RATE: 40 CC/MIN

VIBRATION: STATIC

TIME	T1	T2	T3	T4	T5	T6	T7	T8	T9	T10
110	172	170	143	104	103	98	96	22	22	91
115	172	171	143	104	103	98	95	22	22	92
120	172	170	143	104	102	97	95	22	22	91
125	172	170	143	103	102	97	95	22	22	91
130	173	170	143	103	102	97	94	22	22	91
135	173	170	143	103	102	97	94	22	22	91
140	174	170	143	103	102	96	94	22	22	91
145	174	170	143	103	102	96	94	22	22	91
150	175	171	143	102	101	96	94	22	22	91
155	176	170	142	102	101	96	94	22	22	90
160	176	170	142	102	101	96	94	22	22	90
165	176	170	143	102	101	96	94	22	22	90
170	176	171	143	102	101	96	93	22	22	90
175	177	171	142	102	101	95	93	22	22	89
180	177	171	143	102	101	96	94	22	22	89
185	177	171	143	102	101	96	94	22	22	89
190	177	171	142	102	101	96	93	22	22	89
195	178	171	142	102	101	96	93	22	22	89
200	179	171	142	102	101	95	93	22	22	89
205	180	171	142	102	100	95	93	22	22	89
210	181	171	142	102	100	95	93	22	22	89
215	182	171	142	102	101	95	93	22	22	89
220	183	171	142	102	100	95	93	22	22	88
225	185	171	142	101	100	95	93	22	22	87
230	186	171	142	101	100	95	92	22	22	87
235	189	171	142	101	100	95	91	22	22	88
240	192	171	142	101	100	95	91	22	22	89
245	195	171	142	101	100	95	91	22	22	88
250	197	171	142	101	100	95	91	22	22	88
255	199	170	142	101	99	95	91	22	22	88
260	201	171	142	101	99	94	91	22	22	88
265	204	171	142	100	99	94	90	22	22	88
270	206	171	142	100	99	94	90	22	22	88

DATE: 09-21-1992 TIME: 16:20:12

RUN NUMBER: 16

FLOW RATE: 58 CC/MIN

VIBRATION: STATIC

TIME	T1	T2	T3	T4	T5	T6	T7	T8	T9	T10
285	114	110	95	61	60	56	51	22	21	50
290	115	111	95	61	60	56	51	22	21	50
295	115	111	95	61	60	56	52	22	21	50
300	115	111	96	61	60	57	51	22	21	50
305	116	112	96	61	60	57	52	22	21	50
310	116	112	96	61	60	57	52	22	21	50
315	116	112	96	61	60	57	51	22	21	50
320	117	112	96	62	60	57	51	22	21	50
325	117	112	96	61	60	57	52	22	21	51
330	117	113	97	62	61	57	52	22	21	51
335	118	113	97	62	61	57	51	22	21	51
340	118	113	97	62	61	57	51	22	21	51
345	118	113	97	62	61	58	51	22	21	51
350	119	114	97	62	61	58	51	22	20	51
355	119	114	97	62	61	58	51	22	21	51
360	119	114	97	62	61	58	51	22	21	51
365	119	114	98	62	61	58	51	22	21	52
370	120	114	98	62	61	58	52	22	21	51
375	121	114	98	62	61	58	52	22	21	51
380	121	114	98	62	61	58	52	22	21	51
385	121	115	98	62	61	58	51	22	21	52
390	122	115	98	63	61	58	52	22	21	52
395	122	115	98	63	62	58	52	22	22	52
400	123	115	98	63	62	58	52	22	21	52
405	124	115	98	63	62	58	52	22	21	52
410	125	115	99	63	62	58	51	22	21	52
415	126	115	99	63	62	58	52	22	21	52
420	126	116	99	63	62	58	52	22	21	52
425	127	116	99	63	62	58	52	22	21	52
430	128	116	99	63	62	58	52	22	21	52
435	129	116	99	63	62	58	52	22	21	52
440	129	116	99	63	62	58	53	22	21	52
445	130	116	99	63	62	58	52	22	21	52

DATE: 09-21-1992 TIME: 19:19:13

RUN NUMBER: 17

FLOW RATE: 43 CC/MIN

VIBRATION: STATIC

TIME	T1	T2	T3	T4	T5	T6	T7	T8	T9	T10
330	120	117	100	68	68	65	60	22	22	59
335	120	118	100	69	68	65	60	22	22	59
340	121	118	100	69	68	65	60	22	22	59
345	121	118	100	69	68	65	60	22	22	59
350	121	118	100	69	68	65	60	22	22	60
355	121	119	101	69	68	65	60	22	22	59
360	121	119	101	69	68	65	60	22	22	59
365	122	119	101	69	68	65	60	22	22	60
370	122	119	101	69	69	66	60	22	22	60
375	122	120	101	69	69	66	60	22	22	60
380	123	120	102	70	69	66	60	22	22	60
385	123	120	102	70	69	66	60	22	22	60
390	123	121	102	70	69	66	60	22	22	60
395	124	121	102	70	69	66	60	22	22	60
400	124	121	102	70	70	66	61	22	22	60
405	124	121	103	70	70	67	61	22	22	60
410	125	122	103	70	70	66	61	22	22	61
415	125	122	103	70	70	67	61	22	22	60
420	125	122	103	71	70	67	61	22	22	60
425	126	122	103	71	70	67	62	22	22	60
430	126	123	103	71	70	67	62	22	22	61
435	126	123	104	71	70	67	62	22	22	61
440	126	123	104	71	70	67	62	22	22	61
445	127	123	104	71	71	67	61	22	22	61
450	128	123	104	71	71	67	62	22	22	61
455	129	124	104	72	71	68	62	22	23	61
460	129	124	104	71	71	68	62	22	22	61
465	130	124	105	72	71	68	62	22	22	61
470	130	124	104	72	71	68	63	22	22	61
475	131	125	105	72	71	68	62	22	22	62
480	131	125	105	72	71	68	63	22	22	61
485	132	125	105	72	71	68	63	22	22	61
490	133	125	105	72	72	68	63	22	22	62

DATE: 09-21-1992 TIME: 19:52:34

RUN NUMBER: 18

FLOW RATE: 57 CC/MIN

VIBRATION: STATIC

TIME	T1	T2	T3	T4	T5	T6	T7	T8	T9	T10
420	108	106	90	57	56	53	47	22	20	47
425	108	107	90	58	57	54	47	23	20	48
430	109	106	90	58	56	54	47	22	20	47
435	109	107	90	58	57	54	47	22	20	48
440	109	107	90	58	57	54	47	22	20	48
445	109	107	91	58	57	54	47	22	20	48
450	109	108	91	58	57	54	47	22	20	48
455	110	108	91	58	57	54	48	22	20	48
460	110	108	90	58	57	54	48	22	20	48
465	111	108	91	58	57	54	48	22	20	48
470	111	108	91	58	57	54	48	22	20	48
475	111	109	92	58	57	54	48	22	20	48
480	111	109	92	58	57	54	48	22	20	48
485	112	109	92	59	58	54	48	22	20	49
490	112	110	92	59	58	54	49	22	20	48
495	113	110	92	59	58	54	49	22	20	49
500	113	110	93	59	58	54	49	22	20	48
505	113	110	93	59	58	54	50	22	20	48
510	113	111	93	59	58	55	50	23	21	49
515	114	111	93	59	58	54	51	22	20	49
520	114	111	93	59	58	55	51	22	20	49
525	114	111	93	59	58	55	51	22	20	49
530	114	111	93	60	58	54	51	22	20	49
535	116	112	94	59	58	54	51	22	20	49
540	116	111	93	59	58	54	51	22	20	49
545	117	112	94	59	58	54	51	22	20	49
550	117	112	94	59	58	54	50	22	20	49
555	118	112	93	59	58	54	49	22	20	49
560	119	112	94	59	58	54	49	22	20	49
565	120	112	94	59	58	54	50	22	20	49
570	121	112	93	59	58	54	50	22	20	49
575	122	112	94	59	58	54	50	22	20	49
580	123	112	93	59	58	54	49	22	20	49



DATE: 09-21-1992 TIME: 21:04:02

RUN NUMBER: 19

FLOW RATE: 219 C/MIN

VIBRATION: STATIC

TIME	T1	T2	T3	T4	T5	T6	T7	T8	T9	T10
445	92	87	73	41	40	35	30	22	20	26
450	92	87	73	42	40	35	30	22	20	27
455	93	88	73	42	40	36	30	22	20	27
460	93	88	73	41	40	35	30	22	20	27
465	93	88	73	42	40	35	30	22	20	27
470	93	88	73	42	40	36	30	22	20	26
475	93	88	73	42	40	36	30	22	20	27
480	93	88	73	42	40	36	30	22	20	27
485	93	89	74	42	40	36	30	22	20	27
490	94	89	74	40	40	36	30	22	20	27
495	94	89	74	42	40	36	30	22	20	27
500	94	89	74	42	41	35	30	22	20	27
505	95	90	74	42	41	36	30	22	20	27
510	95	90	75	42	41	36	31	22	20	27
515	95	90	75	42	41	36	31	22	20	27
520	95	90	75	42	41	36	31	22	20	27
525	95	90	75	42	41	36	31	22	20	27
530	96	90	75	42	41	36	31	22	20	27
535	96	91	75	42	40	37	31	22	20	27
540	96	91	75	42	41	37	30	22	20	27
545	97	93	76	42	41	36	30	22	20	27
550	97	93	76	42	41	36	31	22	20	27
555	99	94	77	42	41	36	31	22	20	27
560	101	94	77	42	41	36	31	22	20	27
565	102	94	77	42	41	36	31	22	20	27
570	103	95	77	42	40	35	31	22	20	27
575	104	95	77	42	41	36	31	22	20	27
580	105	95	77	42	41	36	31	22	20	27
585	106	96	77	42	41	36	31	22	20	27
590	107	96	77	42	41	36	31	22	20	27
595	108	97	77	42	41	37	30	21	20	27
600	108	97	78	42	41	37	30	22	20	27

DATE: 09-22-1992 TIME: 13:45:36

RUN NUMBER: 20

FLOW RATE: 61 CC/MIN

VIBRATION: 1000 HZ / 1.0 G (X: .93G, Y: .12G)

TIME	T1	T2	T3	T4	T5	T6	T7	T8	T9	T10
905	118	119	101	63	62	58	52	22	22	52
910	118	119	101	63	62	58	53	22	22	52
915	118	119	101	63	62	58	53	22	22	52
920	119	119	101	63	62	59	52	22	22	52
925	119	119	101	63	62	59	53	22	22	52
930	119	119	101	63	62	59	53	22	22	52
935	119	120	101	63	62	59	53	22	22	52
940	120	120	101	63	62	59	52	22	22	53
945	120	120	102	63	62	59	52	22	22	53
950	121	120	102	63	63	59	51	22	22	53
955	121	120	102	63	62	59	52	22	22	53
960	121	120	102	63	63	59	52	22	22	53
965	121	120	102	63	63	59	52	22	22	53
970	122	121	102	64	63	60	52	22	22	53
975	122	121	102	64	63	60	53	22	22	53
980	122	122	102	64	63	59	53	22	22	53
985	123	122	103	64	63	60	54	22	22	53
990	123	122	102	64	63	60	53	22	22	53
995	123	122	103	64	63	60	53	22	22	54
1000	124	122	103	64	63	60	53	22	22	54
1005	124	122	103	64	63	60	52	22	22	54
1010	124	122	103	64	63	60	53	22	22	54
1015	124	122	103	64	63	60	52	22	22	54
1020	125	123	103	64	62	60	52	22	22	54
1025	127	123	103	64	63	60	53	22	22	54
1030	128	123	103	64	63	60	53	22	22	54
1035	130	123	103	64	63	60	53	22	22	54
1040	131	124	103	64	63	60	53	22	22	54
1045	133	124	103	64	63	59	54	22	22	54
1050	134	125	104	64	63	60	54	22	22	54
1055	135	125	103	64	63	60	55	22	22	54
1060	136	125	104	64	63	60	55	22	22	54
1065	137	125	104	64	63	60	56	22	22	54

DATE: 09-22-1992 TIME: 14:34:49

RUN NUMBER: 21

FLOW RATE: 59 CC/MIN

VIBRATION: 1000 HZ / 2.5 G (X: 1.39G, Y: .25G)

TIME	T1	T2	T3	T4	T5	T6	T7	T8	T9	T10
270	112	109	92	58	57	54	47	22	21	47
275	112	109	92	58	57	54	48	22	21	48
280	112	110	92	59	58	54	48	22	21	48
285	113	110	92	59	58	54	48	21	21	48
290	113	110	93	59	58	54	49	22	21	48
295	113	110	93	59	58	54	49	22	21	48
300	114	111	93	59	58	54	49	22	21	48
305	114	111	93	59	58	54	49	22	21	48
310	114	111	94	59	58	55	49	22	21	48
315	115	111	93	59	58	55	49	22	21	48
320	115	111	94	59	58	55	49	22	21	48
325	115	112	94	60	58	55	49	22	21	49
330	116	112	94	60	58	55	49	22	21	49
335	116	112	94	60	59	55	50	22	20	49
340	116	112	95	60	58	55	50	22	21	49
345	117	112	95	60	59	55	50	22	21	49
350	117	113	95	60	59	55	50	22	21	49
355	118	113	95	60	59	55	50	22	21	49
360	118	113	95	60	59	55	50	22	20	49
365	118	113	95	60	59	55	51	22	21	49
370	118	113	95	60	59	55	51	22	21	50
375	119	114	95	60	59	55	51	22	21	50
380	119	114	95	61	59	55	51	22	21	50
385	120	114	96	61	59	55	51	22	21	50
390	122	114	95	60	59	56	50	22	21	50
395	124	114	95	60	59	56	50	22	21	50
400	125	114	95	60	59	56	50	21	21	50
405	126	114	96	60	59	56	50	21	21	50
410	126	115	96	60	59	56	50	22	21	50
415	127	115	96	60	59	56	49	21	21	50
420	128	115	96	60	59	56	49	21	21	50
425	128	115	96	61	59	56	49	21	21	50
430	129	115	96	60	59	56	51	22	21	50

DATE: 09-22-1992 TIME: 15:57:39

RUN NUMBER: 22

FLOW RATE: 62 CC/MIN

VIBRATION: 1000 HZ / 5.0 G (X: 5.06G, Y: .67G)

TIME	T1	T2	T3	T4	T5	T6	T7	T8	T9	T10
410	105	103	85	55	54	51	45	21	21	45
415	105	103	85	55	54	52	45	21	21	45
420	105	103	85	55	54	51	45	21	21	45
425	105	104	86	55	55	52	45	21	21	46
430	106	104	86	56	55	52	44	21	21	46
435	106	104	86	56	55	52	45	21	21	46
440	106	104	86	56	55	52	45	21	21	46
445	106	104	86	56	55	52	45	23	21	46
450	107	105	86	56	55	52	45	21	21	46
455	107	105	87	56	55	52	45	21	21	46
460	107	105	87	56	55	52	45	21	21	46
465	108	105	87	56	55	52	45	21	21	46
470	108	106	87	56	55	52	45	21	20	46
475	108	106	88	56	55	52	45	21	21	46
480	108	106	88	57	56	52	45	21	21	46
485	108	106	88	56	56	52	45	21	21	46
490	109	106	88	57	56	52	45	21	20	46
495	109	107	88	57	56	52	45	21	21	47
500	109	107	89	57	56	53	45	21	20	47
505	110	107	89	57	56	53	46	21	21	47
510	110	108	89	57	56	53	46	24	21	47
515	110	108	89	57	56	53	46	21	21	47
520	110	108	89	57	56	53	46	21	21	47
525	108	109	89	57	56	53	46	21	21	47
530	111	110	89	57	57	53	46	21	21	47
535	112	110	90	57	56	53	46	21	21	47
540	112	110	90	57	57	53	46	21	21	47
545	112	111	90	57	57	53	46	21	21	47
550	113	111	90	57	57	53	46	21	21	47
555	114	111	89	57	57	53	46	21	21	47
560	115	111	90	57	56	53	46	21	21	48
565	117	111	90	57	56	53	46	21	20	47
570	118	111	91	57	56	53	46	21	21	48

DATE: 09-22-1992 TIME: 16:32:59

RUN NUMBER: 23

FLOW RATE: 65 CC/MIN

VIBRATION: 250 HZ / 1.0 G (X: .53G, Y: .10G)

TIME	T1	T2	T3	T4	T5	T6	T7	T8	T9	T10
725	131	111	90	56	55	52	45	22	21	46
730	131	111	91	54	55	52	46	22	21	46
735	132	111	91	56	55	52	45	22	21	46
740	132	111	91	56	55	52	45	22	21	46
745	133	111	91	56	55	52	46	22	21	46
750	133	111	91	56	55	52	45	22	21	46
755	133	111	91	57	55	52	45	21	21	46
760	134	111	91	57	55	52	45	22	21	46
765	134	111	91	57	55	52	45	22	21	46
770	135	112	91	57	55	52	45	22	21	46
775	135	112	91	56	56	52	45	22	21	46
780	135	112	91	57	53	52	45	22	21	46
785	135	112	91	57	55	52	45	22	21	46
790	135	112	91	57	56	52	45	22	21	46
795	136	112	92	57	55	52	45	22	21	46
800	136	112	92	57	56	53	45	22	21	46
805	136	112	92	57	56	52	45	22	21	46
810	137	113	92	57	55	52	45	21	21	46
815	137	113	92	57	56	52	45	22	21	46
820	138	113	92	57	55	52	45	22	21	46
825	138	113	92	54	55	52	45	21	21	46
830	139	114	92	57	56	52	45	22	21	46
835	139	115	92	57	56	52	45	22	21	46
840	140	116	93	56	55	52	45	22	21	46
845	142	117	92	57	55	52	46	22	23	46
850	143	117	92	56	55	52	45	22	21	47
855	144	118	93	56	55	52	45	22	21	46
860	145	119	93	57	55	51	45	22	21	46
865	146	119	93	57	55	51	46	22	21	47
870	147	119	93	56	55	52	45	21	21	46
875	148	120	93	56	55	52	45	22	21	46
880	149	120	93	57	55	51	46	22	21	46
885	150	120	93	57	55	52	45	22	21	46

DATE: 09-22-1992 TIME: 17:15:15

RUN NUMBER: 24

FLOW RATE: 58 CC/MIN

VIBRATION: 250 HZ / 2.5 G (X: .30G, Y: .15G)

TIME	T1	T2	T3	T4	T5	T6	T7	T8	T9	T10
645	123	112	88	58	56	53	48	22	21	48
650	123	112	89	58	57	53	48	22	21	48
655	124	112	89	58	57	53	48	22	21	48
660	124	112	89	58	57	53	48	22	21	48
665	124	112	89	58	57	54	48	22	21	48
670	124	112	89	58	57	54	48	22	21	49
675	125	113	89	58	57	54	48	22	21	48
680	125	113	89	58	57	54	48	22	21	48
685	125	113	89	58	57	54	48	22	21	48
690	125	113	89	58	57	54	48	22	21	48
695	125	112	89	58	57	54	48	22	21	49
700	125	113	89	58	57	54	48	22	21	49
705	126	113	89	58	57	54	48	22	21	49
710	126	113	90	59	57	54	48	22	21	49
715	126	114	90	59	57	54	48	22	21	49
720	127	114	90	59	57	54	48	22	21	49
725	127	114	89	59	58	54	48	22	21	51
730	128	114	90	59	57	55	48	22	21	49
735	128	114	90	59	58	54	48	21	21	49
740	129	114	90	59	58	55	48	22	21	49
745	129	115	90	59	58	55	48	21	21	49
750	130	115	90	59	58	55	48	21	21	49
755	130	115	91	59	58	54	48	22	21	49
760	131	116	91	59	58	55	48	22	21	49
765	131	116	91	59	58	55	48	22	21	49
770	132	116	91	59	58	54	48	22	21	49
775	132	116	91	59	58	54	48	22	21	49
780	133	117	91	59	58	54	48	22	21	49
785	133	117	91	59	58	55	48	22	24	49
790	134	117	91	60	58	55	49	22	21	49
795	134	117	92	60	58	55	49	22	21	49
800	135	117	92	60	58	55	49	22	21	50
805	135	117	91	60	58	55	49	22	21	49

DATE: 09-23-1992 TIME: 11:42:28

RUN NUMBER: 25

FLOW RATE: 63 CC/MIN

VIBRATION: 250 HZ / 5.0 G (X: .45G, Y: .62G)

TIME	T1	T2	T3	T4	T5	T6	T7	T8	T9	T10
0	100	99	80	53	53	44	45	21	19	43
5	100	99	80	53	52	49	44	21	19	43
10	100	99	81	53	53	49	43	21	19	43
15	101	99	81	53	53	49	43	21	19	44
20	101	99	81	53	53	49	42	21	19	44
25	102	99	81	53	52	50	43	21	20	44
30	103	100	81	53	52	50	43	21	20	44
35	103	100	81	53	53	50	43	21	20	44
40	104	100	80	53	53	50	43	21	20	44
45	105	100	80	53	53	50	43	21	20	44
50	105	100	80	53	53	50	43	21	20	44
55	106	100	80	53	53	50	43	21	20	44
60	105	100	80	53	53	50	43	21	20	44
65	108	100	81	53	52	50	43	21	20	44
70	109	101	81	53	53	50	43	21	20	44
75	111	101	81	53	52	50	43	21	20	44
80	111	101	81	53	53	50	43	21	20	44
85	112	101	82	53	53	50	43	21	20	44
90	113	102	82	53	53	50	43	21	20	44
95	114	102	82	54	53	50	42	21	20	44
100	114	102	82	54	53	50	43	21	20	44
105	115	103	83	54	53	50	43	21	20	44
110	116	102	83	53	53	50	43	21	20	44
115	117	103	83	54	53	50	43	21	20	44
120	117	103	83	51	53	50	43	21	20	44
125	118	103	82	54	53	50	43	21	20	44

DATE: 09-23-1992 TIME: 12:12:58

RUN NUMBER: 26

FLOW RATE: 59 CC/MIN

VIBRATION: 30 HZ / 1.0 G (X: .07G, Y: .05G)

TIME	T1	T2	T3	T4	T5	T6	T7	T8	T9	T10
850	120	117	96	61	60	57	51	21	20	51
855	120	117	95	61	60	57	50	21	20	50
860	121	117	96	61	60	57	51	21	20	51
865	121	117	96	61	61	57	50	21	20	50
870	121	117	96	61	61	57	50	21	20	51
875	122	118	96	62	61	57	50	21	20	51
880	122	117	97	62	61	57	50	21	20	51
885	122	118	97	62	61	57	50	21	20	51
890	123	118	97	62	61	57	50	21	20	51
895	123	118	97	62	61	57	51	21	20	51
900	123	118	97	62	61	57	51	22	20	51
905	124	118	97	62	61	57	52	21	20	51
910	124	118	97	62	61	57	52	21	20	51
915	125	119	97	62	61	57	51	21	20	51
920	125	120	97	62	61	58	51	21	20	51
925	126	120	97	61	61	57	51	21	20	51
930	127	120	98	62	61	57	51	21	20	51
935	127	120	98	62	61	58	51	21	20	51
940	127	120	98	62	61	57	50	21	20	51
945	128	121	98	62	61	58	51	21	20	51
950	128	122	98	63	61	57	52	21	20	52
955	129	122	98	63	61	58	52	21	20	52
960	130	122	98	63	61	58	52	21	20	52
965	132	123	99	63	61	57	52	21	20	51
970	134	123	99	62	61	57	52	21	20	52
975	136	123	98	62	61	57	52	21	20	52
980	137	124	98	62	61	57	51	21	20	52
985	139	124	98	62	61	57	51	21	20	52
990	141	124	98	62	60	57	51	21	20	52
995	144	125	98	61	60	57	50	21	20	51
1000	146	125	98	61	60	56	50	21	20	52
1005	149	126	99	61	60	56	50	21	20	51
1010	150	128	99	61	59	56	50	21	20	51



DATE: 09-23-1992 TIME: 13:16:28

RUN NUMBER: 27

FLOW RATE: 56 CC/MIN

VIBRATION: 30 HZ / 2.5 G (X: .14G, Y: .10G)

TIME	T1	T2	T3	T4	T5	T6	T7	T8	T9	T10
310	110	107	87	58	57	54	47	21	20	48
315	111	107	87	58	57	54	47	21	20	48
320	111	107	88	58	57	54	47	21	20	48
325	111	107	88	58	57	54	47	21	20	48
330	112	107	87	58	57	54	47	21	20	48
335	112	108	87	58	57	54	47	21	20	48
340	112	108	88	58	57	54	48	21	20	48
345	112	108	88	58	57	54	48	21	20	48
350	113	108	88	58	57	54	48	21	20	48
355	113	108	88	58	58	54	48	21	20	48
360	113	108	88	59	57	54	48	21	20	48
365	114	108	88	58	58	54	48	21	20	48
370	115	108	88	58	58	54	47	21	20	48
375	116	109	88	58	58	54	48	21	20	48
380	116	109	89	59	58	55	48	21	20	49
385	116	109	89	59	58	55	48	21	20	49
390	117	109	89	59	58	55	48	21	20	49
395	117	109	89	59	58	55	48	21	20	49
400	118	109	89	59	58	55	48	21	20	49
405	119	110	89	59	58	55	48	21	20	49
410	120	109	89	59	58	55	48	21	20	49
415	121	109	89	59	58	55	48	21	20	49
420	121	109	89	59	58	55	49	21	20	49
425	122	110	89	59	58	55	48	21	20	49
430	123	110	89	58	58	55	48	21	20	49
435	123	110	89	58	58	55	48	21	20	49
440	124	111	89	59	58	55	48	21	20	49
445	125	111	89	58	58	55	48	21	21	49
450	126	111	89	59	58	55	48	21	20	49
455	126	111	89	59	58	55	48	21	20	49
460	127	111	89	59	58	55	48	21	20	49
465	127	111	89	59	58	55	48	21	20	49
470	128	111	89	59	58	55	48	21	20	49

DATE: 09-23-1992 TIME: 13:43:35

RUN NUMBER: 28

FLOW RATE: 54 CC/MIN

VIBRATION: 30 HZ / 5.0 G (X: .66G, Y: .26G)

TIME	T1	T2	T3	T4	T5	T6	T7	T8	T9	T10
610	104	102	82	56	55	52	46	21	20	46
615	105	102	83	57	55	52	46	21	20	47
620	105	102	83	56	55	53	46	22	20	47
625	105	102	83	57	56	53	46	21	20	47
630	106	102	84	57	56	53	47	23	20	47
635	106	103	84	57	55	52	47	21	20	47
640	106	103	84	57	56	53	48	21	20	47
645	106	103	85	57	56	53	48	21	20	47
650	106	104	85	57	56	53	48	21	22	47
655	107	104	85	57	56	53	48	21	20	47
660	107	104	85	57	56	53	48	21	20	47
665	107	104	85	57	56	53	48	21	20	47
670	108	105	86	57	57	53	48	21	20	48
675	108	105	86	58	57	54	48	21	20	48
680	108	105	86	58	57	54	48	22	20	48
685	108	105	87	58	57	54	48	22	20	48
690	109	106	87	58	57	54	48	22	20	48
695	109	106	87	58	57	54	48	22	20	48
700	110	106	88	58	57	54	49	22	20	48
705	110	106	88	58	57	54	49	22	20	48
710	110	106	88	58	57	54	49	22	20	48
715	110	107	89	59	57	54	49	22	20	48
720	111	107	89	58	58	54	49	22	20	48
725	110	107	89	59	57	54	49	21	20	48
730	111	107	89	59	58	55	49	21	20	48
735	112	107	90	59	58	55	49	21	20	49
740	113	107	90	59	58	54	49	21	20	49
745	115	108	90	59	58	55	49	21	20	49
750	115	108	90	59	58	54	49	22	20	49
755	116	108	90	59	58	55	50	21	20	49
760	118	108	91	59	58	55	49	21	20	49
765	119	108	91	59	58	55	49	21	20	49
770	120	108	91	59	58	55	49	21	20	49

DATE: 09-23-1992 TIME: 14:39:05

RUN NUMBER: 29

FLOW RATE: 96 CC/MIN

VIBRATION: STATIC

TIME	T1	T2	T3	T4	T5	T6	T7	T8	T9	T10
620	103	102	86	51	50	47	41	21	20	38
625	103	102	87	51	50	45	41	21	20	38
630	103	102	87	51	50	47	42	23	20	38
635	103	103	86	51	50	47	42	21	20	38
640	104	103	87	51	51	47	42	21	20	38
645	104	103	87	51	51	47	42	22	20	38
650	105	103	87	51	51	47	42	21	20	38
655	105	104	88	51	51	47	42	21	20	39
660	106	104	88	51	51	47	41	21	20	39
665	106	105	88	52	51	47	42	22	20	39
670	107	105	88	52	51	47	42	21	20	39
675	107	105	88	52	51	47	42	21	20	39
680	108	105	88	52	51	47	42	21	20	39
685	108	106	89	52	51	46	42	21	20	39
690	109	106	89	52	51	47	42	22	20	39
695	109	106	89	52	51	47	42	21	20	39
700	110	106	89	52	51	47	42	21	20	39
705	111	106	89	52	51	47	41	21	20	39
710	113	107	89	52	51	47	41	21	20	39
715	114	107	89	52	51	47	41	21	20	39
720	115	107	89	52	51	48	41	21	20	39
725	116	107	89	52	51	47	41	21	20	39
730	117	108	90	52	51	47	41	22	20	39
735	118	109	90	52	51	47	41	22	20	39
740	120	110	90	52	51	47	41	21	20	39
745	122	111	91	52	51	47	41	22	20	39

DATE: 09-23-1992 TIME: 15:12:32

RUN NUMBER: 30

FLOW RATE: 91 CC/MIN

VIBRATION: STATIC

TIME	T1	T2	T3	T4	T5	T6	T7	T8	T9	T10
365	98	94	79	48	47	44	38	21	19	36
370	98	95	80	48	47	44	38	21	20	36
375	99	94	80	48	47	44	38	21	19	36
380	99	95	80	48	48	44	38	21	19	36
385	99	95	80	48	48	44	38	21	20	37
390	99	95	81	49	48	44	38	21	19	37
395	99	95	81	49	48	44	39	21	19	37
400	100	95	81	49	48	44	39	21	19	37
405	100	96	81	49	48	44	39	21	20	37
410	100	96	81	49	48	44	39	21	19	37
415	100	96	81	49	48	44	39	21	19	37
420	101	96	82	49	48	44	39	21	20	37
425	101	97	82	49	48	44	39	21	19	37
430	102	97	82	49	48	44	39	21	19	37
435	102	97	82	49	49	45	40	22	19	37
440	102	97	82	49	48	44	40	21	20	37
445	102	97	82	49	48	44	40	21	20	37
450	103	98	83	49	49	45	40	22	19	38
455	103	98	83	50	49	45	40	21	19	37
460	103	98	83	50	49	45	40	21	19	37
465	103	98	83	50	49	45	40	21	19	38
470	104	98	83	50	49	45	40	21	19	37
475	104	98	83	50	49	45	40	21	20	37
480	105	99	83	50	49	45	40	22	20	38
485	105	99	83	50	49	45	40	21	19	38
490	106	99	84	50	49	45	40	21	20	38
495	106	99	84	50	49	45	40	21	20	38
500	106	99	84	50	49	45	40	22	19	38
505	107	99	84	50	49	45	40	21	20	38
510	107	100	84	50	49	45	40	21	20	38
515	107	100	84	50	49	45	41	21	19	38
520	108	100	84	50	48	45	41	22	19	38
525	108	100	84	51	49	45	41	22	20	38

DATE: 09-23-1992 TIME: 15:46:03

RUN NUMBER: 31

FLOW RATE: 138 CC/MIN

VIBRATION: STATIC

TIME	T1	T2	T3	T4	T5	T6	T7	T8	T9	T10
490	99	96	81	46	45	40	36	22	19	32
495	99	97	81	46	45	40	36	22	19	32
500	99	97	81	46	45	40	36	22	19	32
505	99	97	81	46	45	40	36	22	19	32
510	100	97	81	46	45	40	36	21	19	32
515	100	97	81	47	45	40	36	22	19	32
520	100	98	81	46	45	40	36	22	19	32
525	101	98	82	47	45	40	36	22	19	32
530	101	98	82	47	46	41	36	22	19	32
535	101	98	82	47	46	41	36	22	19	32
540	101	98	82	47	46	41	36	22	19	32
545	102	99	82	47	46	41	36	22	19	32
550	102	99	83	47	46	41	36	22	19	32
555	102	99	82	47	46	41	37	21	19	32
560	102	99	83	47	46	41	37	22	19	32
565	102	99	83	47	46	41	37	22	19	32
570	103	100	83	47	46	41	37	21	19	32
575	103	100	83	46	46	41	37	22	19	32
580	103	100	83	47	46	41	37	22	19	32
585	104	100	83	47	46	41	37	21	19	32
590	104	101	84	47	46	41	37	22	19	32
595	105	101	84	47	46	41	37	22	19	32
600	105	101	84	47	46	41	37	21	19	32
605	106	101	84	47	46	41	36	21	19	32
610	107	102	84	47	46	41	36	22	19	32
615	108	102	84	47	46	41	36	22	19	32
620	109	102	84	47	46	42	35	22	19	32
625	110	102	84	47	46	42	36	22	19	32
630	111	102	85	47	46	42	36	21	19	32
635	111	103	85	47	46	42	36	22	19	32
640	112	103	85	47	46	42	36	22	19	32
645	113	103	85	47	46	42	36	22	19	32
650	115	103	85	47	46	42	35	22	19	32

DATE: 09-23-1992 TIME: 17:08:50

RUN NUMBER: 32

FLOW RATE: 56 CC/MIN

VIBRATION: 250 HZ / 5.0 G (X: .30G, Y: .20G)

TIME	T1	T2	T3	T4	T5	T6	T7	T8	T9	T10
285	99	96	79	53	53	50	43	22	20	44
290	100	96	79	53	53	50	43	22	20	44
295	100	96	79	54	53	50	43	22	20	44
300	101	96	79	53	53	50	43	22	20	44
305	101	96	80	53	53	50	43	22	20	44
310	101	97	80	54	53	50	43	22	20	45
315	101	97	80	54	53	50	43	22	20	45
320	102	96	79	54	53	50	43	22	20	45
325	102	97	80	54	53	50	43	22	20	45
330	102	97	80	54	53	51	44	22	20	45
335	102	97	80	54	53	51	44	22	20	45
340	102	98	80	54	53	51	44	22	20	45
345	103	98	81	54	53	51	44	22	20	45
350	103	98	81	54	53	51	44	22	20	45
355	104	98	81	54	53	51	44	22	20	45
360	104	99	81	54	53	51	44	22	20	45
365	104	99	81	54	54	51	44	22	20	45
370	105	100	81	54	54	51	44	22	20	45
375	105	100	82	55	54	51	45	22	20	45
380	105	100	82	55	54	51	45	22	20	45
385	106	101	82	55	54	51	44	22	20	45
390	106	101	82	55	54	51	45	22	20	46
395	106	101	82	55	54	51	45	22	20	46
400	107	101	82	55	54	51	45	22	20	46
405	108	101	82	55	54	51	45	22	20	46
410	109	102	82	55	54	51	45	22	20	46
415	109	102	81	54	54	51	45	22	20	46
420	110	102	82	55	54	51	45	22	20	46
425	111	102	83	55	54	51	45	22	20	46
430	113	102	82	55	54	51	45	22	20	46
435	114	102	83	55	54	51	45	22	20	46
440	114	103	83	55	54	52	45	22	20	46
445	115	103	82	55	54	52	45	22	20	46

DATE: 09-24-1992 TIME: 09:15:16

RUN NUMBER: 33

FLOW RATE: 131 CC/MIN

VIBRATION: STATIC

TIME	T1	T2	T3	T4	T5	T6	T7	T8	T9	T10
790	108	105	87	49	48	44	35	21	19	34
795	109	105	87	49	48	43	36	21	19	34
800	109	105	88	49	48	44	35	21	19	34
805	109	105	88	50	48	44	35	21	19	34
810	109	105	88	50	48	44	35	21	19	34
815	110	106	88	50	49	44	36	21	20	35
820	110	106	89	50	49	45	36	21	20	35
825	110	106	89	50	49	45	37	21	20	35
830	111	106	89	50	49	44	37	21	19	34
835	111	107	89	50	49	45	38	21	19	34
840	111	107	89	50	49	44	38	21	19	35
845	112	107	89	50	49	45	38	21	20	35
850	112	107	89	50	49	45	38	21	20	35
855	112	107	89	50	49	44	39	21	19	35
860	112	107	89	50	49	45	38	21	20	35
865	113	108	90	50	49	45	37	21	19	34
870	113	108	90	50	50	45	36	21	19	35
875	113	108	90	50	49	45	36	21	19	35
880	113	108	90	50	50	45	38	21	19	35
885	114	108	90	49	50	45	37	21	20	35
890	114	108	90	50	49	45	36	21	20	35
895	114	108	90	50	50	45	38	21	19	35
900	114	108	90	49	50	45	38	21	20	35
905	115	109	90	50	50	44	38	21	19	35
910	116	109	90	50	49	44	39	21	19	35
915	117	109	90	50	49	44	39	21	19	35
920	118	110	90	50	49	44	39	21	19	35
925	120	111	91	50	49	44	38	21	19	35
930	121	111	91	50	49	44	38	21	19	35
935	122	112	91	50	49	44	38	21	19	34
940	123	112	92	50	49	44	37	21	19	35
945	125	113	92	50	49	43	37	21	20	35
950	127	113	92	50	49	43	38	21	20	35

DATE: 09-24-1992 TIME: 10:05:39

RUN NUMBER: 34

FLOW RATE: 40 CC/MIN

VIBRATION: 1000 HZ / 1.0 G (X: .86G, Y: .25G)

TIME	T1	T2	T3	T4	T5	T6	T7	T8	T9	T10
0	125	124	103	72	71	68	62	21	20	61
5	125	124	103	70	71	68	62	21	20	61
10	125	124	103	72	71	68	62	21	20	61
15	125	124	103	72	71	68	62	21	20	61
20	126	125	104	72	71	68	62	21	20	61
25	126	125	104	72	71	68	63	21	20	61
30	126	125	104	72	71	68	63	21	20	62
35	126	126	104	73	71	68	63	21	20	62
40	126	125	104	73	72	68	63	21	20	62
45	127	126	105	73	72	68	63	21	20	62
50	127	126	105	73	72	69	64	21	21	62
55	128	126	105	73	72	69	64	21	21	62
60	128	126	105	73	72	69	64	21	20	62
65	128	127	105	73	72	69	64	21	20	62
70	128	127	106	73	72	69	63	21	20	62
75	129	127	106	73	72	69	64	21	20	62
80	129	127	106	73	73	69	64	21	20	63
85	130	127	106	74	73	69	64	21	20	63
90	130	128	106	74	73	69	64	21	20	63
95	131	128	106	74	73	69	64	21	20	62
100	132	128	106	74	73	69	64	21	20	63
105	133	128	107	74	73	70	64	21	20	63
110	133	128	107	74	73	70	64	21	20	63
115	134	129	107	74	73	70	64	21	21	63
120	134	129	107	74	73	70	64	21	20	64
125	135	129	107	74	73	70	64	21	21	64
130	136	130	107	74	73	70	64	21	20	64
135	136	129	107	75	73	70	64	21	20	64
140	137	130	107	75	73	70	65	21	20	64
145	138	130	108	75	74	70	65	21	21	64
150	138	130	108	74	74	70	65	21	20	64
155	138	130	108	75	74	70	65	21	20	64
160	138	131	108	75	74	71	65	21	20	64



DATE: 09-25-1992 TIME: 10:34:32

RUN NUMBER: 35

FLOW RATE: 47 CC/MIN

VIBRATION: 1000 HZ / 2.5 G (X: 2.4G, Y: .15G)

TIME	T1	T2	T3	T4	T5	T6	T7	T8	T9	T10
695	127	109	97	64	63	60	54	22	20	54
700	128	110	98	64	64	61	55	22	20	54
705	128	110	98	64	64	60	55	22	20	54
710	128	110	98	65	64	60	55	22	20	54
715	128	111	99	65	64	61	55	22	20	54
720	129	111	99	65	64	61	55	22	20	55
725	129	112	99	65	64	61	55	22	20	55
730	129	111	99	65	64	61	55	22	20	55
735	130	111	99	66	64	61	55	22	20	55
740	130	112	99	66	64	61	55	22	20	55
745	130	112	99	66	65	61	55	22	20	55
750	130	112	100	66	65	61	55	22	20	55
755	130	112	100	66	65	62	56	22	20	55
760	131	112	100	66	65	62	55	22	20	55
765	131	112	100	66	65	62	55	22	20	55
770	132	113	100	66	65	62	55	22	20	56
775	132	113	101	66	65	62	55	22	20	56
780	133	113	101	66	66	62	56	22	20	56
785	132	114	101	67	66	62	56	22	20	56
790	133	114	102	67	66	63	57	22	20	56
795	134	114	102	67	66	63	57	22	20	56
800	134	114	102	67	66	63	57	22	20	56
805	134	115	102	67	66	63	57	22	20	57
810	135	115	102	68	66	63	57	22	20	57
815	135	115	102	67	66	63	57	22	20	57
820	136	115	103	68	66	63	58	22	20	57
825	136	116	103	67	66	63	58	22	20	57
830	137	116	103	68	67	63	57	22	20	57
835	137	116	103	68	67	64	58	22	20	57
840	138	116	103	68	67	64	57	22	20	57
845	139	116	103	68	67	64	57	22	20	57
850	140	117	103	68	67	64	58	22	20	57
855	140	117	104	68	68	64	58	22	20	57

DATE: 09-24-1992 TIME: 12:01:52

RUN NUMBER: 36

FLOW RATE: 53 CC/MIN

VIBRATION: 1000 HZ / 5.0 G (X: 5.08G, Y: .45G)

TIME	T1	T2	T3	T4	T5	T6	T7	T8	T9	T10
255	102	101	85	56	55	53	46	21	20	47
260	102	101	85	56	55	53	46	21	20	47
265	102	102	85	57	56	53	46	21	20	47
270	102	102	85	57	56	53	46	21	20	47
275	103	102	85	57	56	53	46	21	20	47
280	103	102	85	57	56	53	46	21	20	47
285	103	102	86	57	56	53	47	21	20	47
290	103	103	86	57	56	53	47	21	20	47
295	104	103	86	57	56	53	48	21	20	48
300	104	103	86	57	56	53	48	21	20	48
305	104	103	86	57	56	53	48	21	20	48
310	104	104	86	57	56	53	48	21	20	48
315	104	104	86	57	56	53	48	21	20	48
320	104	104	87	57	57	54	48	21	20	48
325	105	104	87	58	57	54	48	21	20	48
330	105	104	87	58	57	54	48	21	20	48
335	105	105	87	58	57	54	48	21	20	48
340	105	105	87	58	57	54	48	21	20	49
345	105	105	87	58	57	54	48	21	20	48
350	106	105	88	58	57	54	48	21	20	49
355	106	105	88	58	57	54	48	21	20	49
360	107	105	88	58	57	54	48	21	20	49
365	107	105	88	58	57	54	47	21	20	49
370	108	106	88	58	57	54	48	21	20	49
375	108	106	88	58	57	54	48	21	20	49
380	109	106	88	58	57	54	48	21	20	49
385	109	106	89	58	57	54	48	21	20	49
390	110	107	89	58	57	54	48	21	20	49
395	110	107	89	58	57	54	48	21	20	49
400	111	107	89	58	57	54	48	21	20	49
405	111	108	89	59	58	54	49	21	20	49
410	112	108	89	58	57	54	48	21	20	49
415	114	108	89	58	57	54	48	21	20	49

DATE: 09-24-1992 TIME: 12:28:01

RUN NUMBER: 37

FLOW RATE: 56 CC/MIN

VIBRATION: 250 HZ / 1.0 G (X: .09G, Y: .06G)

TIME	T1	T2	T3	T4	T5	T6	T7	T8	T9	T10
380	100	96	81	53	52	50	43	21	20	43
385	100	96	81	53	52	49	43	21	20	43
390	100	96	81	53	52	49	43	21	20	44
395	100	97	82	53	52	50	43	21	20	44
400	100	97	82	53	52	50	43	21	20	44
405	101	97	82	53	53	50	43	21	20	44
410	101	97	82	53	53	50	43	21	20	44
415	101	97	83	54	53	50	43	21	20	44
420	101	97	83	54	53	50	43	21	20	44
425	102	98	83	54	53	50	43	21	20	44
430	102	98	83	54	53	50	43	21	20	44
435	102	98	83	54	53	50	44	21	20	45
440	103	99	84	54	53	50	44	21	20	45
445	104	99	84	54	53	50	44	21	20	45
450	104	99	84	54	53	50	44	21	20	45
455	104	99	84	54	53	50	44	21	20	45
460	105	99	84	54	53	51	44	21	20	45
465	105	100	85	55	53	51	44	21	20	45
470	105	100	85	54	54	51	45	21	20	45
475	106	100	85	55	54	51	45	21	20	45
480	106	101	85	55	54	51	45	21	20	45
485	107	101	85	55	54	51	45	21	20	45
490	108	101	85	55	54	51	45	21	20	45
495	109	101	85	55	54	51	45	21	20	45
500	109	101	86	55	54	51	46	21	20	45
505	110	102	86	55	54	51	46	21	20	45
510	110	102	86	55	54	51	46	21	20	45
515	111	102	86	55	54	51	46	21	20	45
520	112	102	86	55	54	51	46	21	20	45
525	112	102	86	55	54	51	46	21	20	45
530	112	102	87	56	54	51	46	21	20	45
535	112	103	87	55	55	51	46	21	20	46
540	112	103	87	56	54	52	46	21	20	46

DATE: 09-24-1992 TIME: 13:00:14

RUN NUMBER: 38

FLOW RATE: 49 CC/MIN

VIBRATION: 250 HZ / 2.5 G (X: .15G, Y: .11G)

TIME	T1	T2	T3	T4	T5	T6	T7	T8	T9	T10
530	112	101	85	57	55	53	46	21	20	48
535	112	101	84	57	56	53	46	21	20	47
540	112	101	85	57	56	53	46	21	20	48
545	112	102	85	57	56	53	46	21	20	48
550	113	102	85	57	56	53	47	21	20	48
555	113	102	85	57	56	53	47	21	20	48
560	113	102	85	57	56	53	47	21	20	48
565	113	102	85	57	56	53	47	21	20	48
570	113	102	85	57	56	53	47	21	20	48
575	114	102	85	57	56	53	47	21	20	48
580	114	103	85	57	56	53	47	21	20	48
585	114	103	86	57	56	53	47	21	20	48
590	114	103	86	57	56	54	47	21	20	48
595	114	103	86	57	56	54	47	21	20	48
600	115	103	86	57	56	54	48	21	20	48
605	115	103	86	57	57	54	48	21	20	49
610	115	104	87	58	57	54	48	21	20	49
615	115	104	87	58	57	54	48	21	20	49
620	115	104	87	58	57	54	48	21	20	49
625	115	104	87	58	57	54	48	21	20	49
630	116	105	87	58	57	54	48	21	20	49
635	116	105	88	58	57	54	49	21	20	49
640	116	105	88	58	57	54	49	22	20	49
645	117	105	88	58	57	54	48	22	20	49
650	117	106	89	58	57	54	49	22	20	49
655	118	106	89	58	58	54	49	21	20	49
660	118	106	89	59	58	55	49	21	20	49
665	119	107	89	59	58	55	49	21	20	49
670	119	106	88	59	58	55	48	21	20	49
675	120	107	89	59	58	55	48	21	20	49
680	121	107	89	59	58	55	48	21	20	49
685	121	107	89	59	58	55	48	21	20	49
690	122	108	89	59	58	55	48	21	20	50

DATE: 09-24-1992 TIME: 13:29:35

RUN NUMBER: 39

FLOW RATE: 55 CC/MIN

VIBRATION: 250 HZ / 5.0 G (X: .27G, Y: .19G)

TIME	T1	T2	T3	T4	T5	T6	T7	T8	T9	T10
270	98	92	78	52	51	49	43	22	20	43
275	99	93	78	52	52	49	43	22	20	43
280	98	93	78	53	52	49	43	21	20	43
285	99	93	78	53	52	49	43	21	20	43
290	99	93	78	53	52	49	43	21	20	43
295	99	93	78	53	52	49	43	21	20	43
300	99	93	78	53	52	49	43	21	19	43
305	100	94	79	53	52	49	43	21	20	43
310	100	94	79	53	52	49	43	21	20	43
315	100	94	79	53	52	49	43	21	19	43
320	100	94	79	53	52	50	44	21	20	43
325	100	94	79	53	52	50	43	21	20	44
330	101	95	79	53	52	50	43	21	20	44
335	101	95	80	53	52	49	43	21	19	44
340	101	95	80	53	52	49	43	21	20	44
345	102	95	80	53	53	49	44	21	20	44
350	102	95	80	53	53	49	44	21	20	44
355	102	95	80	54	53	49	44	21	20	44
360	102	95	80	54	53	50	43	21	20	44
365	103	96	80	54	53	50	43	21	20	44
370	103	96	80	53	53	50	43	21	20	44
375	103	96	80	54	53	50	43	21	20	44
380	103	96	81	54	53	50	43	22	20	44
385	104	96	81	54	53	50	43	22	20	44
390	104	96	81	54	53	50	43	22	20	44
395	105	96	81	54	53	50	43	22	20	45
400	105	96	81	54	53	50	43	22	20	45
405	106	96	81	54	52	50	43	21	20	45
410	106	97	81	54	53	50	44	22	20	45
415	107	97	81	54	53	50	44	22	20	45
420	107	97	81	54	53	50	44	21	20	45
425	108	97	82	54	53	50	43	22	20	45
430	108	97	82	54	53	50	44	22	20	45

DATE: 09-24-1992 TIME: 14:07:13

RUN NUMBER: 40

FLOW RATE: 48 CC/MIN

VIBRATION: 30 HZ / 1.0 G (X: .13G, Y: .07G)

TIME	T1	T2	T3	T4	T5	T6	T7	T8	T9	T10
210	111	109	92	61	60	55	51	21	20	51
215	111	109	92	61	60	57	51	22	20	52
220	111	109	92	61	60	57	51	21	20	52
225	112	110	92	61	60	58	51	22	20	52
230	112	110	92	61	60	58	51	22	20	52
235	112	110	93	62	60	58	51	21	20	52
240	112	111	93	62	60	58	51	21	20	52
245	112	111	93	62	61	58	51	21	20	52
250	113	111	93	62	61	58	52	21	20	52
255	113	111	93	62	61	58	52	22	20	52
260	113	111	94	62	61	58	52	22	20	52
265	113	112	94	62	61	58	52	22	20	52
270	114	112	94	62	61	58	52	22	20	52
275	114	112	95	62	61	58	52	21	20	52
280	114	112	95	62	61	58	52	21	20	53
285	115	113	95	62	62	58	52	21	20	53
290	115	113	95	63	62	59	53	21	20	53
295	115	113	95	63	62	59	53	21	20	53
300	115	113	95	63	62	59	53	21	20	53
305	115	114	95	63	62	58	53	21	20	53
310	116	114	96	63	62	59	54	21	20	53
315	116	114	96	63	62	59	53	21	20	53
320	116	115	96	63	62	59	53	21	20	53
325	117	115	96	63	62	59	53	21	20	53
330	118	115	97	63	62	59	53	21	20	53
335	119	115	97	63	62	59	53	21	20	53
340	120	115	97	63	62	59	53	21	20	53
345	121	115	97	63	62	59	53	21	20	53
350	122	116	97	63	62	59	53	21	20	53
355	123	116	97	64	62	59	53	22	20	54
360	124	116	97	64	62	59	53	22	20	54
365	125	116	98	64	62	59	53	21	20	54
370	126	117	98	64	62	59	53	21	20	53

DATE: 09-24-1992 TIME: 14:31:33

RUN NUMBER: 41

FLOW RATE: 47 CC/MIN

VIBRATION: 30 HZ / 2.5 G (X: .49G, Y: .30G)

TIME	T1	T2	T3	T4	T5	T6	T7	T8	T9	T10
335	101	95	80	57	56	53	48	21	20	47
340	101	95	79	57	56	53	48	21	20	47
345	101	95	80	57	56	53	48	21	20	47
350	102	95	81	57	56	53	48	21	20	47
355	102	96	81	57	56	53	48	22	20	47
360	102	96	80	57	56	53	48	21	20	47
365	102	96	81	57	57	54	48	22	20	48
370	103	96	81	57	57	54	48	21	20	48
375	103	96	82	58	57	54	48	21	20	48
380	103	97	82	57	57	54	48	21	20	48
385	103	97	82	58	57	54	48	21	20	48
390	104	97	82	58	57	54	48	22	20	48
395	104	97	82	56	57	54	48	21	20	48
400	104	98	82	58	57	54	48	22	20	48
405	105	98	82	58	57	54	48	22	20	48
410	105	98	83	58	57	55	48	21	20	48
415	105	98	83	58	57	54	48	21	19	48
420	106	98	83	58	57	55	48	21	20	49
425	106	99	83	58	57	55	48	21	20	49
430	106	99	83	58	57	54	48	22	19	49
435	107	99	83	58	57	55	48	22	20	49
440	107	99	83	58	57	55	48	22	20	49
445	107	99	83	58	58	55	48	22	20	49
450	108	99	83	58	58	55	48	21	20	49
455	109	100	83	58	58	55	48	21	20	49
460	109	100	83	58	58	55	49	21	20	49
465	110	100	83	58	58	55	49	22	20	49
470	111	100	84	59	58	55	49	22	20	49
475	111	100	84	59	58	55	49	22	20	49
480	112	100	84	59	58	55	49	22	20	49
485	112	100	84	59	58	55	49	22	20	50
490	112	101	84	59	58	55	49	22	20	49
495	113	101	84	59	58	55	49	22	20	50

DATE: 09-25-1992 TIME: 11:19:20

RUN NUMBER: 42

FLOW RATE: 49 CC/MIN

VIBRATION: 30 HZ / 5.0 G (X: .22G, Y: .20G)

TIME	T1	T2	T3	T4	T5	T6	T7	T8	T9	T10
595	126	104	94	62	61	58	53	23	20	52
600	127	104	94	62	61	58	53	23	20	52
605	127	105	95	62	61	58	53	23	20	53
610	127	105	95	62	61	58	53	22	20	53
615	127	105	95	63	61	58	53	22	20	53
620	127	105	95	63	62	58	53	23	20	53
625	128	105	95	63	62	58	53	22	20	53
630	128	106	95	63	62	58	53	22	20	53
635	128	105	95	63	62	59	54	22	20	53
640	129	106	95	63	62	59	54	22	20	53
645	129	106	95	63	62	59	54	23	20	53
650	130	106	96	63	62	59	53	22	22	54
655	130	106	95	63	62	59	53	22	20	53
660	131	107	96	63	62	59	53	22	20	53
665	131	107	96	63	62	59	54	22	20	53
670	132	107	96	63	62	59	54	23	20	54
675	132	107	96	63	62	59	54	22	20	53
680	133	107	96	63	62	59	54	22	20	53
685	133	107	96	63	62	59	54	22	20	54
690	133	108	97	63	62	59	54	22	20	53
695	133	109	97	63	62	59	54	22	20	54
700	134	109	97	63	62	59	54	22	20	53
705	134	109	97	63	62	59	53	22	20	54
710	136	110	97	63	62	59	53	22	20	54
715	136	109	97	63	62	59	53	22	20	54
720	137	110	97	63	62	59	54	22	20	54
725	138	110	97	63	62	59	54	22	20	54
730	139	110	97	63	62	59	54	22	20	54
735	140	110	97	63	62	59	54	22	20	54
740	141	110	97	63	62	59	53	23	20	54
745	142	110	97	63	62	59	53	22	20	54
750	143	111	97	63	62	59	53	22	20	54
755	144	111	97	63	62	59	53	22	20	54



DATE: 09-24-1992 TIME: 17:00:21

RUN NUMBER: 43

FLOW RATE: 77 CC/MIN

VIBRATION: STATIC

TIME	T1	T2	T3	T4	T5	T6	T7	T8	T9	T10
695	120	110	90	55	54	50	45	23	20	43
700	120	110	90	55	54	50	45	23	20	43
705	120	110	91	55	54	50	45	23	20	43
710	121	111	91	55	54	50	45	23	20	43
715	121	111	91	55	54	51	45	23	20	43
720	121	111	91	55	54	51	45	23	20	43
725	121	111	91	55	54	51	45	23	20	43
730	121	111	91	55	54	51	45	23	20	44
735	122	111	91	56	54	51	45	23	20	44
740	122	112	92	56	54	51	45	23	20	44
745	122	112	92	56	54	51	45	23	20	44
750	123	112	92	56	55	51	45	23	20	44
755	123	112	92	56	55	51	45	23	20	44
760	123	113	92	56	55	51	45	23	20	44
765	123	113	92	56	55	51	45	23	20	44
770	124	113	93	56	55	51	45	23	20	44
775	124	113	93	56	55	51	46	23	20	44
780	124	114	93	56	55	51	46	23	20	44
785	125	114	93	56	55	51	46	23	20	44
790	125	114	93	56	55	51	46	23	20	44
795	125	114	93	57	55	52	46	23	20	44
800	125	115	93	57	56	52	46	23	20	44
805	125	114	93	57	56	52	46	23	20	44
810	126	114	94	57	56	52	46	23	20	45
815	126	115	94	57	56	52	46	23	20	45
820	127	115	94	57	56	52	46	23	20	45
825	127	115	94	57	56	52	46	23	20	45
830	128	115	94	57	56	52	46	23	20	45
835	128	115	94	57	56	52	47	23	20	45
840	129	116	95	57	56	52	47	23	20	45
845	129	116	95	57	56	52	47	23	20	45
850	130	116	95	57	56	52	47	23	20	45
855	131	116	95	57	56	52	46	23	20	45

DATE: 09-24-1992 TIME: 17:36:36

RUN NUMBER: 44

FLOW RATE: 57 CC/MIN

VIBRATION: STATIC

TIME	T1	T2	T3	T4	T5	T6	T7	T8	T9	T10
445	124	108	91	59	58	54	49	23	20	48
450	124	108	92	59	58	54	50	23	20	48
455	124	109	92	59	58	55	50	23	20	49
460	125	109	92	59	58	55	50	23	20	49
465	125	109	92	59	58	55	50	23	20	49
470	125	109	92	59	58	55	49	23	20	49
475	125	109	92	59	58	55	49	23	20	49
480	125	109	92	60	58	55	50	23	20	49
485	126	109	92	60	58	55	49	23	20	49
490	126	110	92	59	58	55	49	23	20	49
495	126	110	92	59	58	55	49	23	20	49
500	127	110	93	60	58	55	49	23	20	49
505	127	110	93	60	59	56	49	23	20	50
510	127	110	93	60	59	56	49	23	20	50
515	127	111	93	60	59	55	49	23	20	50
520	128	111	93	60	59	56	49	23	20	50
525	128	111	93	60	59	56	49	23	20	50
530	128	111	93	60	59	56	49	23	20	50
535	129	111	93	60	59	56	49	23	20	50
540	129	111	94	60	59	56	49	23	20	50
545	130	111	94	60	59	56	49	23	20	50
550	130	112	94	60	59	56	49	23	20	50
555	130	112	94	60	59	56	49	23	20	50
560	131	112	94	60	59	56	49	23	20	50
565	131	112	94	60	59	56	49	23	20	50
570	132	112	94	60	59	56	49	23	20	50
575	132	112	94	60	60	56	50	23	20	51
580	133	112	94	61	60	56	50	23	20	51
585	133	112	95	61	60	56	51	23	20	51
590	134	113	95	61	60	56	51	23	20	51
595	134	113	95	61	60	56	51	23	20	51
600	134	113	95	61	60	56	51	23	20	50
605	134	113	95	61	60	57	51	23	20	51

DATE: 09-25-1992 TIME: 09:53:43

RUN NUMBER: 45

FLOW RATE: 52 CC/MIN

VIBRATION: STATIC

TIME	T1	T2	T3	T4	T5	T6	T7	T8	T9	T10
850	130	114	101	66	66	62	56	22	22	56
855	130	115	101	66	66	62	56	22	22	56
860	130	115	102	66	66	62	56	22	22	56
865	131	115	102	67	66	62	56	22	22	56
870	130	115	102	67	66	62	56	22	22	56
875	131	115	102	67	66	63	56	22	22	57
880	131	115	102	67	66	63	56	22	22	57
885	132	116	102	67	66	63	57	22	22	57
890	132	116	103	67	66	63	57	22	22	57
895	133	116	103	67	66	63	56	22	22	57
900	133	116	103	67	67	63	57	22	22	57
905	133	117	103	67	66	63	57	22	22	57
910	134	117	104	67	67	63	57	22	22	57
915	134	117	104	68	67	63	58	22	22	57
920	135	117	104	68	67	63	59	22	22	57
925	135	118	104	68	67	63	59	22	22	57
930	135	118	105	68	67	63	59	22	22	57
935	136	118	105	68	67	64	59	22	21	58
940	136	118	105	68	68	64	60	22	22	58
945	136	118	105	69	68	64	60	22	22	57
950	137	118	105	69	68	64	60	22	22	58
955	137	119	106	69	68	64	61	22	22	58
960	137	119	106	69	68	64	60	22	22	58
965	138	119	106	69	68	64	60	22	22	58
970	138	119	106	69	68	64	59	22	22	58
975	139	119	106	69	68	64	59	22	22	58
980	140	119	106	69	68	64	59	22	22	58
985	141	119	106	69	68	64	60	22	22	58
990	143	119	106	69	68	64	61	22	22	58
995	144	120	106	69	68	64	61	22	21	58
1000	145	120	106	69	68	64	62	22	22	59
1005	147	120	106	69	68	64	61	22	22	59
1010	148	120	107	69	68	64	61	22	21	59

DATE: 09-25-1992 TIME: 11:57:34

RUN NUMBER: 46

FLOW RATE: 45 CC/MIN

VIBRATION: STATIC

TIME	T1	T2	T3	T4	T5	T6	T7	T8	T9	T10
785	131	115	103	68	67	64	59	23	20	58
790	131	115	103	68	67	64	58	23	20	58
795	132	115	103	69	67	64	59	23	20	58
800	132	115	103	68	67	64	59	22	20	58
805	132	115	104	69	67	64	59	23	20	58
810	132	115	104	69	67	65	58	23	20	58
815	133	116	104	69	68	65	58	23	20	58
820	133	116	104	69	68	65	58	23	20	58
825	133	116	104	69	68	65	59	23	20	58
830	133	116	104	69	68	65	59	23	20	59
835	133	116	104	69	68	65	58	23	20	59
840	134	116	104	69	68	65	59	23	20	59
845	134	116	105	69	68	65	59	23	20	59
850	134	116	105	69	68	65	59	23	20	59
855	134	117	105	69	68	65	59	23	20	59
860	135	117	105	69	68	65	59	23	20	59
865	135	117	105	70	68	66	59	23	20	59
870	135	117	105	70	69	66	60	23	20	59
875	135	117	105	70	69	66	60	23	20	60
880	136	117	106	69	69	66	60	23	20	60
885	136	118	106	70	69	66	60	23	20	60
890	136	118	106	70	69	66	60	23	20	60
895	136	118	106	70	69	66	60	23	20	60
900	137	118	106	70	69	66	60	23	20	60
905	138	118	106	70	69	66	60	23	20	60
910	138	119	106	70	69	66	60	23	20	60
915	139	119	106	70	69	66	60	23	20	60
920	141	119	106	70	69	66	60	23	20	60
925	141	119	106	70	69	66	60	23	20	60
930	142	119	107	70	69	66	60	23	20	60
935	144	119	107	70	69	66	60	23	20	60
940	145	119	107	70	69	66	60	23	20	60
945	147	119	107	70	69	66	61	23	20	60

DATE: 09-25-1992 TIME: 16:06:12

RUN NUMBER: 47

FLOW RATE: 49 CC/MIN

VIBRATION: 250 HZ / 1.0 G (X: .10G, Y: .06G)

TIME	T1	T2	T3	T4	T5	T6	T7	T8	T9	T10
580	124	107	96	63	61	58	53	23	20	53
585	124	106	96	63	62	58	53	23	20	53
590	125	106	96	63	62	58	53	23	20	53
595	125	107	97	63	62	59	53	24	20	53
600	125	107	97	63	62	59	53	23	20	53
605	125	107	97	63	62	59	53	23	20	53
610	126	107	97	63	62	59	53	23	20	53
615	126	107	97	63	62	59	53	24	20	53
620	126	108	97	63	62	59	53	23	20	53
625	127	108	97	63	62	59	53	23	20	54
630	127	108	98	64	63	59	53	23	20	54
635	127	108	97	63	62	59	54	23	20	54
640	127	109	98	64	63	59	54	23	20	54
645	127	109	98	64	63	59	54	23	20	54
650	128	109	98	64	63	60	54	23	20	54
655	128	109	98	64	63	60	54	23	20	54
660	128	109	98	64	63	60	54	23	20	54
665	129	109	98	64	63	60	54	23	20	54
670	129	110	99	65	63	60	54	23	20	54
675	129	110	99	65	63	60	54	23	20	54
680	130	110	99	65	63	60	55	23	20	54
685	130	111	99	65	64	60	55	23	20	54
690	130	111	100	65	64	60	56	24	20	54
695	131	111	100	65	64	60	56	24	20	54
700	131	112	100	65	64	60	56	24	20	55
705	132	111	100	65	64	60	56	23	20	55
710	133	112	100	65	64	61	56	24	20	55
715	134	112	100	65	64	61	56	24	20	55
720	136	112	101	65	64	61	55	23	20	55
725	137	112	101	65	64	61	55	23	20	55
730	138	112	101	66	64	61	55	23	20	55
735	139	112	101	66	64	61	56	23	20	55
740	139	113	101	66	65	61	56	23	20	55

DATE: 09-25-1992 TIME: 15:30:30

RUN NUMBER: 48

FLOW RATE: 49 CC/MIN

VIBRATION: 250 HZ / 2.5 G (X: .33G, Y: .24G)

TIME	T1	T2	T3	T4	T5	T6	T7	T8	T9	T10
370	126	109	97	64	63	59	53	23	21	54
375	126	109	97	64	62	59	53	23	20	54
380	127	109	97	64	63	59	54	23	21	54
385	127	110	97	64	63	60	55	24	21	54
390	127	110	97	64	63	60	55	24	21	54
395	127	110	97	64	63	60	55	23	20	54
400	128	110	97	64	63	60	55	23	21	54
405	128	110	98	64	63	60	54	24	20	54
410	128	111	98	64	63	60	54	23	20	54
415	128	111	98	64	63	60	54	23	20	55
420	128	111	98	64	63	60	55	23	21	54
425	129	111	98	64	64	60	54	24	20	55
430	129	111	98	64	63	60	54	23	20	55
435	129	111	98	64	63	60	55	24	21	55
440	130	111	98	64	63	60	54	24	21	55
445	130	111	99	64	63	60	54	24	21	55
450	131	111	99	64	63	60	55	24	21	55
455	131	112	99	65	64	60	54	23	20	55
460	131	112	99	65	64	60	54	23	20	55
465	132	112	99	65	64	61	54	24	21	55
470	132	112	99	65	64	60	55	24	21	55
475	133	112	99	64	64	60	54	23	20	55
480	133	112	99	65	64	61	55	24	21	55
485	134	113	99	65	64	61	55	24	21	55
490	136	113	99	65	64	60	54	24	21	55
495	137	113	99	65	64	60	55	23	20	55
500	138	113	99	65	63	60	55	24	21	55
505	140	113	100	65	64	61	54	24	20	55
510	141	114	100	65	64	60	54	23	20	55
515	141	114	100	65	64	60	54	24	21	55
520	142	114	100	65	64	60	54	23	20	55
525	143	114	100	65	64	60	54	23	20	55
530	144	115	100	65	64	60	54	23	20	55

DATE: 09-25-1992 TIME: 14:46:57

RUN NUMBER: 49

FLOW RATE: 50

VIBRATION: 250 HZ / 5.0 G (X: .32G, Y: .35G)

TIME	T1	T2	T3	T4	T5	T6	T7	T8	T9	T10
485	121	105	95	63	62	59	54	23	21	53
490	121	105	96	63	62	59	54	23	21	53
495	122	105	96	63	62	59	54	23	21	53
500	122	106	96	63	63	59	54	23	22	53
505	123	106	96	63	63	60	54	23	21	53
510	123	106	96	64	62	60	54	23	22	54
515	123	106	97	64	63	60	54	23	21	54
520	124	107	97	64	63	60	54	23	22	54
525	124	107	97	64	63	60	54	23	21	54
530	124	107	97	64	63	60	54	23	21	54
535	124	107	97	64	63	60	54	23	21	54
540	125	108	98	64	63	60	55	23	22	54
545	125	108	98	64	64	60	54	23	22	54
550	125	109	98	64	63	60	54	23	21	54
555	126	109	98	65	64	60	54	23	21	54
560	126	109	98	65	64	60	54	23	21	54
565	126	109	98	65	64	60	55	23	21	55
570	127	109	98	65	64	60	54	23	21	55
575	127	110	99	65	64	60	54	23	21	55
580	127	110	98	65	64	61	54	23	21	55
585	127	110	99	65	64	61	54	23	21	55
590	128	110	99	65	64	61	54	23	21	55
595	128	111	99	65	64	61	55	23	21	55
600	129	111	99	65	64	61	54	23	21	55
605	130	111	99	65	64	61	54	23	22	55
610	130	111	99	65	64	61	54	23	21	55
615	132	112	99	65	64	61	55	23	21	55
620	135	112	99	65	64	61	54	23	21	55
625	136	112	99	65	64	61	54	23	21	55
630	138	113	99	65	64	61	54	23	21	55
635	140	113	99	65	64	60	55	23	21	55
640	141	113	99	65	64	60	55	23	21	55
645	142	114	99	65	64	61	55	23	21	55

DATE: 09-25-1992 TIME: 16:47:12

RUN NUMBER: 50

FLOW RATE: 55 CC/MIN

VIBRATION: 30 HZ / 1.0G (X: .06G, Y: .06G)

TIME	T1	T2	T3	T4	T5	T6	T7	T8	T9	T10
205	116	96	86	56	55	52	46	23	20	46
210	116	96	86	56	55	52	46	23	20	46
215	116	96	87	56	55	52	46	23	20	46
220	116	96	87	56	55	52	47	23	20	47
225	116	96	87	56	55	52	47	24	20	46
230	116	97	87	57	55	52	47	24	20	47
235	117	97	87	56	55	52	47	23	20	47
240	117	97	87	57	55	52	47	24	20	47
245	117	97	87	56	55	52	46	23	20	47
250	118	97	88	57	55	52	46	23	20	47
255	118	97	88	57	56	52	47	23	20	47
260	118	97	88	57	55	52	47	23	20	47
265	119	98	88	57	56	52	47	23	20	47
270	119	98	88	57	56	52	48	23	20	47
275	119	98	88	57	56	53	48	23	20	47
280	120	98	89	57	56	52	48	24	20	47
285	120	98	88	57	56	53	48	23	20	47
290	120	99	89	57	56	53	48	23	20	47
295	121	99	89	57	56	53	48	23	20	48
300	121	99	89	57	56	53	48	24	20	48
305	121	99	89	57	56	53	48	23	20	48
310	121	99	89	57	56	53	48	23	20	47
315	121	99	89	57	56	53	48	23	20	48
320	122	99	89	57	56	53	48	23	20	48
325	122	99	89	57	56	53	48	23	20	48
330	123	100	89	56	56	53	48	23	20	48
335	123	100	90	57	56	53	48	23	20	48
340	124	100	90	58	56	53	48	23	20	48
345	124	100	90	58	57	53	48	23	20	48
350	125	100	90	58	57	53	48	23	20	48
355	125	100	90	58	57	54	47	23	20	48
360	125	101	90	58	57	53	48	23	20	48
365	126	101	90	58	56	53	48	23	20	48



DATE: 09-28-1992 TIME: 13:09:08

RUN NUMBER: 51

FLOW RATE: 54 CC/MIN

VIBRATION: 30 HZ / 2.5 G (X: .15G, Y: .10G)

TIME	T1	T2	T3	T4	T5	T6	T7	T8	T9	T10
665	122	106	98	63	62	58	53	23	20	53
670	122	106	97	63	62	58	53	23	20	52
675	122	107	98	63	62	59	54	23	21	53
680	123	107	98	63	62	59	54	23	21	52
685	123	107	98	64	63	59	54	23	21	53
690	123	107	98	64	62	59	54	23	21	53
695	123	107	98	64	63	59	55	23	21	53
700	124	107	99	64	63	59	54	23	20	53
705	124	108	99	64	62	59	54	23	20	53
710	124	108	99	64	63	59	55	23	21	53
715	124	108	99	64	63	59	54	23	20	53
720	125	108	99	64	63	59	54	23	20	53
725	125	108	99	64	63	59	54	23	21	53
730	125	108	99	64	63	59	54	23	21	53
735	125	108	99	64	63	60	55	24	20	53
740	126	108	100	64	63	59	55	23	21	53
745	126	109	100	64	63	59	54	23	21	54
750	126	109	100	64	63	60	54	23	20	53
755	126	109	100	65	64	60	54	23	21	54
760	126	109	100	65	64	60	54	23	21	54
765	127	109	100	65	64	60	54	23	20	54
770	127	109	100	65	63	60	55	23	21	54
775	127	110	100	65	64	60	55	23	20	54
780	128	110	100	65	64	60	55	23	20	54
785	129	110	100	65	64	60	55	23	20	54
790	131	110	100	64	63	60	55	23	21	54
795	133	110	100	64	63	59	55	23	21	54
800	134	110	100	64	63	60	55	23	21	54
805	135	110	100	64	63	59	55	23	21	54
810	136	110	100	64	63	59	55	23	21	54
815	136	110	100	64	63	60	55	23	21	54
820	137	110	100	64	63	60	55	23	21	54
825	137	111	100	65	63	60	55	23	21	54

DATE: 09-25-1992 TIME: 18:09:41

RUN NUMBER: 52

FLOW RATE: 49 CC/MIN

VIBRATION: 30 HZ / 5.0 G (X: .21G, Y: .16G)

TIME	T1	T2	T3	T4	T5	T6	T7	T8	T9	T10
855	125	110	100	66	65	62	58	24	20	56
860	126	110	100	66	65	62	58	24	20	56
865	126	110	100	66	65	62	58	24	21	56
870	126	110	100	66	65	62	58	24	20	56
875	126	111	101	66	66	62	58	24	20	56
880	127	111	101	66	66	62	58	24	21	56
885	127	111	101	66	66	62	58	24	20	56
890	128	111	101	66	66	62	58	24	20	56
895	128	111	101	66	66	62	58	24	20	56
900	128	111	101	66	66	62	58	24	20	57
905	129	112	102	67	66	63	59	24	21	57
910	129	112	101	67	66	62	59	24	20	57
915	129	112	101	67	66	62	59	24	20	57
920	129	112	102	67	66	63	59	24	21	57
925	129	112	102	67	66	63	59	24	21	57
930	129	112	102	67	66	63	59	24	20	57
935	130	112	102	67	66	63	59	24	21	57
940	130	113	102	68	66	63	59	24	21	57
945	130	113	102	67	66	63	60	24	20	57
950	131	113	103	67	66	63	58	24	20	58
955	131	113	103	67	67	63	58	24	20	57
960	131	113	103	68	67	63	58	24	20	57
965	131	113	103	68	67	63	59	24	20	58
970	132	114	103	68	67	64	59	24	21	57
975	132	115	103	68	67	63	58	24	20	57
980	133	115	103	68	67	63	59	24	21	57
985	134	116	104	68	67	64	59	24	20	57
990	136	116	104	68	67	64	59	24	20	58
995	137	116	104	68	67	63	59	24	20	58
1000	139	117	104	68	67	64	58	24	21	58
1005	141	117	104	67	67	64	58	24	20	58
1010	143	117	104	67	67	64	58	24	20	58
1015	144	118	104	67	67	64	58	24	20	58

DATE: 09-28-1992 TIME: 15:17:40

RUN NUMBER: 53

FLOW RATE: 50 CC/MIN

VIBRATION: STATIC

TIME	T1	T2	T3	T4	T5	T6	T7	T8	T9	T10
230	116	103	93	60	59	56	51	23	20	51
235	117	103	93	61	60	56	51	23	20	51
240	117	103	93	61	60	56	51	23	20	51
245	117	103	94	61	60	57	52	23	20	51
250	117	104	94	61	60	57	52	23	20	51
255	117	104	94	61	60	57	52	23	20	51
260	118	104	94	61	60	57	52	23	20	51
265	118	104	94	61	60	57	51	23	20	51
270	119	105	95	61	60	57	51	23	20	51
275	119	104	95	61	60	57	51	23	20	51
280	119	105	95	61	60	57	51	23	20	52
285	120	105	95	61	60	57	51	23	20	51
290	120	105	95	62	60	57	51	23	20	52
295	120	105	95	62	60	57	51	23	20	52
300	120	106	95	62	60	57	51	23	20	52
305	120	106	96	62	60	57	52	23	20	52
310	120	106	96	62	61	57	52	23	20	52
315	121	106	96	62	61	57	52	23	20	52
320	121	106	96	62	61	58	52	23	20	52
325	121	107	96	62	61	57	53	23	20	52
330	122	107	96	62	61	58	53	23	20	52
335	123	107	97	62	61	58	53	23	20	53
340	123	107	97	62	61	58	53	23	20	53
345	124	108	97	62	61	58	53	23	20	52
350	124	108	97	63	61	58	53	23	20	52
355	125	108	97	63	62	58	53	23	20	52
360	126	110	97	63	62	58	52	23	20	52
365	127	111	97	63	61	58	52	23	20	52
370	129	111	97	62	61	58	52	23	20	52
375	131	111	98	62	61	58	52	23	20	53
380	133	112	98	62	61	58	52	23	20	53
385	135	112	98	62	61	58	52	23	20	53
390	136	113	98	62	61	57	52	23	20	53

### *Bibliography*

1. Chi, S. W. *Heat Pipe Theory and Practice: A Sourcebook*. Washington: Hemisphere Publishing Corporation, 1976.
2. Deverall, J. E. *The Effect of Vibration on Heat Pipe Performance*. LA-3798. Los Alamos Scientific Laboratory, October 1967.
3. Doebelin, Ernest O. *Measurement Systems: Application and Design*. New York: McGraw-Hill Book Company, 1983.
4. Dunn, P. D. and D. A. Reay. *Heat Pipes*. Oxford: Pergamon Press, 1976.
5. Incopera, Frank P. and David P. DeWitt. *Introduction to Heat Transfer*. New York: John Wiley & Sons, 1990.
6. Richardson, John Wilson et al. "The Effect of Longitudinal Vibration on Heat Pipe Performance," *Journal of the Astronautical Sciences*, 17 [5]: 249-266 (March-April 1970).

### Vita

Captain Mark C. Charlton was born 12 March 1966 in Sacramento, California. He is the son of Colonel and Mrs. James Charlton and is married to April Dawn Hogland of Albuquerque, New Mexico. He graduated from Saint Pius X High School in Albuquerque, New Mexico in 1984 and attended the U.S. Air Force Academy, graduating as a Distinguished Graduate with a Bachelor of Science in Astronautical Engineering in June 1988. Upon graduation, he received a regular commission in the USAF and served his first tour of duty at Los Angeles AFB, California. He began as a project engineer in the Titan IV System Program Office providing technical evaluation and oversight of the Centaur Upper Stage development and production. He was chosen to enter the Astronautical Engineering program in the School of Engineering, Air Force Institute of Technology, in May 1991.

Permanent Address: 10200 Oso Redondo NE

Albuquerque, New Mexico 87111

# REPORT DOCUMENTATION PAGE

1. AGENCY USE ONLY (Leave blank)		2. REPORT DATE DEC 92	3. REPORT TYPE AND DATES COVERED Master's Thesis
4. TITLE AND SUBTITLE Effect of Transverse Vibration on the Capillary Limit of a Wrapped Screen Wick Copper/Water Heat Pipe			5. FUNDING NUMBERS
6. AUTHOR(S) MARK C. CHARLTON, Captain, USAF			
7. PERFORMING ORGANIZATION NAME(S) AND ADDRESS(ES) Air Force Institute of Technology WPAFB OH 45433-6583			8. PERFORMING ORGANIZATION REPORT NUMBER AFIT/GA/ENY/92D-02
9. SPONSORING/MONITORING AGENCY NAME(S) AND ADDRESS(ES) Dr. Jerry Beam WL/POOS-3 Wright-Patterson AFB OH 45433			10. SPONSORING/MONITORING AGENCY REPORT NUMBER
11. SUPPLEMENTARY NOTES			
12a. DISTRIBUTION/AVAILABILITY STATEMENT APPROVED FOR PUBLIC RELEASE; DISTRIBUTION UNLIMITED			12b. DISTRIBUTION CODE
13. ABSTRACT (Maximum 200 words) The effect of transverse vibration on the capillary limit of a copper/water heat pipe with a tightly wrapped screen wick was investigated. The capillary limit was measured over a range of operating temperatures under static conditions. A bench-top shaker was used to provide vibration normal to the longitudinal axis of the pipe, and the capillary limit was measured at vibration frequencies of 30, 250, and 1000 Hz. At each of these frequencies, tests were run at vibration levels of 1.0, 2.5, and 5.0 G. The pipe was maintained at a zero degree inclination angle and power throughput was increased until dryout was achieved. The power throughput at dryout was considered to be the capillary limit under the conditions imposed for that test. The measured capillary limit from each vibration test was compared to those from the static tests. The results spanned pipe operating temperatures from 50° C to 75° C. For the frequencies and amplitudes tested, there was found to be little or no effect on the capillary limit due to vibration normal to the longitudinal axis. It is recommended that further study in this area be concentrated on vibration parallel to the longitudinal axis.			
14. SUBJECT TERMS HEAT PIPES; VIBRATION; VIBRATION TESTING; THERMAL PROTECTION; WORKING FLUIDS; CONDUCTIVE HEAT TRANSFER; HEAT FLUX			15. NUMBER OF PAGES 172
			16. PRICE CODE
17. SECURITY CLASSIFICATION OF REPORT UNCLASSIFIED	18. SECURITY CLASSIFICATION OF THIS PAGE UNCLASSIFIED	19. SECURITY CLASSIFICATION OF ABSTRACT UNCLASSIFIED	20. LIMITATION OF ABSTRACT UL